
Science

The sedimentary rocks of Sinus Meridiani: Five key observations from data acquired by the Mars Global Surveyor and Mars Odyssey orbiters

Kenneth S. Edgett

Malin Space Science Systems, P.O. Box 910148, San Diego, CA, 92191-0148, USA

Citation: Mars 1, 5-58, 2005; [doi:10.1555/mars.2005.0002](https://doi.org/10.1555/mars.2005.0002)

History: Submitted July 18, 2005; Reviewed September 13, 2005; Revised October 12, 2005; Accepted October 26, 2005; Published November 2, 2005

Editor: Jeffrey B. Plescia, Applied Physics Laboratory, Johns Hopkins University

Reviewers: Larry S. Crumpler, New Mexico Museum of Natural History and Science; Ellen Stofan, Proxemy Research

Open Access: Copyright © 2005 Malin Space Science Systems. This is an open-access paper distributed under the terms of a [Creative Commons Attribution License](https://creativecommons.org/licenses/by/2.0/), which permits unrestricted use, distribution, and reproduction in any medium, provided the original work is properly cited.

Abstract

Background: The sedimentary rocks explored by the Mars Exploration Rover (MER-B), Opportunity, occur within a greater stratigraphic context that is visible from orbit. In the Sinus Meridiani region, vast exposures of light-toned, layered, sedimentary rock cover an area greater than that of the sedimentary rock outcrops of the Colorado Plateau in North America.

Method: This is a photogeologic study focused on observations made from examination of images acquired by the Mars Global Surveyor (MGS) Mars Orbiter Camera (MOC) and the Mars Odyssey Thermal Emission Imaging System (THEMIS) visible (VIS) and infrared (IR) subsystems. The work is supplemented by observations from use of MGS Mars Orbiter Laser Altimeter (MOLA) data and pictures from MER-B and the Mariner 9, Viking 1, Viking 2, and Phobos 2 orbiters.

Results: Five key observations help place the ~7 m of stratigraphic section examined by the MER-B team in 2004 into context. (1) The rocks outcropping in Sinus Meridiani are more diverse than the suite of materials explored at the MER-B site. (2) Former valleys and impact craters (of a range of diameters from 10s of meters to 10s of kilometers) are interbedded with the rocks exposed in Sinus Meridiani. (3) The stratigraphic section explored by the MER-B team covers < 1% of the > 800 m of section exposed in the region. (4) The bedrock of the heavily cratered terrain to the south, north, west, and east of Meridiani Planum is layered, possibly light-toned, and includes interbedded impact craters. (5) Light-toned, layered, plains-forming rocks are not unique to the Sinus Meridiani region; similar rocks are cut by Mawrth Vallis and by some of the troughs of the Valles Marineris.

Conclusions: The sedimentary rocks of Sinus Meridiani preserve a rich and complex geologic history, of which very little is presently known. The bedrock of both Meridiani Planum and the adjacent heavily cratered terrains can be described as a layered, cratered, and "valley-ed" volume. Orbiter images show a diversity of rocks in the form of erosional expression, relative albedo, and bedding styles. Material deposited in impact craters is usually different from the material deposited outside the crater, suggesting different depositional environments in close proximity (e.g., the crater may have been a lake or pond at the same time that the surrounding areas were not). No unambiguous, primary volcanic landforms or rock units are discerned. When deposited, the rocks were generally horizontally bedded except where dipping locally in response to previous, buried topography. Interbedded craters and valleys indicate the presence of buried surfaces, including erosional surfaces, representing unconformities in the rock record. Four basic rock units are identified in western Sinus Meridiani; they represent a stratigraphic section of > 800 m thickness. Near (but not quite at) the top of this stratigraphic section lies the ~7 m of section explored by the MER-B team in Eagle, Fram, and Endurance craters. The occurrence of similar rocks in the plains cut by the Valles Marineris (considered to be Hesperian in age) and Mawrth Vallis (considered to be Noachian) suggests that conditions for deposition, lithification and diagenesis of sedimentary materials in the presence of water or groundwater might have persisted on Mars beyond the end of the period of heavy impact cratering (i.e., beyond the Noachian).

Introduction

The Mars Exploration Rover (MER-B), Opportunity, landed on 25 January 2004 (~05:05 UTC) near 2.0°S , 5.6°W (areographic latitude, west-positive longitude). Opportunity's Meridiani Planum landing site is located in the classical low albedo region, Sinus Meridiani ([Golombek et al. 2003](#)). The first navigation camera images received during Opportunity's first sol showed that the spacecraft landed near an outcrop of light-toned, layered rock ([Squyres et al. 2004](#)). Further analysis demonstrated that the rover was in a small impact crater and that the rocks are sedimentary ([Squyres et al. 2004](#)).

During the first Earth year of MER-B operations, the rover team explored ~7 m of stratigraphic section exposed in the walls of the craters Eagle, Fram, and Endurance ([Grotzinger et al. 2004](#)). Compared to sedimentary rock exposures located elsewhere in the Sinus Meridiani region, the outcrops explored by the rover are quite small—so small that they are not well distinguished in some of the highest spatial resolution Mars Global Surveyor (MGS) Mars Orbiter Camera (MOC) images ever acquired (Figure 1).

The light-toned, layered rocks of Meridiani Planum were anticipated prior to the MER-B landing, but their exact nature and genesis were unknown. The context in which

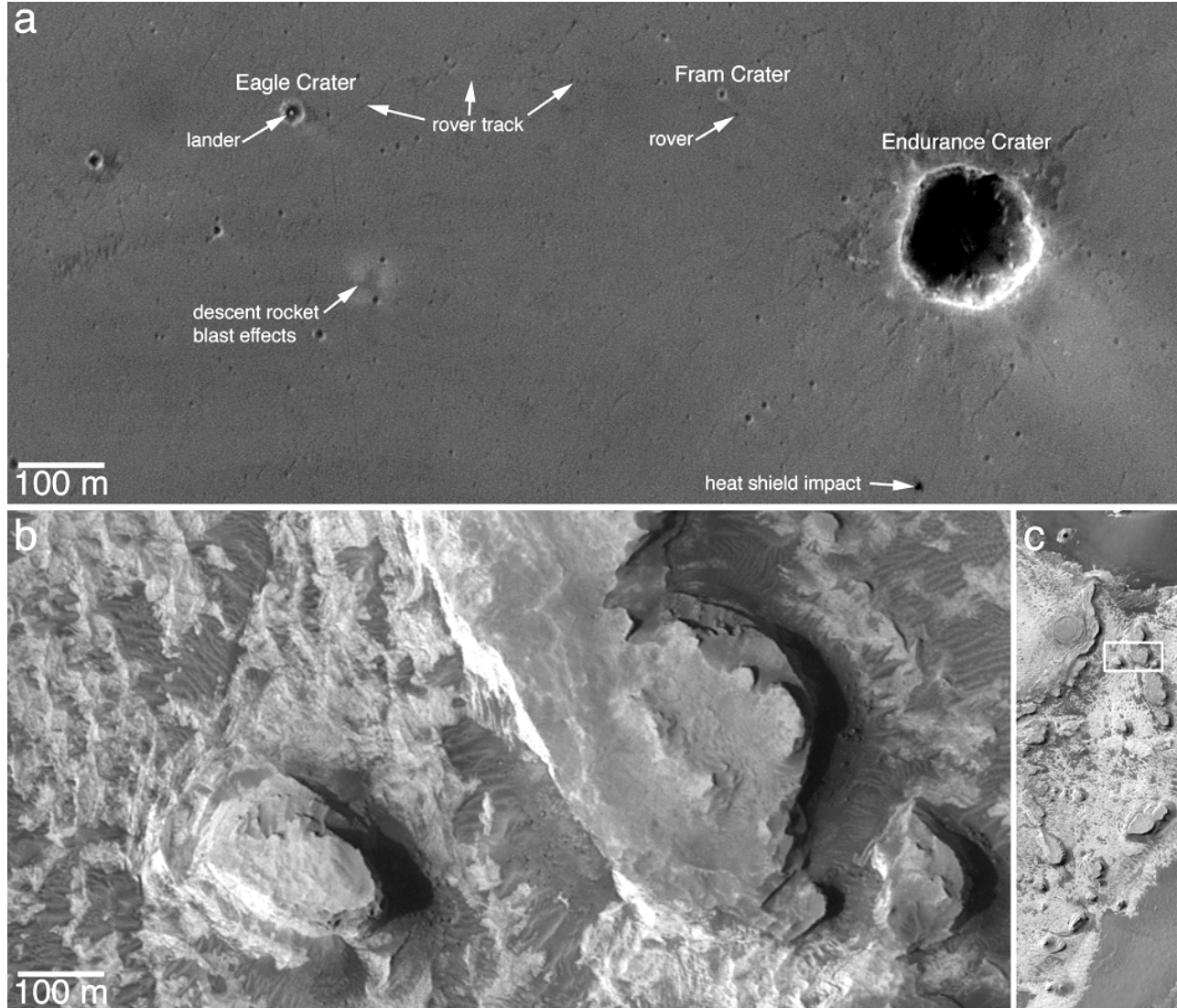


Figure 1. (a) The Mars Exploration Rover (MER-B) Opportunity site explored in 2004 (north is up; sunlight is from the left). The spatial resolution of this MGS MOC image is sufficient to see the rover, but the sedimentary rock outcrops known to occur in Eagle, Fram, and Endurance craters are too small to be seen. The image was acquired with a downtrack spatial resolution of ~0.5 m/pixel; crosstrack of ~1.5 m/pixel. This is a sub-frame of R16-02188 ([figure01a.png](#)). (b) An image of light-toned, layered rock outcrops, including buttes and mesas, in northern Sinus Meridiani, acquired and presented at the same scale as the image of the MER-B site. While the sedimentary rock outcrops at the MER-B site are small, other areas in Sinus Meridiani exhibit extensive outcrops. This is a sub-frame of MOC image S05-00383, located near 2.3°N , 353.6°W ([figure01b.png](#)). (c) The white box shows the location of the image in (b) among other light-toned rock outcrops, mesas, buttes, and spires. This is a sub-frame of MOC image E20-00994; it covers an area 3 km wide ([figure01c.png](#)).

these rocks occur was explored and discussed through the products of research conducted with data from the Viking 1, Viking 2, Phobos 2, MGS, and Mars Odyssey orbiters (e.g., Edgett and Parker 1997; [Christensen et al. 2000](#); [Edgett and Malin 2002](#); [Hynek et al. 2002](#); [Arvidson et al. 2003](#); [Newsom et al. 2003](#); [Ormö et al. 2004](#); [Christensen and Ruff 2004](#); [Hynek 2004](#)).

However, several key observations relevant to placing the rocks at the MER-B site into context were not described in detail until now. Just as early geologic reconnaissance of the sedimentary rocks of the Colorado Plateau (e.g., Darton 1910; Baker 1936) provided a framework for the details that would emerge from later field studies of the region, the purpose of this paper is to present a framework for the geology of the Sinus Meridiani region. This framework is summarized through the following five key observations:

- 1) The rocks outcropping in the Sinus Meridiani region are more diverse than the suite of materials explored at the MER-B site.
- 2) Impact craters—of a range of diameters (from tens of meters to tens of kilometers)—and former valleys are interbedded with the layered bedrock of the Sinus Meridiani region.
- 3) The ~7 m of section observed by MER-B covers < 1% of the stratigraphic section exposed in the Sinus Meridiani region. The rocks at the MER-B site are near, but not at the top, of the region's stratigraphic section.
- 4) The bedrock of the cratered terrain adjacent to Meridiani Planum is layered, possibly light-toned, and contains interbedded, filled, buried, and exhumed impact craters.
- 5) Light-toned, layered, plains-forming sedimentary rocks are not unique to Meridiani Planum; similar rocks are cut by Mawrth Vallis and form the plains cut by the Valles Marineris.

Spacecraft data and methods

Data

This research is focused on 0.5–20 m/pixel images acquired by the MGS MOC and Mars Odyssey Thermal Emission Imaging System (THEMIS) visible (VIS) subsystem. Additional details were observed in THEMIS infrared (IR) ~100 m/pixel images and data from the Mariner 9, Viking 1, Viking 2, and Phobos 2 orbiters. These were supplemented with examination of images of Endurance Crater acquired by the MER-B cameras in May 2004.

The MOC images were obtained September 1997 through September 2005. Data acquired through March 2005 are available from the NASA Planetary Data System (PDS); the subsequent MOC images are scheduled for release to the PDS in April 2006. MOC images not yet archived that were used in the figures are in the accompanying directory of supporting data. The MOC investigation was described by Malin et al. (1992) and [Malin and Edgett \(2001\)](#). Data from

THEMIS ([Christensen et al. 2004](#)) are available from the PDS and cover images obtained through December 2004. The relevant MER-B data are also from the NASA PDS; the Pancam and navigation cameras were described by [Bell et al. \(2003\)](#) and [Maki et al. \(2003\)](#).

In addition to images, MGS Mars Orbiter Laser Altimeter (MOLA) data (altimetry profiles expressed as elevations relative to the martian datum) obtained 1999–2001 and archived with the PDS were used to determine elevations and the stratigraphic placement of layered rocks. The MOLA investigation, including its data products and uncertainties, were described by Zuber et al. (1992) and [Smith et al. \(2001\)](#).

Methods

This paper presents results of a photogeologic study. As with work done using aerial photographs and topographic maps for field studies on Earth, this effort emphasizes the geomorphic details and stratigraphic relations that can be determined by examining landforms presented in images. The multispectral and thermophysical capabilities of THEMIS were not used to reach the conclusions drawn here.

Research regarding Observation 3 included construction of a rudimentary geologic map. Traditional planetary geologic mapping, which dates back four decades and builds on the concepts of Shoemaker and Hackman (1962), is focused on definition of materials units that might or might not, in reality, reflect the nature of a true bedrock unit (Wilhelms 1972; Wilhelms 1990). Unlike the case for the majority of planetary geologic maps, the rock outcrops of Sinus Meridiani offer opportunities to produce maps that portray observable, mappable layers of rock. Indeed, part of the region examined here was noted by Wilhelms (1990) in his 12th figure as having this potential.

Production of true geologic maps from Mars orbiter images is fraught with the same suite of challenges that face the terrestrial geologist working with aerial photographs. The field geologist uses the aerial photographs to understand the general character of an area, identify good exposures and clear relationships, and help pinpoint locations where the contact relations between rock units are unclear or unresolved. These, then, become key sites to be visited in the field. For Mars, the field site cannot be visited and the mapping effort is frustrated by difficulties in recognizing and tracing contacts (where they are obscured), decisions regarding whether to lump or split different materials, and understanding where it is appropriate to use relative albedo as one of the indicators of a mappable rock unit (rock albedo can be affected by surface roughness or obscured by mantles of sand or dust).

Conventions

Latitude and longitude. In keeping with the pre-MGS tradition for Mars exploration and mapping, which dates back more than a century, throughout this paper the coordinate locations of features on the planet are described in terms of areographic latitude and west-positive longitude.

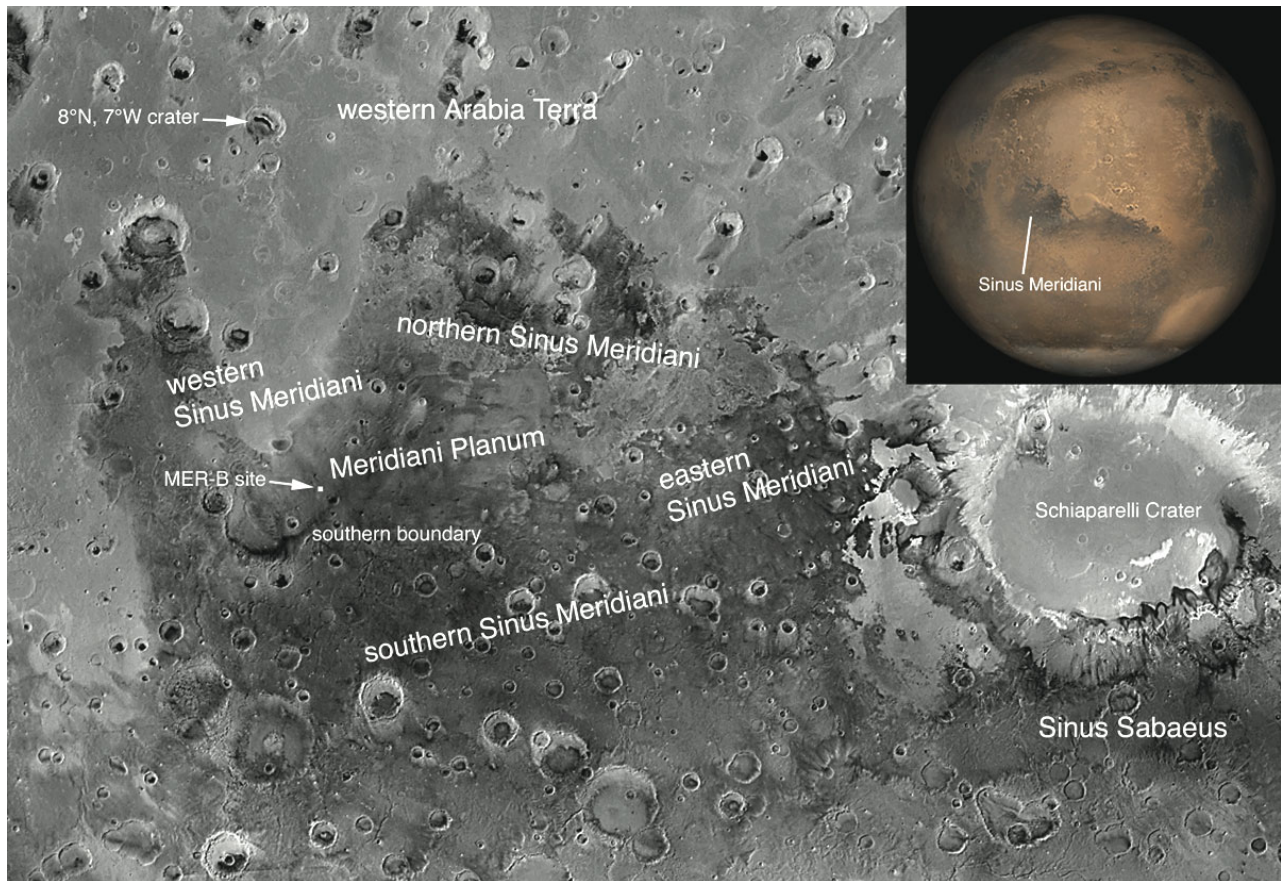


Figure 2. The Sinus Meridiani region of Mars. The inset shows a composite of MGS MOC daily global images, acquired 5–7 June 2001, and indicates the location of the classical low albedo feature, Sinus Meridiani ([figure02inset.png](#)). The grayscale map is a mosaic of MGS MOC red wide angle images acquired in May 1999 during the MOC Geodesy Campaign described by [Caplinger and Malin \(2001\)](#). The map shows the location of places and sub-regions described in this paper. The location of the Mars Exploration Rover (MER-B), Opportunity, site on Meridiani Planum is indicated. The map is a simple cylindrical projection, spanning across the equator and prime meridian from about 11.3°N to 13.0°S and 14.3°W right to 339.0°W ([figure02.png](#)).

MER-B site. Throughout the paper, only the information that was published about the MER-B site from investigations conducted in 2004 is discussed. In late 2004, the rover was driven out of Endurance Crater and began a journey southward, out of the area shown in Figure 1a.

Age of materials. In recent years, it has become clearer that Mars is a world on which burial, exhumation, and destruction of impact craters presents challenges to the utility of impact craters as indicators of relative or absolute age ([Malin and Edgett 2001](#)). Formation of secondary craters might complicate the record for smaller martian craters ([McEwen et al. 2005](#)), and the resistance of a rock unit to erosion translates into the capability of the material to retain small impact craters. For discussion purposes, however, it is useful to put the rock units studied here into a known context. The framework established following the Mariner 9 mission divides martian time into three periods, the Noachian, Hesperian, and Amazonian (Scott and Carr 1978). In this paper, the only distinction of relevance is the time that the Noachian ended and the Hesperian began. Thus, the term, Noachian, is used here to refer to the earliest part of martian history, with no implication as to absolute age, but

with the assumption that the Noachian period began with planetary accretion and ended when the rate of large impact crater formation (sometimes referred to as “heavy bombardment”) tapered off to near-modern values. The Hesperian is here considered to be the period that immediately followed the end of the time of heavy cratering, and this work assumes that the mare-type ridged plains of Lunae and Hesperia date to that period (Scott and Carr 1978). Tanaka (1986) and Hartmann and Neukum (2001) provide further discussion of the definitions of the martian time periods and their interpretations regarding absolute ages; [Hartmann \(2005\)](#) recently reviewed these topics and the issues of burial, exhumation, secondary cratering, and crater retention.

Nomenclature. Where they exist, the formal names of features—approved by the International Astronomical Union (IAU)—are used. Sinus Meridiani is the IAU-approved name for the low albedo feature that encompasses the region investigated. For ~30 years, Sinus Meridiani was named Terra Meridiani. That name was disallowed by the IAU in 2003, and a smaller portion of Sinus Meridiani, characterized by a relatively flat, lightly cratered plain, was given the name

Meridiani Planum. The names of craters investigated by the MER-B rover team are not IAU-approved, but they are used here to provide commonality with papers that discuss MER-B results. In addition to these conventions, directional names are used for sub-regions that have no name (e.g., northern Sinus Meridiani, eastern Sinus Meridiani). Rock units are not named but are given designations for discussion purposes. To formally name a rock unit, detailed field investigation and establishment of a type section, plus clear distinction of the top and bottom of the unit, must be described (North American Commission on Stratigraphic Nomenclature 1983).

Setting and previous studies

Sinus Meridiani was known for nearly four centuries from telescopic observations (Figure 2; Antoniadi 1930). The name, Meridiani, comes from use of the region to establish the martian prime meridian in the 1830s by Wilhelm W. Beer and Johann H. von Mädler. Southern and eastern Sinus Meridiani are distinct from central and northern Sinus Meridiani, as they have relatively heavily cratered surfaces that are grossly similar to the other heavily cratered regions of Mars (Figure 2). Northern Sinus Meridiani is distinct for its occurrence of light-toned, layered rock outcrops (Malin and Edgett 2000; [Christensen et al. 2003](#); [Hynek 2004](#)), while central Sinus Meridiani (Meridiani Planum) is distinguished by its relative lack of craters, generally flat character, and association with hematite detected by the MGS Thermal Emission Spectrometer (TES; [Christensen et al. 2000](#); [Christensen et al. 2001](#)).

Mariners 6 and 7 acquired the earliest spacecraft views of Sinus Meridiani. Near-encounter images 6N11, 6N13, 7N5, and 7N7 included the light-toned outcrop areas but had insufficient spatial resolution for their nature to be discerned. Mariner 9 and Viking orbiter images provided additional details of the region's geomorphology. In this context, the light-toned outcrops of northern Sinus Meridiani were described as "etched" terrain, perhaps eroded by wind (Presley 1986; Scott and Tanaka 1986; Greeley and Guest 1987; [Murchie et al. 1993](#)). The plains of central Sinus Meridiani were described as "smooth" terrain (Edgett and Parker 1997; [Christensen et al. 2000](#)) and were considered to be the upper surface of the same sequence of layered materials as the light-toned, etched terrain ([Schultz and Lutz 1988](#); Edgett and Parker 1997). Zimbelman and Craddock (1991) described the light-toned surfaces as "an eroded layer of competent material" in their assessment of possible occurrences of bedrock outcrops in the region.

The nature of the light-toned materials—that they are outcrops of layered rock—was not fully appreciated prior to the acquisition of high spatial-resolution MOC images (Malin and Edgett 2000). The materials were interpreted to be rock, and to have the physical properties of sedimentary rocks, on the basis of geomorphic observations (layering, cliffs, buttes, boulders, impact crater morphology) conducted using Viking and MOC images as well as infrared thermophysical observations from the Viking Infrared

Thermal Mappers (IRTM), Phobos 2 Termoscan, and Mars Odyssey THEMIS (Malin and Edgett 2000; [Edgett and Malin 2002](#); [Christensen et al. 2003](#)). The outcrops in northern Sinus Meridiani cover an area greater than that of North America's Colorado Plateau, famous for its diverse, layered, sedimentary rocks.

Working with data from MGS and Mars Odyssey, some investigators interpreted the light-toned, layered outcrops as the products of explosive volcanism (pyroclastic flows, airfall tephra, or wind re-worked tephra) ([Chapman and Tanaka 2002](#); [Hynek et al. 2002](#); [Arvidson et al. 2003](#)). However, the Sinus Meridiani region lacks obvious, unequivocal lava flows, and it lacks the faults, fissures, and vents typically associated with volcanism. Thus, other investigators favored non-volcanic forms of subaqueous or subaerial sedimentation (Malin and Edgett 2000; [Edgett and Malin 2002](#); [Christensen and Ruff 2004](#)). In addition, a few researchers considered that the rocks might have been subjected to diagenesis in the presence of groundwater ([Christensen et al. 2003](#); [Örmo et al. 2004](#)), an interpretation later found consistent with MER-B results (e.g., [Squyres et al. 2004](#); [Herkenhoff et al. 2004](#); [McLennan et al. 2005](#)).

Much recent work has focused on the mechanisms by which the hematite, detected by MGS TES, might have formed ([Christensen et al. 2000](#); [Christensen et al. 2001](#); [Allen et al. 2001](#); [Hynek et al. 2002](#); [Lane et al. 2002](#); [Arvidson et al. 2003](#); [Catling and Moore 2003](#); [Christensen and Ruff 2004](#); [Chan et al. 2004](#); [Chan et al. 2005](#)). Others focused on terrestrial analogs to the environments in which the rocks at the MER-B site might have been subjected (e.g., [Varekamp 2004](#)), or whether organic molecules could have been preserved in the rocks ([Sumner 2004](#)). MER-B results showed that the hematite occurs largely in spherical concretions of very coarse sand and granule size that are in—and have weathered out of—light-toned, layered, sedimentary rock ([Squyres et al. 2004](#); [Christensen et al. 2004](#); [Klingelhöfer et al. 2004](#)).

The main results from MER-B during 2004 centered on the observation that the light-toned rocks at the landing site are largely cross-bedded siliciclastic sandstones altered by diagenesis in the presence of sulfur-rich, acidic groundwater ([Squyres et al. 2004](#); [Klingelhöfer et al. 2004](#); [Rieder et al. 2004](#); Grotzinger et al. 2004; [McLennan et al. 2005](#)). In addition to MER-B's activities, near-infrared hyperspectral images from the Mars Express Observatoire pour la Minéralogie, l'Eau, les Glaces, et l'Activité (OMEGA) were acquired in 2004 for a portion of the Sinus Meridiani region; these data were interpreted to indicate the presence of adsorbed molecular water and sulfate minerals, with differences in the occurrence of these in different layered units in northern Sinus Meridiani ([Arvidson et al. 2005](#)).

Observation 1: Diversity of rocks

MOC and THEMIS images show that there is a diversity of rock types or rock physical properties in the Sinus Meridiani region. The key observation is that the rocks are more

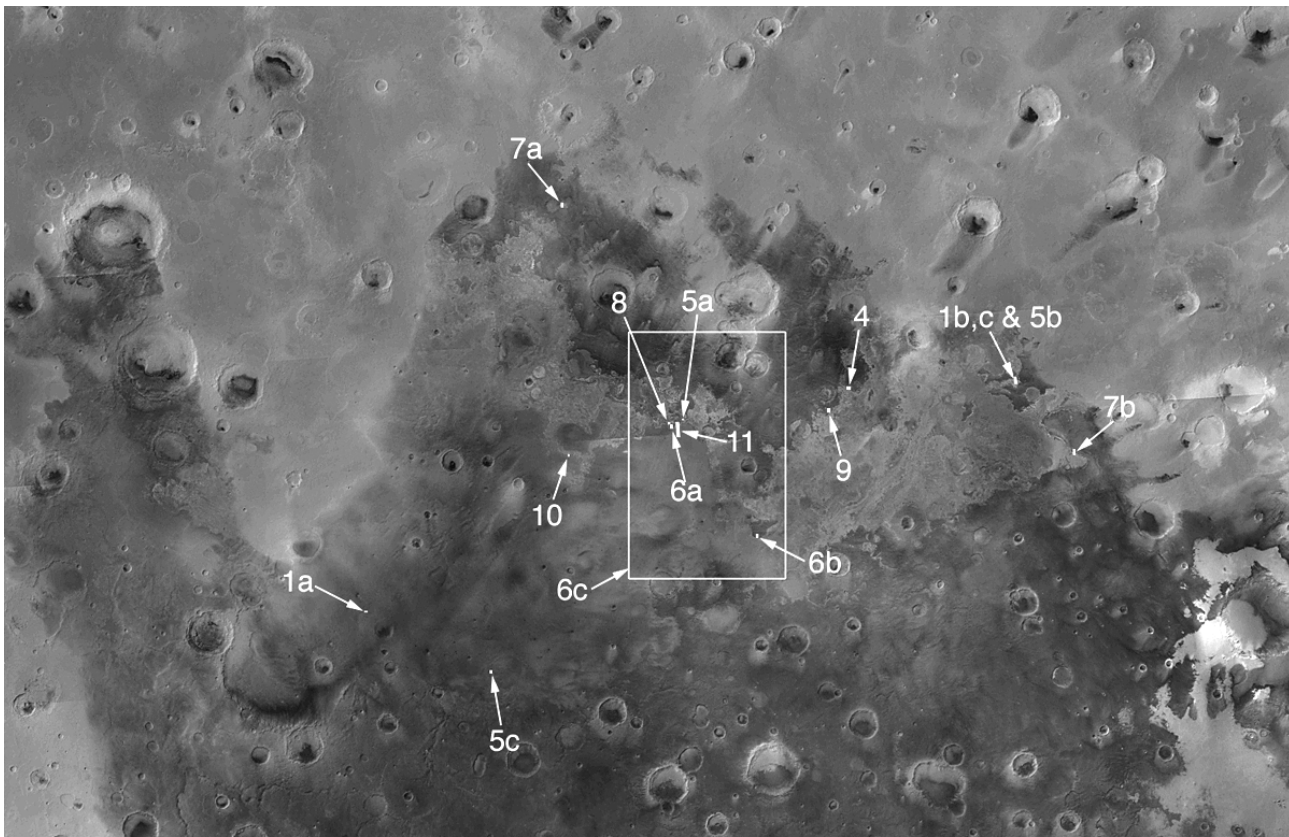


Figure 3. Map of the Sinus Meridiani region, showing the location of MOC and THEMIS images in Figures 1 and 4–11. The map is a mosaic of MOC red wide angle images acquired in May 1999, during the MOC Geodesy Campaign described by [Caplinger and Malin \(2001\)](#) ([figure03.png](#)).

diverse than those explored in Eagle, Fram, and Endurance craters at the MER-B site. While the rocks exhibit diversity, the diversity is not vast. For example, none of the orbiter images provide information to permit a unique determination of the presence of igneous rocks, and, given all that is known about the tectonic history of Mars, the likelihood of metamorphic rocks (except contact metamorphic) is slim. Thus, the diversity of materials appears to lie within the realm of sedimentary rocks or clastic igneous rocks that have the gross physical attributes of sedimentary rock. The observed diversity likely includes differences in hardness as a function of the degree of induration and weathering of the materials. Figure 3 shows the location of orbiter images described in this section.

Case for sedimentary rock

The light-toned, layered outcrops of northern Sinus Meridiani are interpreted to be rock because the material is indurated well enough to hold near-vertical cliffs (Figure 4). Some of the materials have been eroded to form mesas, buttes, and spires (Figures 1b, 4), and some produce boulders when subjected to impact cratering and scarp retreat (Figure 5). Discussion of thermophysical observations made by the Phobos 2 Termoskan and Mars Odyssey THEMIS also favored interpretation that the materials are rock ([Edgett and Malin 2002](#); [Christensen et al. 2003](#)). Indeed, the rock abundance map of Christensen (1986) showed the Sinus

Meridiani outcrops to have the highest abundances on the planet at the scale he examined (> 25%).

The rocks do not exhibit the morphologic characteristics of lava flows or pyroclastic flows (e.g., lobate fronts, break-out lobes, pressure ridges, leveed channels or collapsed tubes), and no volcanic landforms are uniquely identified in Sinus Meridiani and neighboring regions (although some were previously speculated to occur in the region by Scott and Tanaka 1986, [Chapman and Tanaka 2002](#), [Hynek et al. 2002](#), and [Arvidson et al. 2003](#)). The rocks of Sinus Meridiani occur many thousands of kilometers from unambiguous, inarguable volcanic landforms, such as the Tharsis volcanoes and flows, Syria Planum shields, and Syrtis Major calderae; and any tephra that could have been produced by these sources would have been smaller than fine silt and expressed as airfall deposits if they found their way to the Sinus Meridiani region. Extensional landforms, such as horst and graben (from which fissure eruptions of flows or tephra might have come), do not occur in Sinus Meridiani. Finally, the fact that the sandy regolith at the MER-B site has been interpreted to be basaltic ([Soderblom et al. 2004](#); [Christensen et al. 2004](#)) is not evidence that volcanism occurred in the region—the term is prematurely applied because it requires knowledge that there was an extrusive genesis, yet there is insufficient spatial resolution in the MER-B microscopic imager data to be certain that the < 150 μm -sized grains have the microcrystalline texture that

volcanism would produce, and the sand source and distance from the source are unknown ([Christensen et al. 2004](#)).

Some of the layered rocks in northern Sinus Meridiani are quite laterally extensive. The elevation information presented in Figure 6 shows examples of two rock units repeated in sequence at two locations more than 150 km apart. Figure 6 also shows that these rock units lie nearly horizontal, sloping $< 0.02^\circ$, over the distance between them. The plains on which the MER-B rover has been operating are also relatively flat ([Arvidson et al. 2004](#)), attesting to the near-horizontality of the bedrock.

The combined properties of lateral extent, horizontality, and bedding (especially in cases of repeated bedding of units of similar thickness and erosional expression), all contribute to the interpretation that the light-toned, layered materials of Sinus Meridiani are sedimentary rocks, as has been confirmed by MER-B investigators for the rocks exposed at that site ([Squyres et al. 2004](#)).

Case for diversity

The erosional expression of rock outcrops provides clues regarding the diversity of rock types and properties at a given location. For example, on Earth, shales are slope-formers because of their relatively low resistance to erosion, while more competent rock resists erosion and can form benches, shelves, and vertical cliffs. Resistant cap rocks protect underlying, less-resistant rock to form cliffs, mesas, and buttes. The very presence of buttes and mesas (Figure 4) requires there to be two or more rock types, or at least an erosion-resistant lag—with rock less resistant to erosion

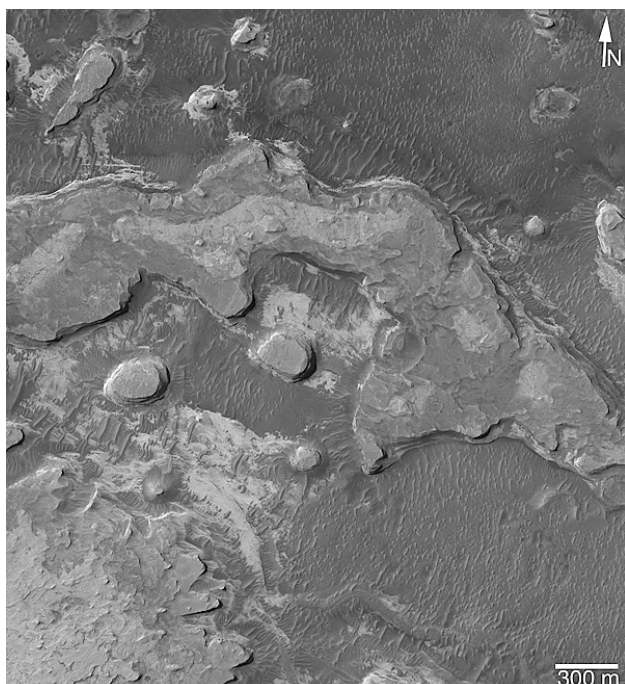


Figure 4. The sedimentary rocks of Sinus Meridiani include cliff-, mesa-, and butte-forming materials. This is a sub-frame of MOC image R20-01497, located near 2.2°N, 356.7°W ([figure04.png](#)).

underlying the more resistant material (Stokes 1969).

Images that illustrate some of the diversity among the rocks of the region include Figure 5, which shows the production of boulders derived from resistant rock, and Figure 7, which exhibits some of the diversity of bedding styles in the region. Other indicators of rock diversity include the terracing of the walls of small impact craters in the 2 to 10 km diameter range, which indicates differences in the impact target properties with depth (Figure 5c), and differences in relative albedo (tone) between vertically adjacent rock units (Figures 4, 8). Differences in albedo can be functions of differences in composition or sub-resolution roughness (a product of weathering and erosion), both of which can be the result of differing rock type. Because the light-toned, layered rock outcrops of Sinus Meridiani exhibit a variety of erosional expressions, more than one rock type must be present and the rocks at the MER-B site must merely be a subset of the diversity found in the region.

Dark mesa- and small ridge-forming materials

In addition to light-toned, layered rock, Sinus Meridiani also exhibits a suite of intermediate- and dark-toned materials that lie unconformably above the light-toned rocks. Orbiter images show that eolian dunes are extremely rare (Edgett 1997), but images from MOC and MER-B show that megaripples are common; rover images also show smaller sand ripples and a generally sandy regolith ([Greeley and Thompson 2003](#); [Soderblom et al. 2004](#); [Sullivan et al. 2005](#); [Thomas et al. 2005](#)).

Two other materials occur above and in an unconformable relation to the light-toned, layered bedrock: dark mesa-forming material and small ridge-forming material. These are discussed here—in the context of diversity of rock types and properties—because one or both of them might be legitimate rock units rather than geologically recent regolith materials. If they are not rock, then they are materials that are at least indurated or crusted to some depth.

An example of the dark mesa-forming material is shown in Figure 9. The dark mesas are generally several meters high, have steep bounding scarps, and in some places are pitted and cratered. The ability to hold a bounding scarp and retain pits and impact craters is evidence that these materials are indurated. Similar dark mesa-forming materials are found in other sedimentary rock settings, such as Mawrth Vallis and the chasms of west Candor and Tithonium (Malin and Edgett 2000). In all cases, dark mesa-forming materials lie unconformably above previously eroded surfaces, usually light-toned layered rock outcrops. Their origin is not known.

Small ridge-forming materials consist of fields of dark and intermediate-toned, closely-spaced ridges and sharp-crested mounds like those in Figure 10. The small ridge-forming materials occur in a variety of locations in central and northern Sinus Meridiani. In some cases, the light-toned substrate beneath the small ridge-forming materials may be seen on the inter-ridge flats, suggesting that the material is not much thicker than the ridges are high. Figure 10 shows

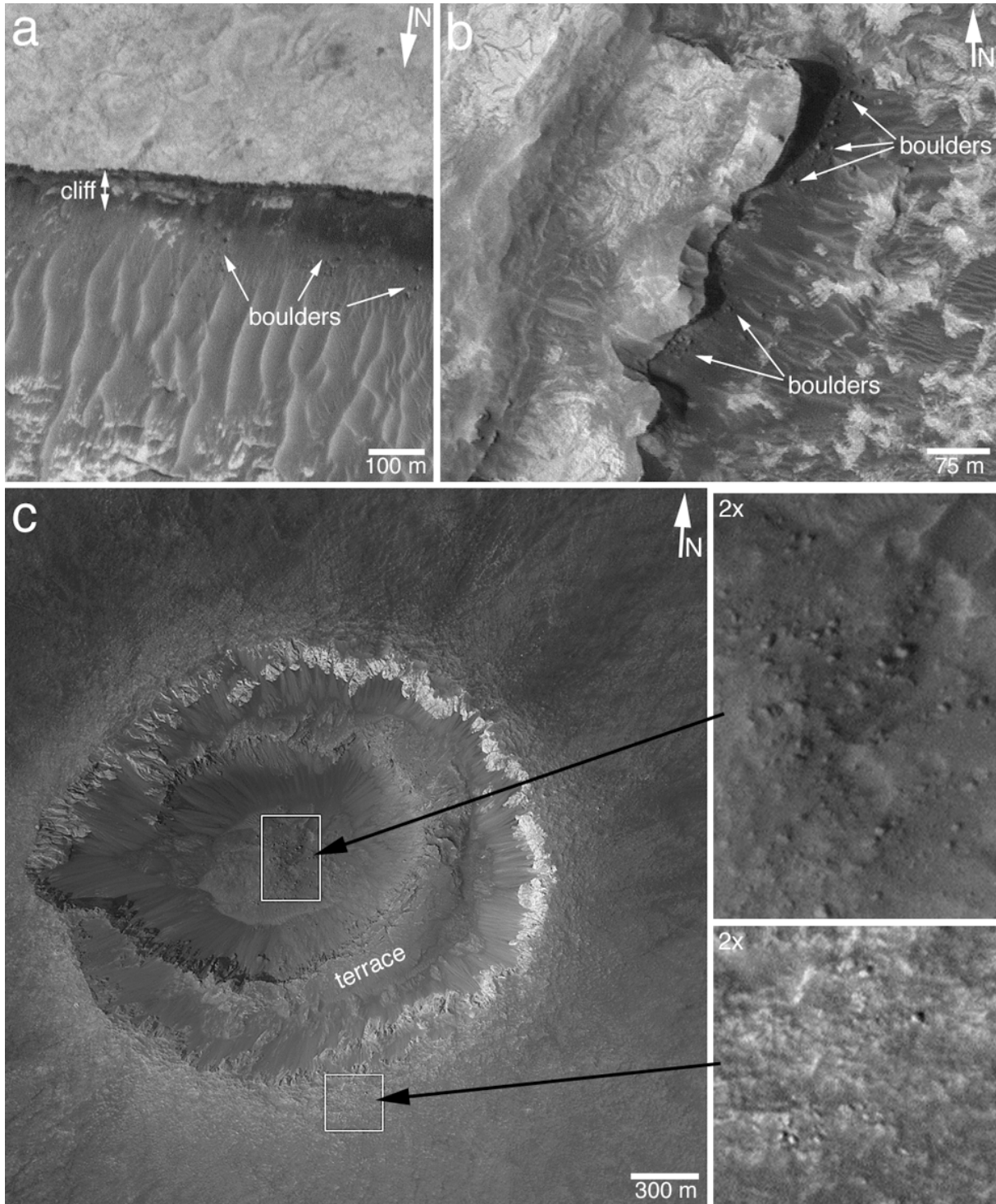


Figure 5. Examples of boulder production along steep slopes and among impact craters in the light-toned, layered sedimentary rocks of Sinus Meridiani. **(a)** Boulders at base of cliff in sub-frame of MOC image R07-00563 near 1.6°N , 359.8°W ([figure05a.png](#)). **(b)** Boulders at base of mesa slopes in sub-frame of MOC image S05-00383 near 2.3°N , 353.6°W ([figure05b.png](#)). **(c)** Impact crater in Meridiani Planum; areas in white boxes are shown at 2x scale and illustrate some of the boulders on the crater floor and rim; sub-frame of MOC R09-00731, located near 3.1°S , 3.3°W ([figure05c.png](#)).

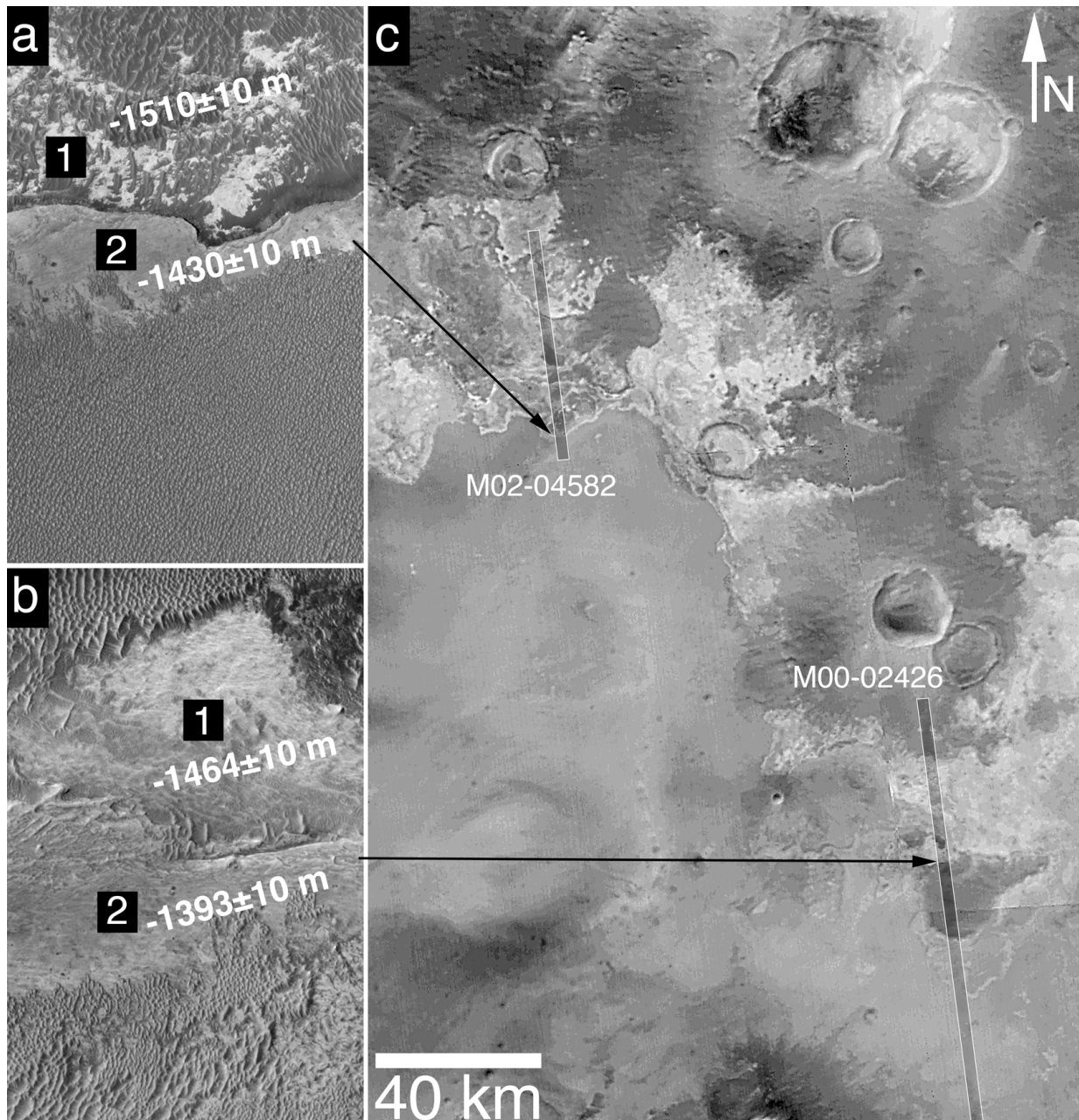


Figure 6. Some of the light-toned, layered rock units in Sinus Meridiani have great lateral extent. In this example, two MOC images (**a**) sub-frame of M02-04582 ([figure06a.png](#)), and (**b**) sub-frame of M00-02426 ([figure06b.png](#)) show two rock units (labeled 1, 2) of similar erosional expression and albedo that are separated by a distance of about 150 km. The rocks in this case are nearly horizontal, as indicated by the elevations (in white) of the rock exposures derived from MGS MOLA observations. The elevations were obtained by examination of individual MOLA laser shots from MGS orbits 458, 1137, 1376, 2030, and 8802. These elevations translate to a dip of $\sim 0.02^\circ$. (**c**) The basemap is a mosaic of sub-frames of MOC red wide angle camera images M01-01236, M01-01238, M01-01627, and M01-01629 ([figure06c.png](#)).

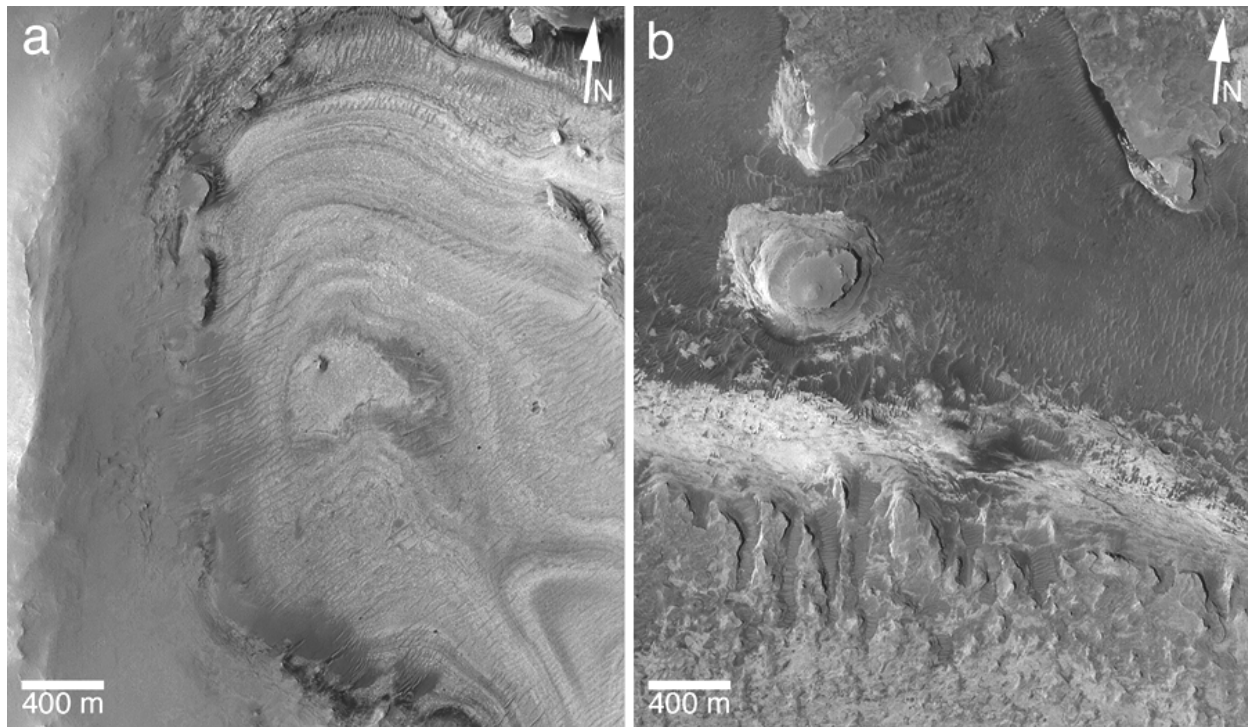


Figure 7. Examples of differing bedding styles and erosional expressions in Sinus Meridiani. Note that both images are presented at the same scale. **(a)** Dozens of layers of similar thickness forming bands on the floor of an elliptical crater in sub-frame of MOC image R16-01694 near 1.5°N, 2.0°W ([figure07a.png](#)). **(b)** Variety of light- and intermediate-toned layered rock outcrops in northeast Sinus Meridiani; bedding in these cases is more massive than in the previous example. This is a sub-frame of MOC image R15-02235, located near 1.0°N, 352.6°W ([figure07b.png](#)).

that the materials form distinct, sharp boundaries and hold steep slopes (e.g., in pits, craters, and depressions). These attributes suggest that the small ridge-forming material is indurated and somewhat resistant to erosion. The small ridge-forming materials always lie unconformably and stratigraphically above a surface eroded into older, light-toned, layered rock (e.g., Figure 11). The small ridges might be the eroded remains of old, crusted, or indurated eolian bedforms ([Malin and Edgett 2001](#)).

Observation 2: Interbedded craters and valleys

The erosional expression of bedrock outcrops in Sinus Meridiani suggests the presence of a diversity of rock types and properties. Some of this diversity is captured in differences between the materials deposited inside and outside of craters and valleys that are interbedded with the light-toned rock. The key observation described in this section is that the Sinus Meridiani rock record includes filled, buried, and exhumed valleys and impact craters. The interbedding of craters and valleys within the layered upper crust of Mars is a theme repeated all over the planet ([Malin and Edgett 2001](#); [Frey et al. 2002](#)), and some aspects of this story have long been recognized, including layering and crater exhumation (Malin 1976) and extremely old eroded and filled impact basins (e.g., Schultz et al. 1982). Indeed, the upper crust of Mars can be described as a layered, cratered, and “valley-ed” volume (Edgett and Malin 2004).

Figure 12 shows the location of images described in this section.

Interbedded and exhumed impact craters

In Sinus Meridiani, impact craters as small as a few tens of meters to tens of kilometers in diameter are interbedded with the light-toned, layered rocks. Some formerly buried craters have been exhumed ([Hynek et al. 2002](#); [Edgett and Malin 2002](#); [Arvidson et al. 2003](#)). Examples of exhumed and partially exhumed craters are shown in Figure 13. Impact craters occur at different levels within the exposed stratigraphy, suggesting that they, and the rocks into which they impacted, formed over an extended period of time ([Edgett and Malin 2002](#)). Exhumed impact craters—as well as those that were never buried—can also be destroyed by erosion.

Although it is impossible to show evidence of a crater that has been destroyed and removed from the rock record, examples of impact crater remnants, indicating the near-destruction of these landforms, occur throughout the region. Figure 14 shows an example of a crater interpreted to have been exhumed. It occurs with several examples of landforms that may result from the near destruction of smaller craters. The present rim of the larger, exhumed crater stands at about -1360 m elevation—about the same as that of the eroded bedrock it is thought to have once been encased within. Today, the crater interior remains mostly filled with eroded sedimentary rock with a bedding character (dozens of

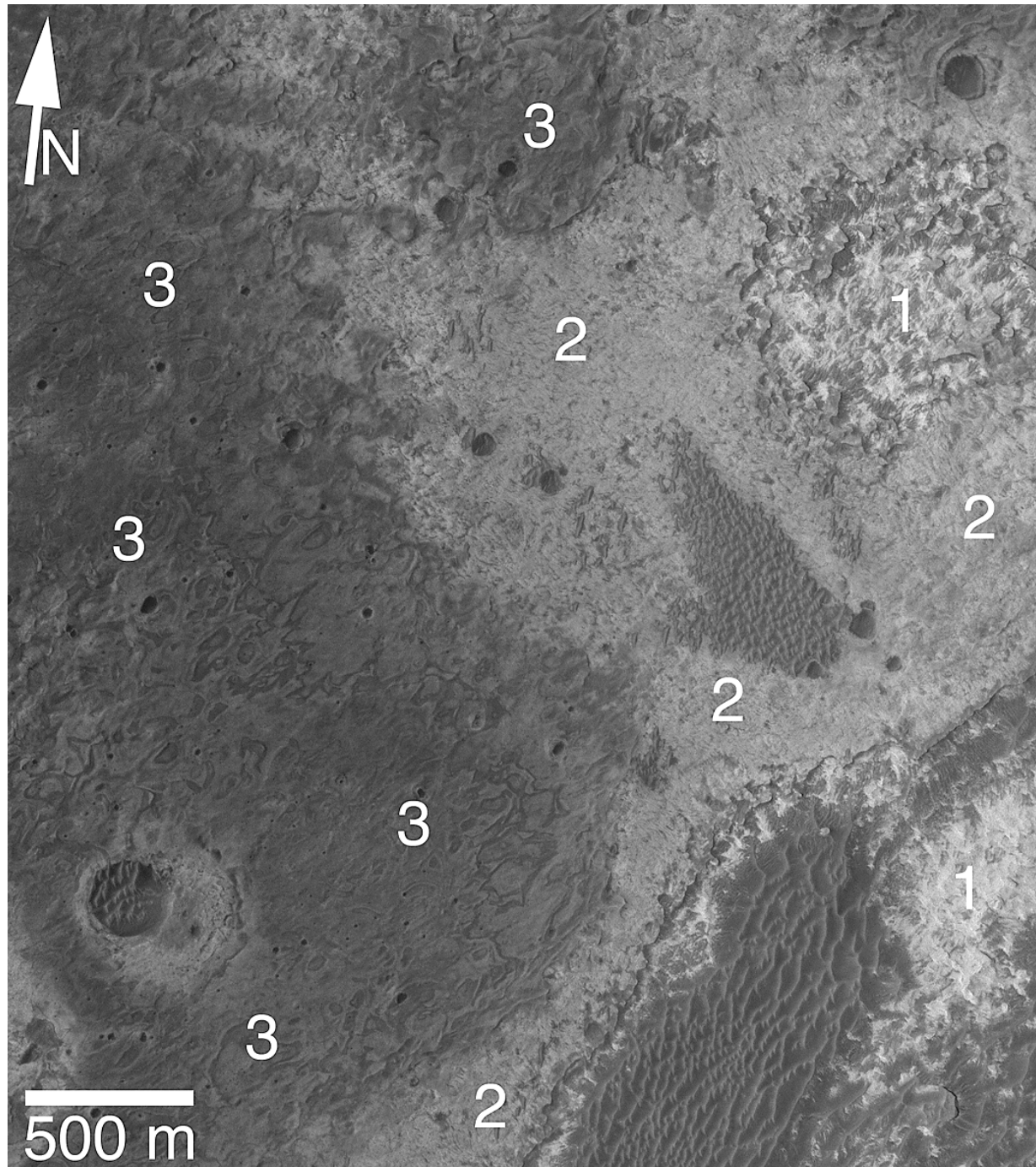


Figure 8. The relative albedo or tone of unmantled rock exposures in Sinus Meridiani also gives an indication of lithologic diversity. Three rock units are evident in this scene. The lowermost, or oldest, rocks (1) have the lightest tone. The stratigraphically highest, youngest rocks have the darkest tone (3). Even darker than unit (3) are windblown megaripples and other patches of dark mantling material. This is a sub-frame of MOC S05-00568, located near 1.5°N , 0°W ([figure08.png](#)).

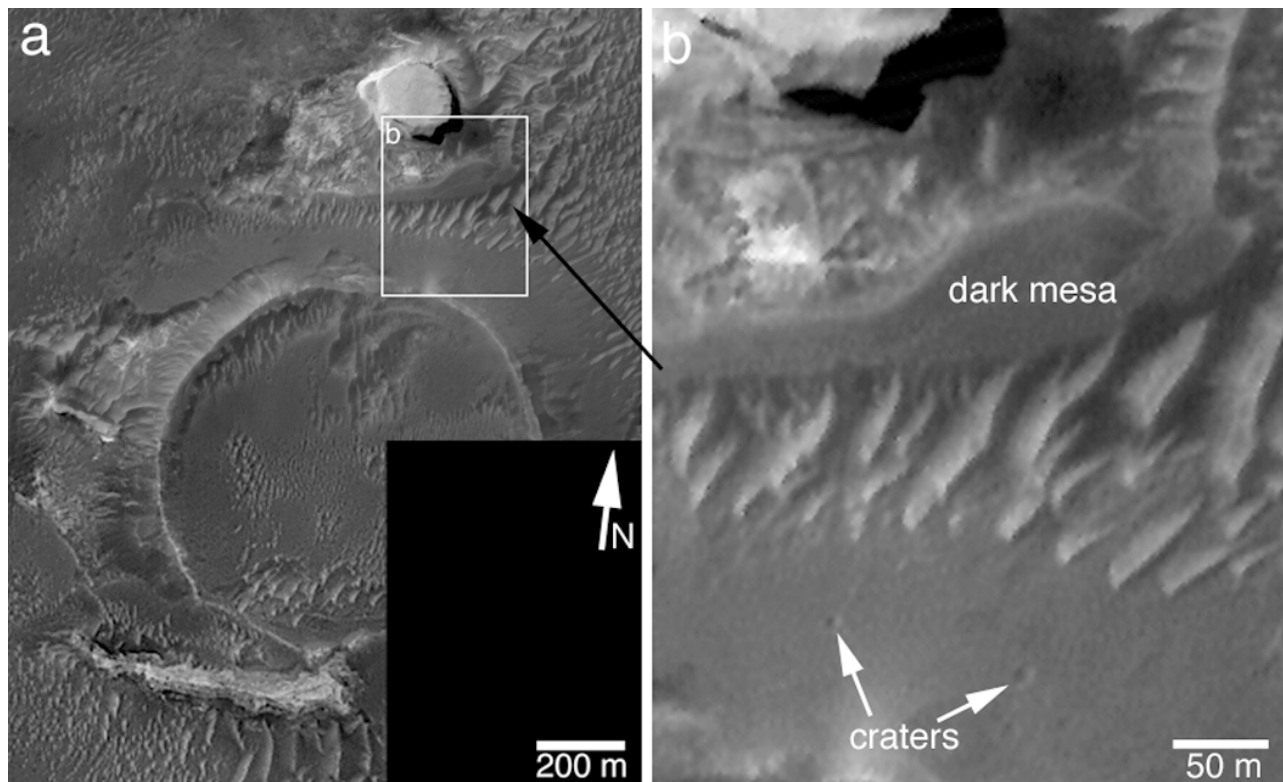


Figure 9. Examples of dark, mesa-forming material in Sinus Meridiani. (a) A crater being exhumed from beneath dark mesa-forming material. The white box shows the location of the close-up in the picture to the right. This is a mosaic of sub-frames of MOC images M10-02028 and FHA-00674, located near 1.7°N, 357.1°W ([figure09a.png](#)). (b) Close-up view of a dark mesa and two small craters formed in a neighboring dark material. The ability of dark mantling materials in Sinus Meridiani to hold cliffs and impact craters suggests that the material is indurated ([figure09b.png](#)).

repeated beds of similar thickness) unlike that of any of the rocks that represent the remains of those that once surrounded the crater. The near-destruction of smaller impact craters superimposed on the larger crater is evident in the form of smaller, circular patches that contain small ridge-forming material (Figure 14b).

Craters that have been exhumed from within the strata in Sinus Meridiani commonly have a suite of layered rock within them that is different from the rock occurring outside of the crater. Typically, the layers in a crater exhibit repeated beds of similar thickness and erosional expression (implying similar physical properties and composition), whereas the layers outside of a crater are more massively bedded and have a different erosional expression (e.g., Figure 15). Differences in layering and other physical properties between rocks inside and outside of a crater suggest that there were differences in depositional setting in these adjacent locations (for example, one might speculate that the contrast in depositional setting could be the product of subaqueous—in the crater—versus subaerial—outside the crater).

Interbedded, exhumed, and inverted valleys

Like impact craters, valleys and sinuous ridges interpreted to be the inverted remains of valleys are interbedded with the rocks of Sinus Meridiani. Although not widely reported, MOC and THEMIS images show that inverted valleys are

common on Mars and are usually found in association with eroded, layered rock. Examples include inverted channels of a fossil delta in the provisionally-named (by the IAU) Eberswalde Crater described by [Malin and Edgett \(2003\)](#), networks of fine ridges near western Juventae Chasma (Williams et al. 2005), abundant sinuous ridges in eastern Arabia Terra, and a fan of sinuous ridges in Aeolis (Williams and Edgett 2005). In Sinus Meridiani, [Newsom et al. \(2003\)](#) recognized a few examples of negative-relief valleys being exhumed from beneath or within a suite of northern Sinus Meridiani strata. Figure 16 shows examples of the negative-and positive-relief features interpreted to be the remains of valleys in the Sinus Meridiani region. Examples on Earth demonstrate that stream courses can become inverted if the floor or valley-filling material is more resistant to erosion than the rock that the stream originally cut (Miller 1937; Rhodes 1987; Maizels 1990).

Observation 3: Local Stratigraphic placement of MER-B rocks

On a planet such as Earth or Mars, it is possible in limited locations where rocks are well exposed to construct a rudimentary geologic map and stratigraphic section using high-resolution satellite images or aerial photographs. The sequences of layered rocks in Figures 6 and 8 demonstrate that the materials exposed in Sinus Meridiani are amenable

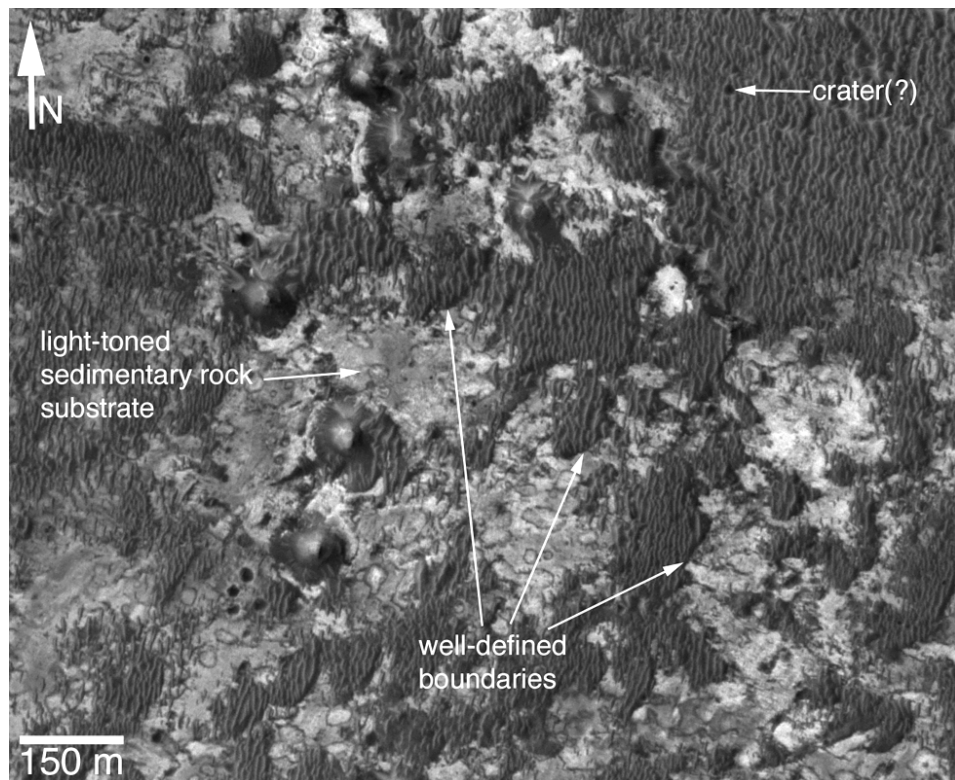


Figure 10. Examples of small ridge-forming material overlying a previously eroded light- and intermediate-toned substrate of sedimentary rock. The small ridge-forming materials may be indurated; their erosion produces sharp, well-defined boundaries and the material may retain small impact craters. Located near 1.0°N , 1.9°W , this is a sub-frame of MOC image R21-00090 ([figure10.png](#)).

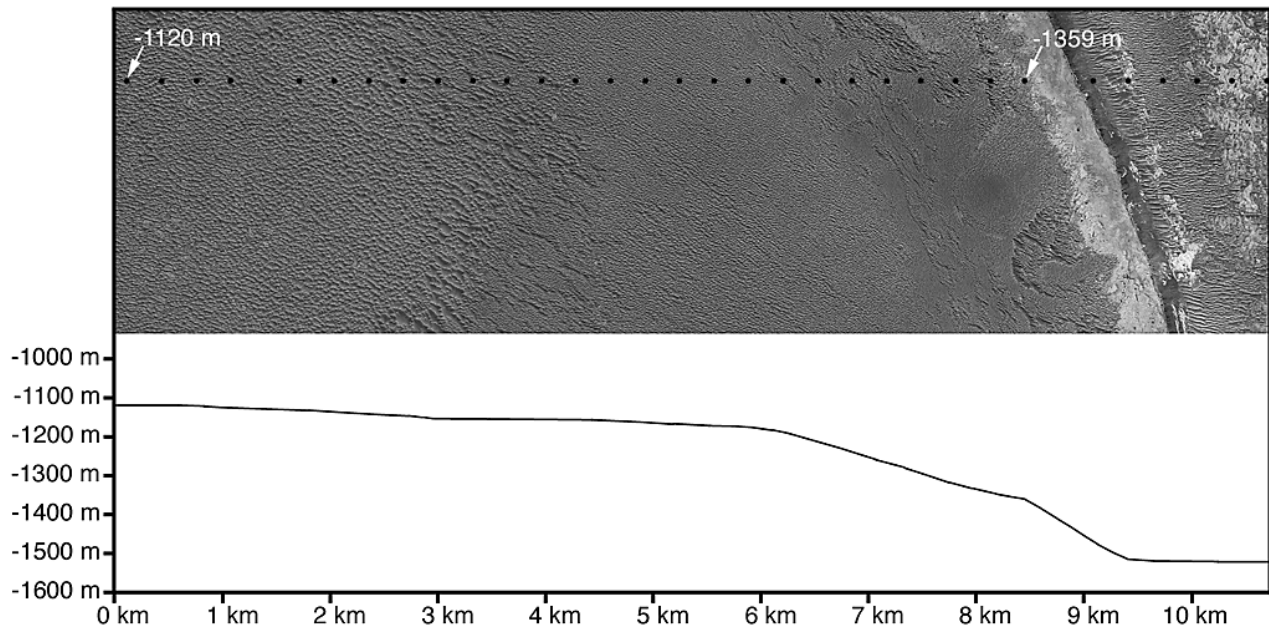


Figure 11. Small ridge-forming materials lie unconformably over a previously-eroded substrate of sedimentary rock. In this figure, topography changes ~ 200 m in ~ 9 km, although the small-ridge-forming material is of nearly uniform thickness (from trough floors to ridge crests, that is). The topographic profile is from MGS MOLA observations; the dark dots indicate the location of individual laser shots acquired on orbit 1703 at the same time the MOC image, M03-04970, was obtained. North is toward the lower right, sunlight illuminates the scene from the top ([figure11.png](#)).

to geologic mapping and stratigraphic interpretation.

The purpose of this section is to describe the stratigraphy of a portion of Sinus Meridiani at a regional scale. It should be understood that MOC images and the MER-B results show that the rocks of Sinus Meridiani exhibit tremendous complexity at finer scales than described in this section; the situation is akin to the presence of multiple lithologies within any given geologic formation on Earth. The goal, here, is to place the rocks explored by the MER-B team in 2004 into the larger context of the bedrock of western Sinus Meridiani.

The region studied and mapped is shown in Figure 17. The rudimentary geologic map of the region is in Figure 18. Figure 19 illustrates the location of the MOC and THEMIS images used throughout the section. The images, together with MOLA topography, show that the rocks of the MER-B site are part of a stratigraphic section that is > 800 m thick.

Stratigraphic overview

Four basic rock units, each acknowledged to likely contain many layers exhibiting a range of complexity and local variation, are recognized (Figure 18):

- 1) The rocks of the MER-B site are located within strata of the Meridiani Planum plains-forming unit (P). The rocks at the rover site are not at the top of this stratigraphy, but probably near the top (it is not possible to know exactly how much material has been removed from the surface into which Eagle, Fram, and Endurance craters formed).
- 2) Below the plains-forming unit (P) lies a distinct ridge-

forming unit (R). Exposures of this unit are pervasive across northern Sinus Meridiani.

- 3) Below the ridge-forming unit (R) lies a unit that is only clearly distinguished as a scarp-forming material (S) in northwestern Sinus Meridiani. Occurrences of this unit are usually mantled by intermediate- or dark-toned material; it is in this unit that many of the region's inverted and negative-relief valleys/channels occur.
- 4) Below the scarp-forming unit (S) lies other rock units, not well distinguished from orbit, that are exposed in terrain west of Sinus Meridiani and are generally mantled by intermediate-toned materials. However, windows into these lower materials show light-toned, layered rock. The lower unit is here designated (L).

The four-unit stratigraphy described by [Edgett and Malin \(2002\)](#) is similar to that presented in Figure 18, except that unit (R) in this case incorporates both unit R and unit B from that paper because it was difficult, upon further analysis, to be certain whether this is a single unit or two. In the case of all four units described here, there is considerable lumping of materials that have grossly similar erosional expression—at any given location (planimetric or vertical) there is likely to be a variety of thinner rock units present, as known, for example, from the ~7 m of strata examined at the MER-B site. In addition, little attempt has been made in this initial stratigraphic exercise to correlate rocks identified in Sinus Meridiani west of 1°W longitude with those that occur east of 1°W except for unit (R).

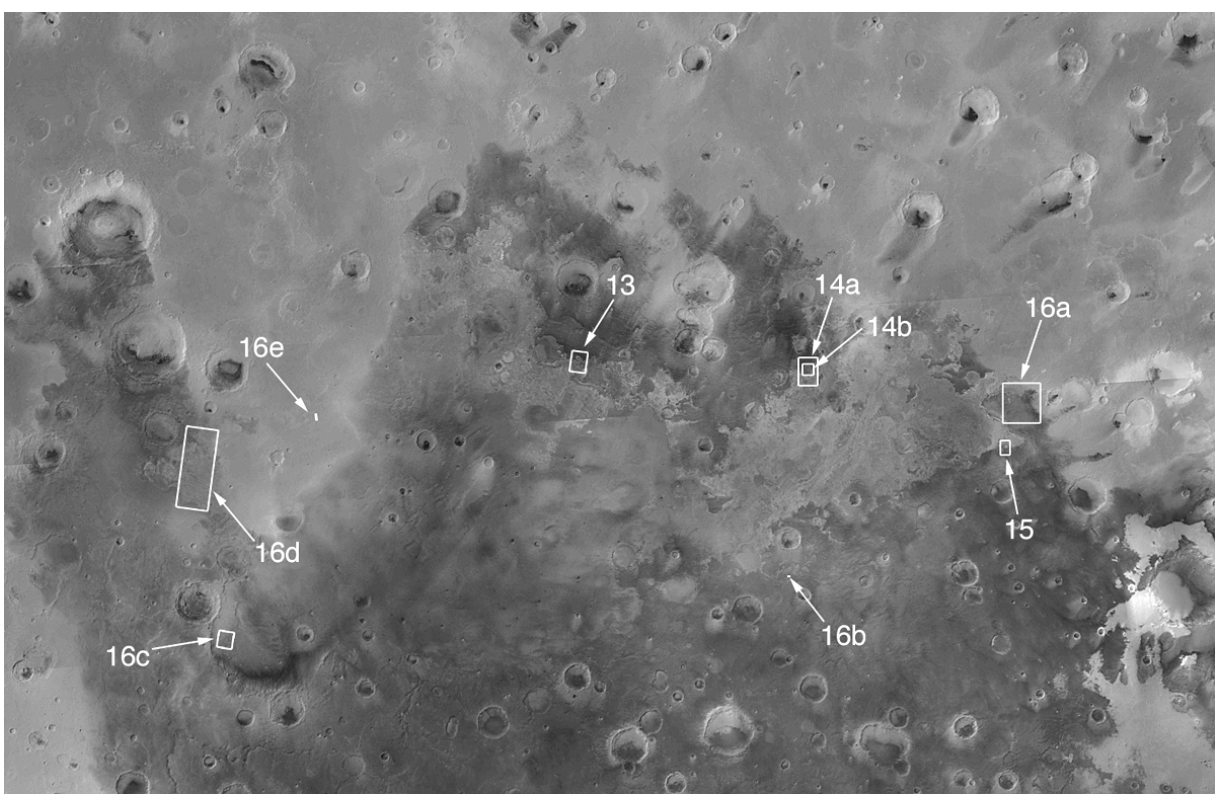


Figure 12. Map of Sinus Meridiani, showing the location of images in Figures 13–16 ([figure12.png](#)).

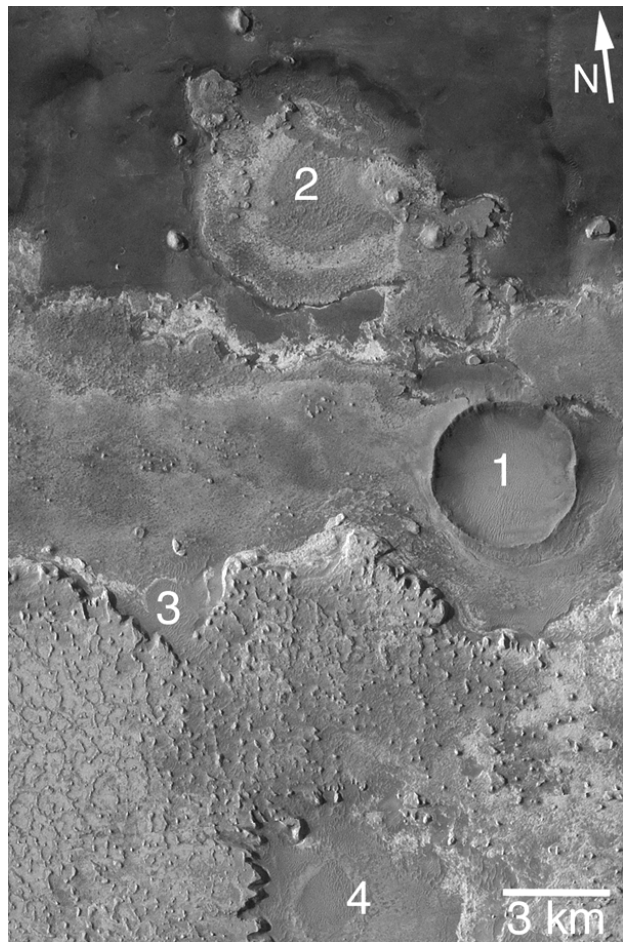


Figure 13. Examples of impact craters interbedded with the sedimentary rocks of Sinus Meridiani. The craters labeled 1–4 formed at different levels within the stratigraphy, and each exhibits a different state of preservation and exhumation. This is a sub-frame of THEMIS VIS image V02459003, located near 2.4°N, 1.1°W ([figure13.png](#)).

The plains-forming unit

The four rock units are described here in reverse-chronologic order, so as to begin with the unit (P) that contains the rocks at the MER-B site. The rocks of the plains-forming unit are light-toned and are not well exposed to view from above. The rocks are largely covered by a mantle of low-albedo fines. At the MER-B site, this mantle, generally considered to be an eolian lag, is typically no more than a meter or so thick and its surface displays abundant granules and sand, including spherules of hematite ([Soderblom et al. 2004](#)). Figures 1a and 20 show typical MOC views of western Meridiani Planum. Outcrops of light-toned sedimentary rock most commonly occur in crater walls and in small patches or windows eroded through the dark-toned lag and between ridges of small ridge-forming material. The erosional expression of the plains-forming rock creates a surface that is distinct from other terrain in the region; it appears at MOC and THEMIS VIS scale to be relatively flat, smooth, and only lightly cratered ([Christensen et al. 2000](#); [Christensen and Ruff 2004](#)).

Circular depressions, such as the one located just south of the center of Figure 20, are interpreted to be the expression of filled, nearly-buried impact craters ([Hartmann et al. 2001](#); [Lane et al. 2003](#)), although other depressions on the plains might be the remains of craters that formed in higher strata that were later eroded away. MOC images of craters near the MER-B site suggest that the plains-forming unit exhibits a progression of crater expressions, from those that are buried to those that are partially to fully exhumed (Figure 21). Endurance Crater, explored by MER-B, might have once been partially filled like the crater in Figure 21a. Victoria Crater (Figure 21b) illustrates the next stage in the exhumation of a crater in the plains-forming unit. The U-shaped alcoves eroded into rock around the crater's circumference indicate erosion by undermining and collapse as less-resistant crater-filling material and/or brecciated crater wall material was broken down and removed from the crater, perhaps by wind. The rock into which the U-shaped alcoves formed overlies the original (presently buried) Victoria Crater rim. Endurance Crater (Figure 21c, d) might be showing the next stage in the process. At Endurance, the raised crater rim is topographically expressed, as are some aspects of ejecta blanket, but none of the original rim nor ejecta are fully exhumed. For comparison, Figure 21e shows a fresh crater—one never buried—on Meridiani Planum.

The area outlined in black in Figure 21c, located on the southeast rim of Endurance Crater, was visited by MER-B and found to have a surface of eroded, broken plates of sedimentary rock. Unlike the fresh crater in Figure 21e, the rim and ejecta areas outside Endurance do not exhibit any ejected boulders. MER-B images confirm the lack of ejecta materials—boulders, cobbles, overturned beds—enhancing the case that these materials might still be buried (Figure 22). In addition, blocks of sedimentary rock like those that the rover encountered at the rim are found to have dropped down into the crater, covering what should otherwise be layered rock outcrops in the crater wall (Figure 22). The original wall is interpreted to be obscured by rocks that fell when the rock unit that lies stratigraphically above the crater rim was undermined and collapsed. How the materials that once filled or partially-filled Endurance were removed is a difficulty for this interpretation, but the same problem exists for larger craters like Victoria and even larger craters elsewhere on Mars, like Gale and Henry (Malin and Edgett 2000).

The lag of hematite spherules on the plains at the MER-B site suggests that the ~7 m of strata investigated there are not at the stratigraphic top of the plains-forming unit. To create such a lag, some amount of rock bearing the hematitic material must have once existed above the surface on which MER-B has been operating, an idea that was captured in one of the several original working hypotheses described by [Christensen et al. \(2000\)](#). The topography of Meridiani Planum rises from west to east. Some of this topographic form could be the result of a warped upper crust and dipping strata, but, as noted in Figure 6, dips are generally slight (<1°). Thus, it is possible that tens to as much as a few hundred meters of strata once existed above the present surface at the rover site.

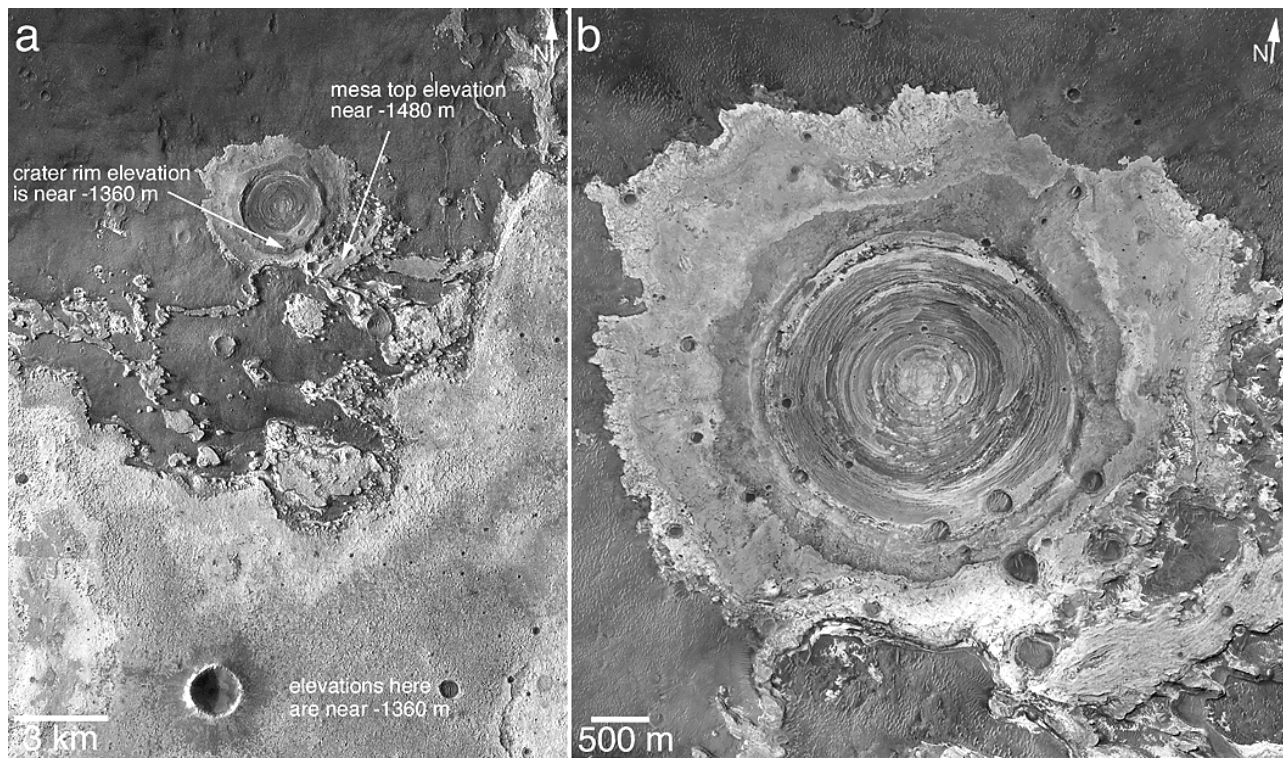


Figure 14. Crater in northern Sinus Meridiani interpreted to have been filled, buried, then exhumed. **(a)** Context; elevations come from MOLA observations on orbits 2501, 4312, 7513, 7689, and 9348. The elevation of the rock in the south third of the image is similar to the elevation of the exhumed crater rim; erosion and scarp retreat progressed southward to reveal the formerly buried crater. This is a mosaic of sub-frames of THEMIS images V05717012 and V02721007 ([figure14a.png](#)). **(b)** The exhumed crater is located near 2.3°N, 356.6°W. This is a mosaic of sub-frames of MOC images M04-01289, E17-01676, and E20-01346. Dark, circular features superimposed on the crater may be the remains of smaller craters that have been nearly destroyed by erosion ([figure14b.png](#)).

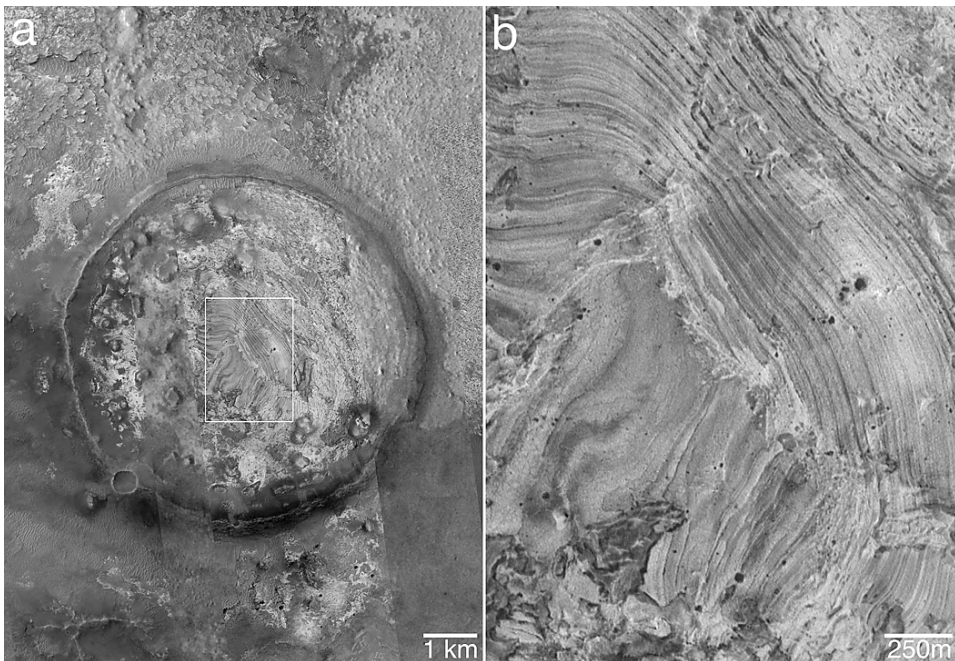


Figure 15. Filled impact craters in Sinus Meridiani usually exhibit a different bedding style inside the crater relative to the bedding outside the crater. **(a)** An exhumed crater near 0.7°N, 252.7°W, in a mosaic of portions of MOC and THEMIS images M10-02183, E14-01674, and V09499005 ([figure15a.png](#)). **(b)** Close-up view of layers in the crater ([figure15b.png](#)).

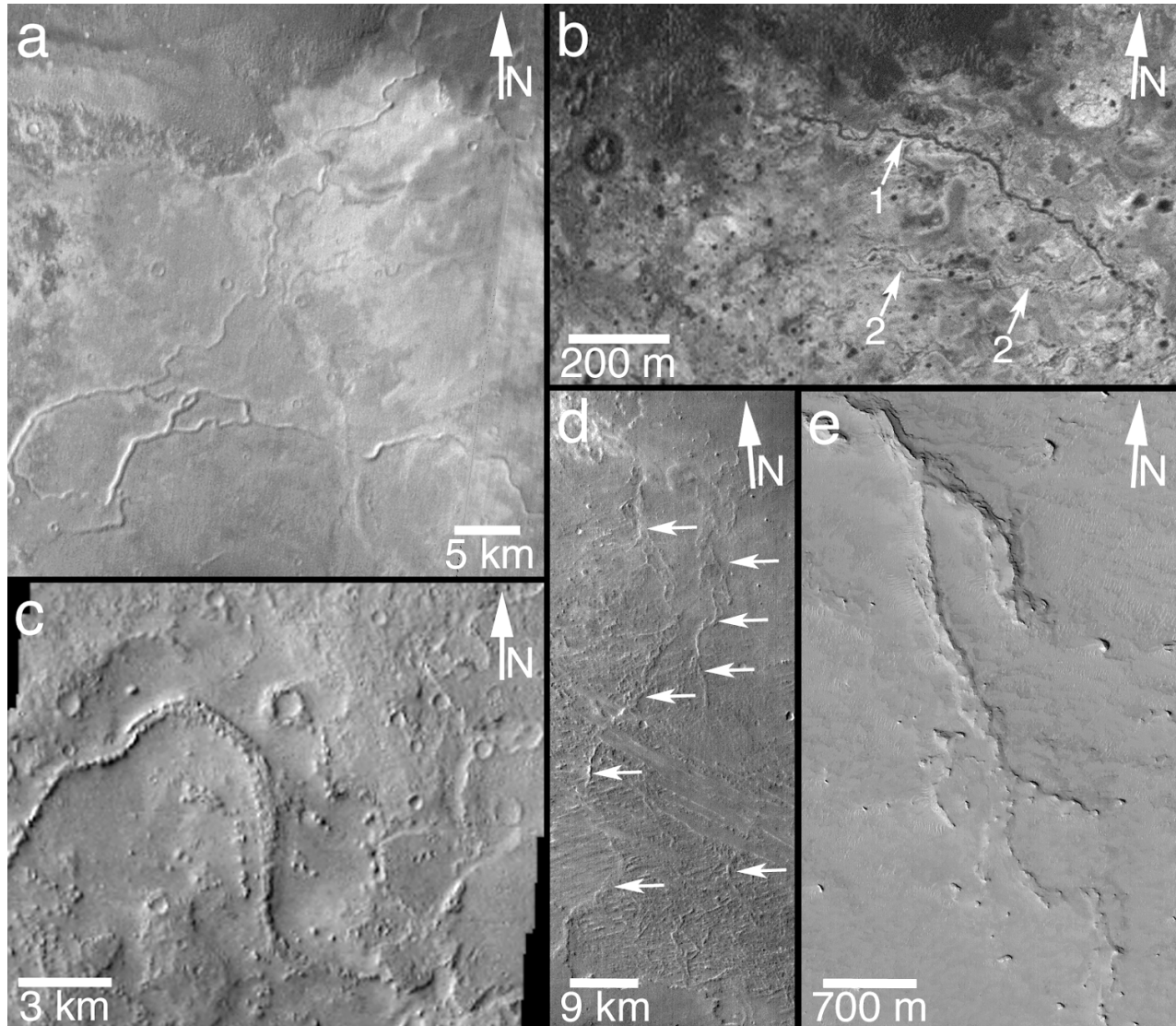


Figure 16. Examples of inverted valleys, filled valleys, and exhumed negative-relief valleys that are part of the stratigraphic story of the Sinus Meridiani region. (a) Inverted valleys; mosaic of THEMIS band 9 IR images I01173002, I03707002, and I08176017, near 1.5°N , 352.5°W ([figure16a.png](#)). (b) Negative-relief channel (1) and filled, exhuming tributary (2) in mosaic of MOC images S09-02562 and S10-01115, near 1.9°S , 356.9°W ([figure16b.png](#)). (c) Inverted valley in sub-frame of THEMIS V11360001, located near 3.0°S , 8.0°W ([figure16c.png](#)). (d) Inverted stream courses (arrows) in THEMIS band 9 IR image I11072009, near 0° , 8.5°W ([figure16d.png](#)). (e) Inverted valley system in MOC image M11-01050, near 1.4°N , 6.2°W ([figure16e.png](#)).

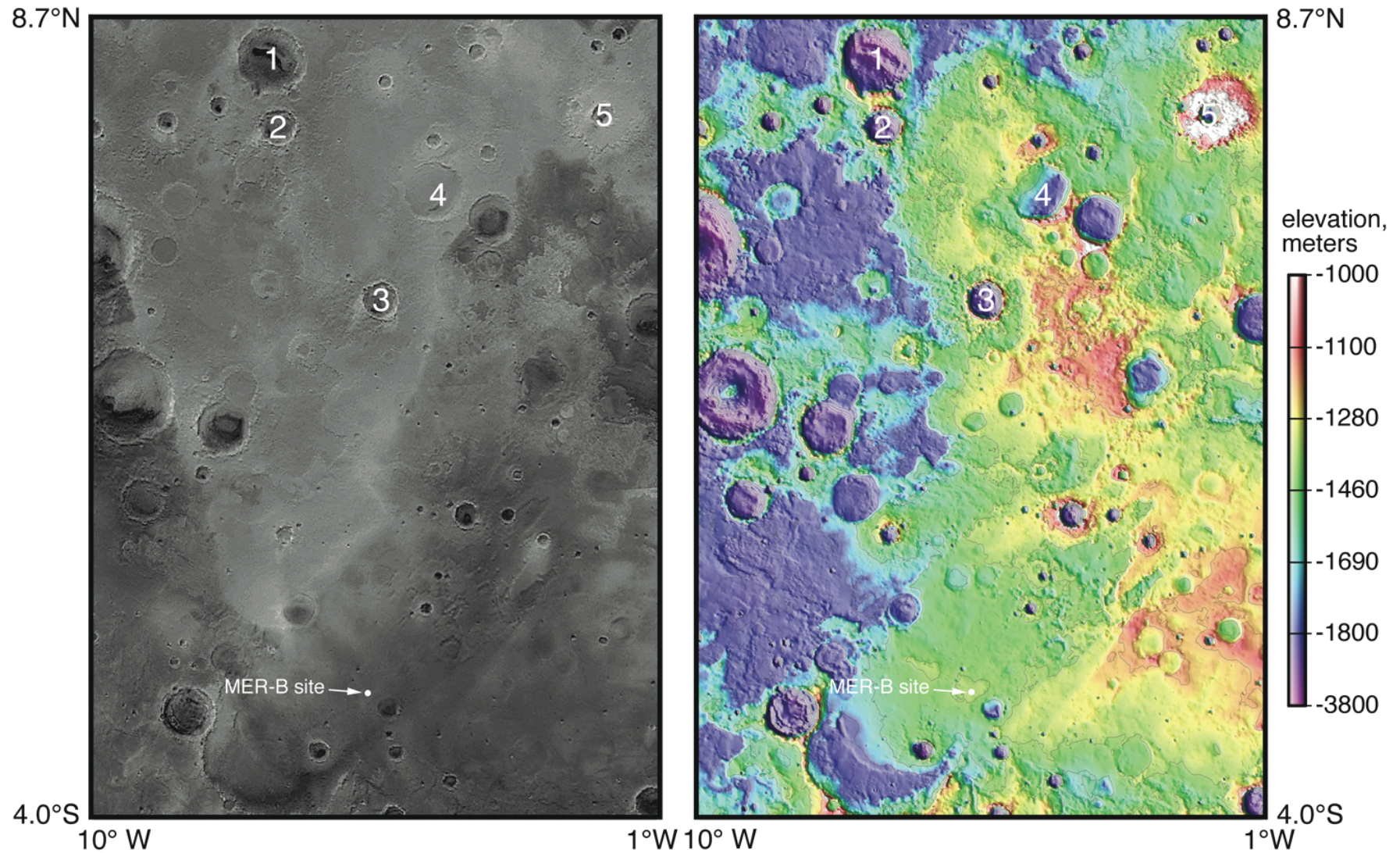


Figure 17. A mosaic of MOC red wide angle camera images ([figure17a.png](#)) and a MOLA topographic map ([figure17b.png](#)) of western Sinus Meridiani. The area shown is the region for which a geologic sketch map was compiled (Figure 18). The craters labeled 1–5 are described in the text. Crater 4 is partially exhumed and partially buried. The MOC images were acquired during the MGS Geodesy Campaign in May 1999. The topographic map is derived from MOLA observations obtained 1999–2001. Note that the elevation/contour scale is non-linear and designed to emphasize details in the western Sinus Meridiani landscape.

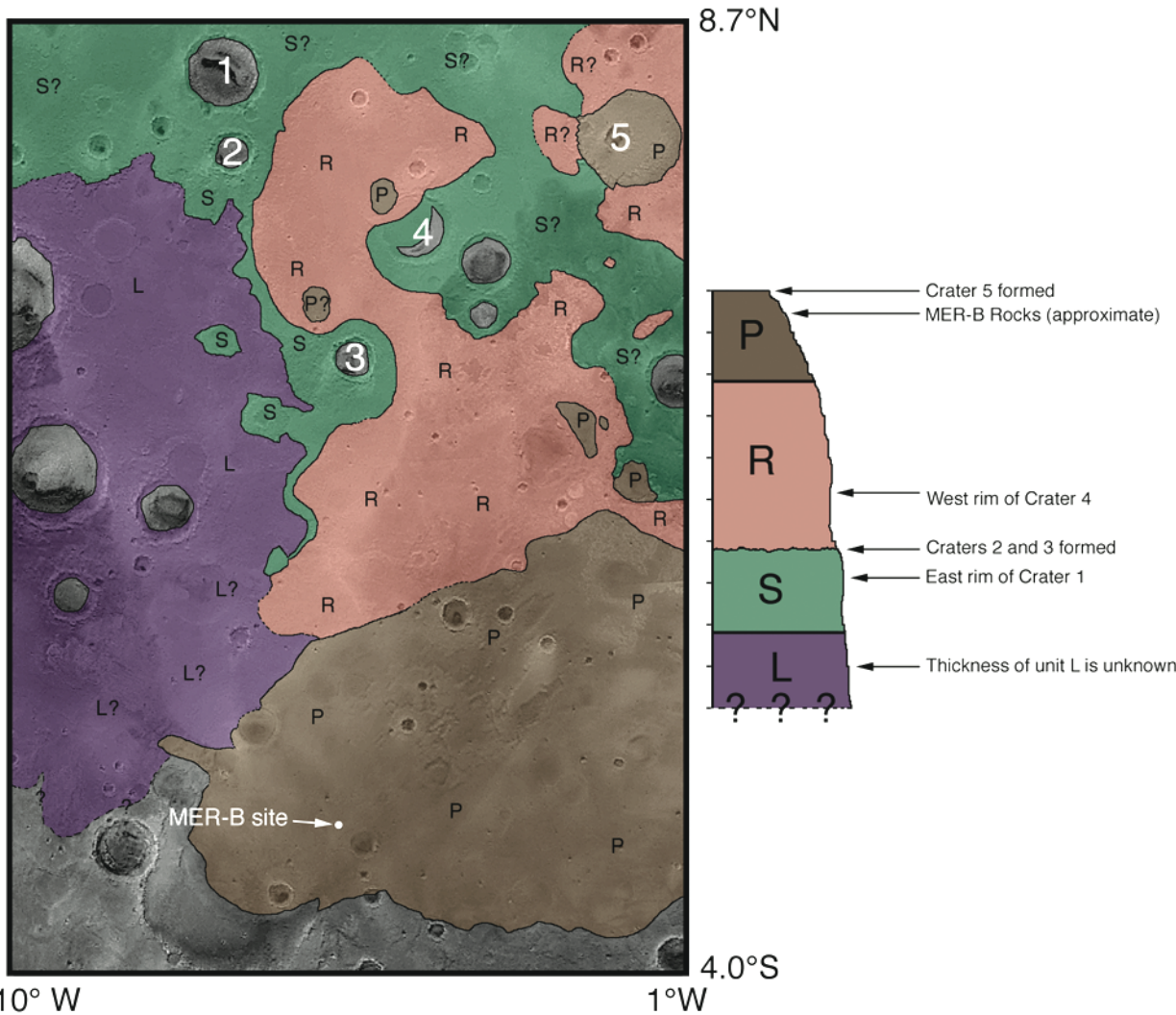


Figure 18. Rudimentary geologic map of western Sinus Meridiani. Dashed contacts and question marks indicate uncertainties; areas not colored do not exhibit rocks that can be classified as belonging to one of the four stratigraphic units. Tick marks on the stratigraphic column are in 100 m intervals; thicknesses were estimated from MOLA topographic observations. The craters 1–5 are described in the text ([figure18.png](#)).

The ridge-forming unit

If one were to hike or drive a rover ~165 km north of the MER-B site, one would encounter a scarp which, in places, is 50–100 m high (measured from individual MOLA ground tracks) where the plains-forming unit (P) drops down to the uppermost rocks of the underlying, ridge-forming unit (R). The relation between the plains on which MER-B has been operating, and the stratigraphic position of the ridge-forming unit, is shown in Figure 23. Another example of the relationship between these units is shown in Figure 24.

Figure 25 provides examples of the rugged, criss-crossing ridge patterns developed by erosion in the ridge-forming unit (R). The unit is present across northern Sinus Meridiani. The ridges are more resistant to erosion than surrounding light-toned bedrock in which the ridges were previously embedded. Figure 26 shows the occurrence of the ridge-forming material within rock that is less-resistant to erosion

and can be eroded away to leave only the ridges as the high-standing remains of this unit. Figure 27 shows a case in which the ridges of the ridge-forming unit have been eroded to reveal that the rock comprising the ridges is layered. In other words, the ridges of the ridge-forming unit are not monolithic. The observations presented here contrast with the perspectives of [Arvidson et al. \(2003\)](#), who considered the ridges to be the products of fracturing (and filling of fractures) in lava flows and/or dike emplacement, as well as those of [Ormö et al. \(2004\)](#), who considered the ridges to result from alteration/diagenesis of rock along fractured zones in the presence of groundwater.

The ridges show no preferred orientation. That is, they do not form distinct networks suggestive of inverted valley network systems, nor do they resemble other inverted valleys elsewhere on Mars. Figure 24 shows that some of the ridges form circles and are thus interpreted to have an affinity for,

or at least correspond with, the location of buried or formerly buried craters. While the origin of the ridges can only be speculated upon, their pattern and scale bears some resemblance, although in inverted form, to the troughs of the “giant polygon” areas in Acidalia Planitia and northern Elysium Planitia, particularly the Adamas Labyrinthus troughs (Figure 28). While Figure 28 does not show a relationship to craters, it has been known for several decades that the troughs of the “giant polygon” regions form circular troughs where the rock in which the troughs occur has been draped over buried crater rims (e.g., McGill and Hills 1992; [Buczkowski and McGill 2002](#)). The speculation here, one that was also suggested by Edgett and Parker (1997), is that the ridges of the ridge-forming unit were once troughs similar to those of the Adamas Labyrinthus. The troughs were subsequently filled (layer by layer) with sediment, and eventually buried by additional sediment (including that of the plains-forming unit), before later being re-exposed and eroded to create inverted forms.

Scarp-forming and lower units

The scarp-forming unit (S) and the lower unit (L) occur below the ridge-forming (R) unit (Figure 29). The scarp-forming unit is named for the prominent scarp that it displays in Figure 29 and along its continuance in western Sinus Meridiani. Other places in western Sinus Meridiani where the scarp-forming unit is inferred to occur are much more speculative because, in northern Sinus Meridiani, the rock that lies below the ridge-forming unit is usually covered by a

low-albedo, smooth-surfaced (at MOC image scale) mantle. The dark surface in the eastern half of Figure 30 is proposed to be a dark-toned mantle covering the rock of the scarp-forming unit. Figure 30 also illustrates that valleys and inverted valleys (in this case, a valley with both negative- and positive-relief elements) are found in this rock unit.

The lower unit (L) lies below the scarp-forming unit (Figure 29). It is largely covered by intermediate-toned mantles of material, but there is one area in which some of the rock in this unit is well exposed (Figure 31). This rock is light-toned and layered like the other rock units in the Sinus Meridiani region. The inverted valleys in Figure 16d occur in this area.

Geologic map of western Sinus Meridiani

Comparison of the geologic map in Figure 18 with the topographic map in Figure 17b suggests that, in the northern half of the geologic map, the rocks are generally flat-lying and there is a steady progression down-section and west-southwest from the rocks contained within the pedestal surrounding the crater labeled 5, to the rocks of the ridge-forming unit (R), to the rocks of the scarp-forming (S) and lower (L) units. A complication, however, is evident when one examines the southern half of the geologic map and compares it with the topography in Figure 17b. Here, the elevation of the MER-B site is lower than the elevation of some of the exposures of ridge-forming unit (R). The rover site is also lower than other exposures of the plains-forming unit (P) to the east of the MER-B site.

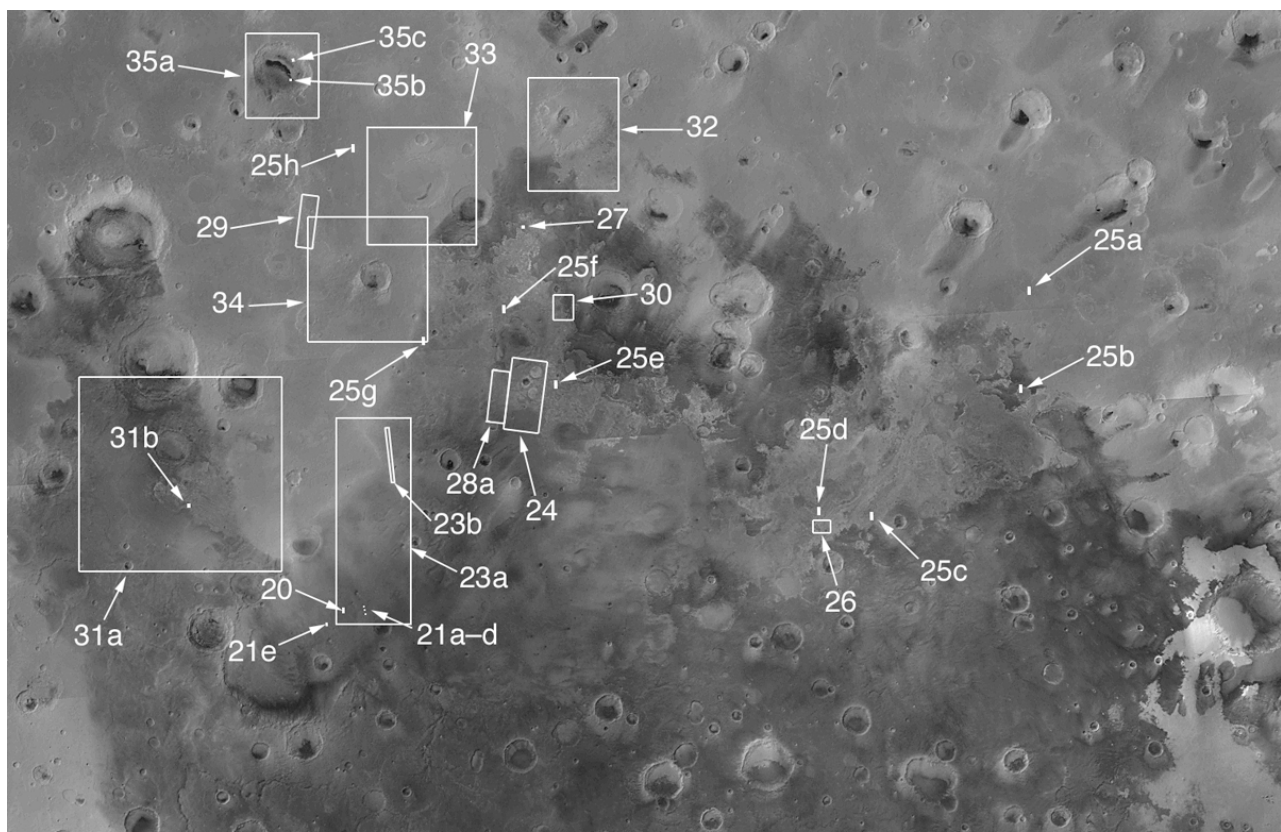


Figure 19. Map of Sinus Meridiani, showing the location of images in Figures 20, 21, and 23–35 ([figure19.png](#)).



Figure 20. Typical MOC-scale view of Meridiani Planum surfaces. As known from the MER-B site, the plains-forming unit (P) bedrock lies beneath a dark-toned regolith. This is a sub-frame of MOC image E12-03255, located near 2.0°S, 6.0°W ([figure20.png](#)).

That some of the plains-forming unit rocks may be at a higher elevation than those of the MER-B site could be explained as the product of erosion; that is, that a hundred or more meters of material have been removed from the plains upon which MER-B has been operating. But this explanation would not hold for the higher-elevation ridge-forming unit materials to the north. In this case, the explanation may require that rocks are dipping toward the southwest or that the rocks have been faulted and vertically offset relative to one another. In either case, the stratigraphic relation between the ridge-forming unit and the plains-forming unit illustrated in Figures 23 and 24 must be preserved.

Problems aside, the geologic map and four unit stratigraphy (Figure 18) is intended to make one key point: the rocks examined by MER-B are near the top of a sequence of >800 m of rock. The thickness of the rock units was

estimated using MOLA topography of the exposures in the northern half of the area in Figure 18. Four critical stratigraphic relations emerge from this mapping exercise:

- 1) The ejecta from the crater labeled 5 in Figures 17 and 18 formed a resistant cap that protected a layered sequence of rocks more than 150 m thick from erosion (Figure 32). Below the rocks within the pedestal are rocks of the ridge-forming unit (R); thus the pedestal-forming rocks are inferred to be the time-stratigraphic equivalent to those of the plains-forming unit (P). Rocks of about the same age as those examined by MER-B, whatever that age may be, are probably preserved in the layers of rock in the pedestal.
- 2) The crater labeled 4 in Figures 17 and 18 is embedded and only partly exhumed from within the rocks of the ridge-forming (R) and scarp-forming (S) units. Illustrated in Figure 33, this crater has a diameter of about 55 km, attesting to the fact that large craters, like the smaller craters in Figures 13–15, have been filled, buried, and incorporated into the stratigraphy of Sinus Meridiani.
- 3) The ejecta blanket of the crater labeled 3 in Figures 17 and 18 is being exhumed from beneath the ridge-forming unit (Figure 34). Crater 3 and crater 2 formed after the rocks of the scarp-forming unit (S) were deposited and lithified, but before the sediments comprising the rocks of the ridge-forming unit (R) were deposited. The amount of time that occurred between deposition of unit S and R is unknown, but it was long enough for the rocks of unit S to be exposed at the surface and experience formation of two relatively large, nearby impact craters. In other words, the upper surface of unit S was exposed to the elements and to potential large impactors for some considerable period before the sediments of unit R were deposited.
- 4) The east rim of the crater labeled 1 in Figures 17 and 18 lies below the top of the scarp-forming unit (S). This crater therefore lies below more than 600 m of the > 800 m of strata exposed in western Sinus Meridiani. The crater may therefore have once been filled, buried, and covered by the additional ~600 m of strata; that this is possible is illustrated by crater 4 which is only 5 km smaller in diameter than crater 1. Figure 35 shows that the interior of crater 1 exhibits hundreds of repeated layers of sedimentary rock of similar thickness and erosional expression. Rocks like those in crater 1 are found in other craters > 20 km in diameter in northern Sinus Meridiani, western Arabia Terra, and in some of the chasms of the Valles Marineris (Malin and Edgett 2000). Similar rocks do not occur as part of the units P, R, S, and L, and suggest that the depositional environment within the crater (and in other craters of Sinus Meridiani and western Arabia) was different than the depositional environment(s) outside the crater. The rocks examined by the MER-B team in Eagle, Fram, and Endurance craters lie more than 600 m, stratigraphically, above the rim of crater 1.

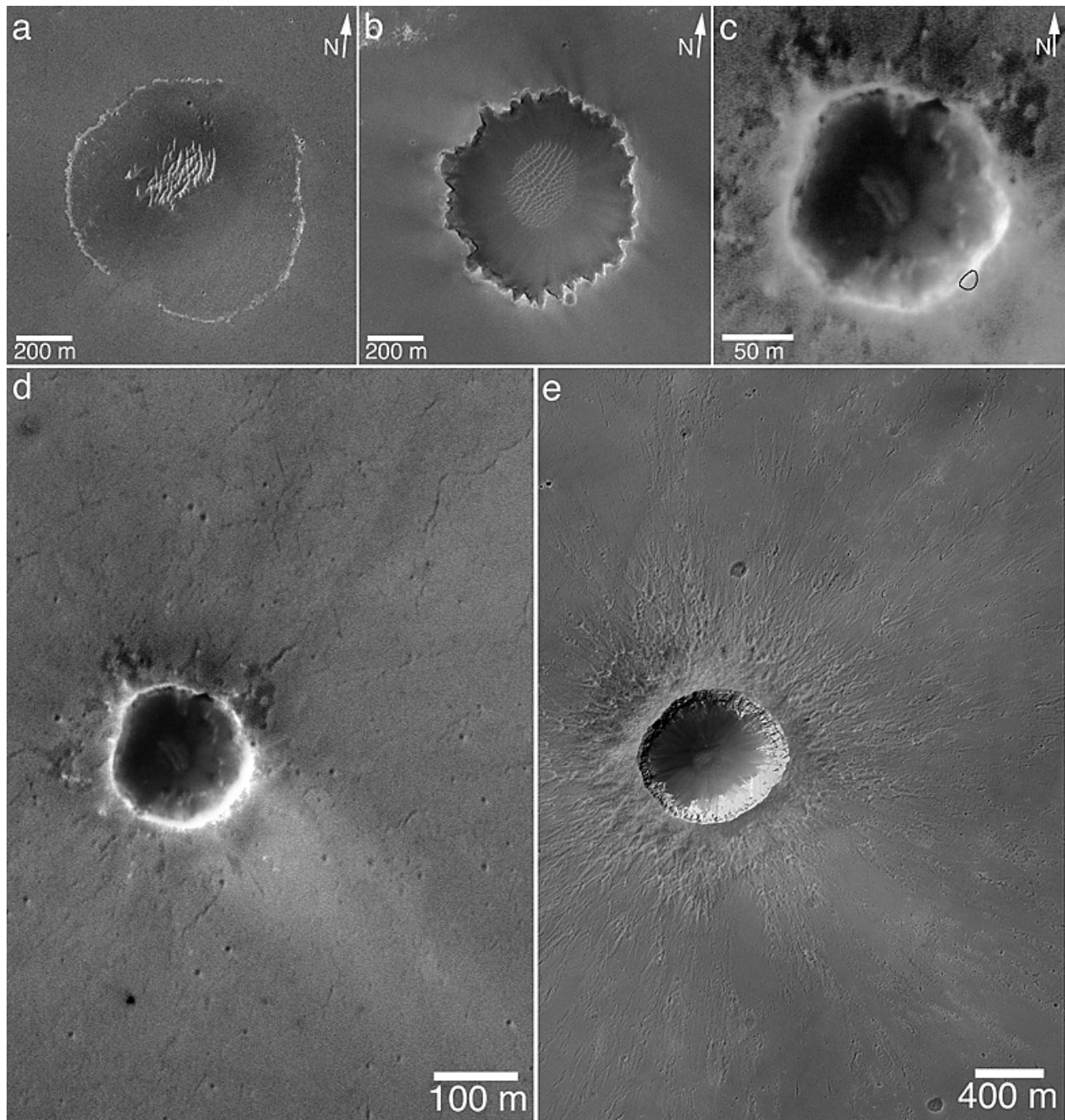


Figure 21. Possible sequence for exhumation of craters in the plains-forming bedrock of Meridiani Planum. **(a)** A shallowed, nearly-filled crater located a few kilometers north of the MER-B landing site in a sub-frame of MOC image R14-00021, near 1.9°S , 5.6°W ([figure21a.png](#)). **(b)** Victoria Crater, located several kilometers south of the MER-B landing site, is nearly the size of the shallowed crater in (a). Victoria's original rim is buried beneath the uppermost strata of the plains; the scalloped nature of the present rim was produced by undermining and collapse as less-resistant material was eroded away. This is a sub-frame of MOC R14-00021, near 2.1°S , 5.6°W ([figure21b.png](#)). **(c)** Expanded (4x) view of Endurance Crater. This crater has a raised rim, but it may once have been buried like the craters in (a) and (b). The dark polygon indicates the location visited by MER-B in May 2004, illustrated in Figure 22. This is a sub-frame of MOC R16-02188, located near 2.0°S , 5.6°W ([figure21c.png](#)). **(d)** Endurance Crater in a sub-frame of R16-02188, to be compared with crater to the right ([figure21d.png](#)). **(e)** Example of a relatively fresh impact crater in Meridiani Planum. Although about 4 times larger, this crater provides an example of how Endurance Crater looked when it was young. Examination of the full-resolution view of this crater shows that it has boulders of ejecta on its rim—a feature not seen at Endurance Crater. This is a sub-frame of MOC image E17-00918, located near 2.3°S , 6.3°W ([figure21e.png](#)).

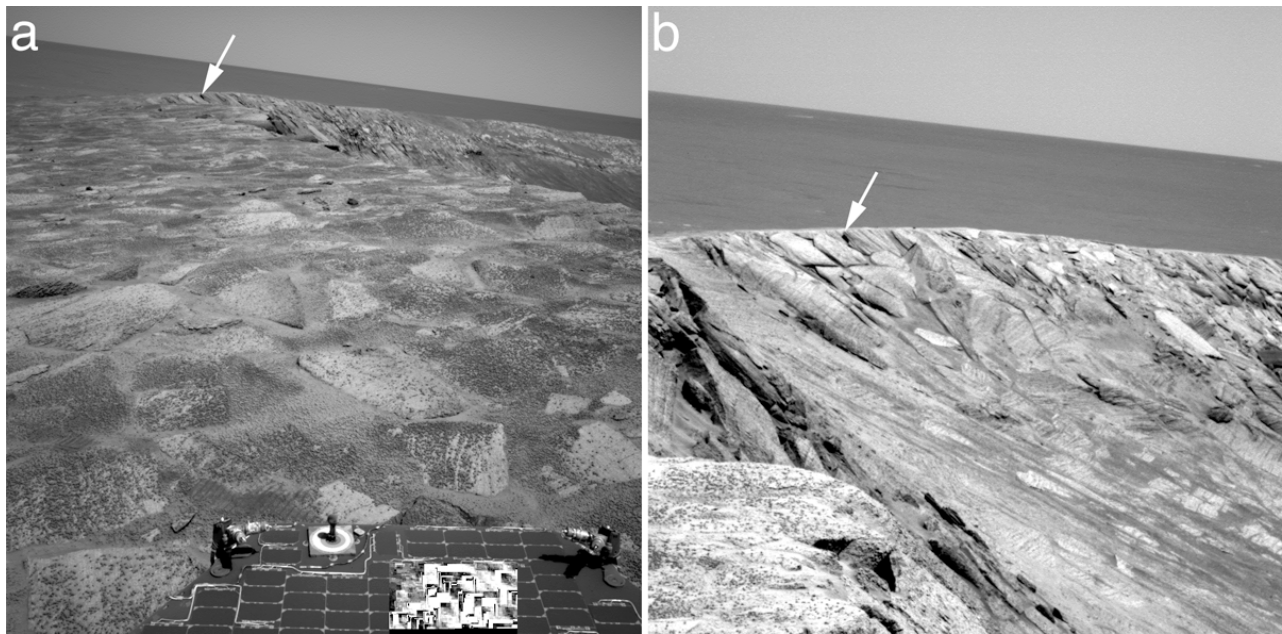


Figure 22. Images from MER-B acquired May 2004 on the southeast rim of Endurance Crater. The bedrock in this area is exposed at the surface; its configuration suggests that the crater has been exhumed. No primary ejecta materials, including boulders and cobbles, are present. Rocks that form the surface that the rover was driving upon are also the same materials that draped over the rim and have collapsed, covering much of the original upper crater wall and the rock that was exposed by the impact. The rocks presently at the surface, and those that have collapsed onto and obscuring the crater wall, are interpreted to be the remains of strata that once buried the crater. For reference, the arrows point to the same location on the rim. (a) View looking southwest; the rover hardware provides scale. Image 1N138388315EFF2700P1994L0M1 is from Left Navigation Camera on Sol 115, 21 May 2004, near 10:55 local time ([figure22a.png](#)). (b) Close-up of rocks draped over upper wall. Image 1P138566784EFF2809P2297L2C1 is from Left Pancam (753 nm filter) on Sol 117, 23 May 2004, near 11:11 local time ([figure22b.png](#)).

Observation 4: Light-toned, layered rock and interbedded craters in neighboring heavily cratered terrain

Implicit in the geologic map and stratigraphic study is the inference that some of the rocks in the Sinus Meridiani stratigraphic column are intimately interbedded with some of the large (tens of kilometers in diameter) impact craters in the region. In other words, these rocks are not superimposed on a heavily cratered terrain—as suggested, for example, in the second figure of [Arvidson et al. \(2003\)](#)—they are a part of the bedrock of the cratered terrain in the areas north and west of Meridiani Planum ([Edgett and Malin 2002](#)). This section explores the nature of the cratered terrain to the east and south of Meridiani Planum. Figure 36 shows the location of images described in this section.

Cratered terrain east of Meridiani Planum

The terrain of eastern Sinus Meridiani is more rugged and heavily cratered than Meridiani Planum (Figure 37a). Like Meridiani Planum, most of this surface is covered by a low-albedo mantle, although this material differs in that it lacks the thermal infrared spectral signature of hematite found on

Meridiani Planum ([Christensen et al. 2000](#)). THEMIS VIS and MOC narrow angle images of the boundary between light-toned rock outcrops and the dark, mantled intercrater plains of eastern Sinus Meridiani do not in all locations show a clear, distinct geologic contact (Figure 37). Light-toned rocks of the ridge-forming unit (R) stand higher than the immediately adjacent dark, mantled surfaces of eastern Sinus Meridiani, but the inter-ridge depressions exhibit light-toned rock; this observation suggests that the material beneath the adjacent dark, mantled plains may be of a similar nature (Figure 37b). A narrow valley cut into the dark-toned plains in Figure 37c also suggests that the substrate may have a light tone provided that the light-toned material in the valley is the bedrock into which it was cut, rather than a material that later filled the valley.

As there is no certainty about the light-toned material in the valley in Figure 37c, other MOC images of rock exposures in the region must be examined. Figure 38 shows three examples of light-toned rock outcrops in eastern Sinus Meridiani. One of them, Figure 38b, illustrates light-toned, layered rock exposed in the wall of an impact crater. The other two show patches of light-toned rock in the intercrater plains. Wherever the dark-toned mantle is not present in eastern Sinus Meridiani, a light-toned substrate is seen.

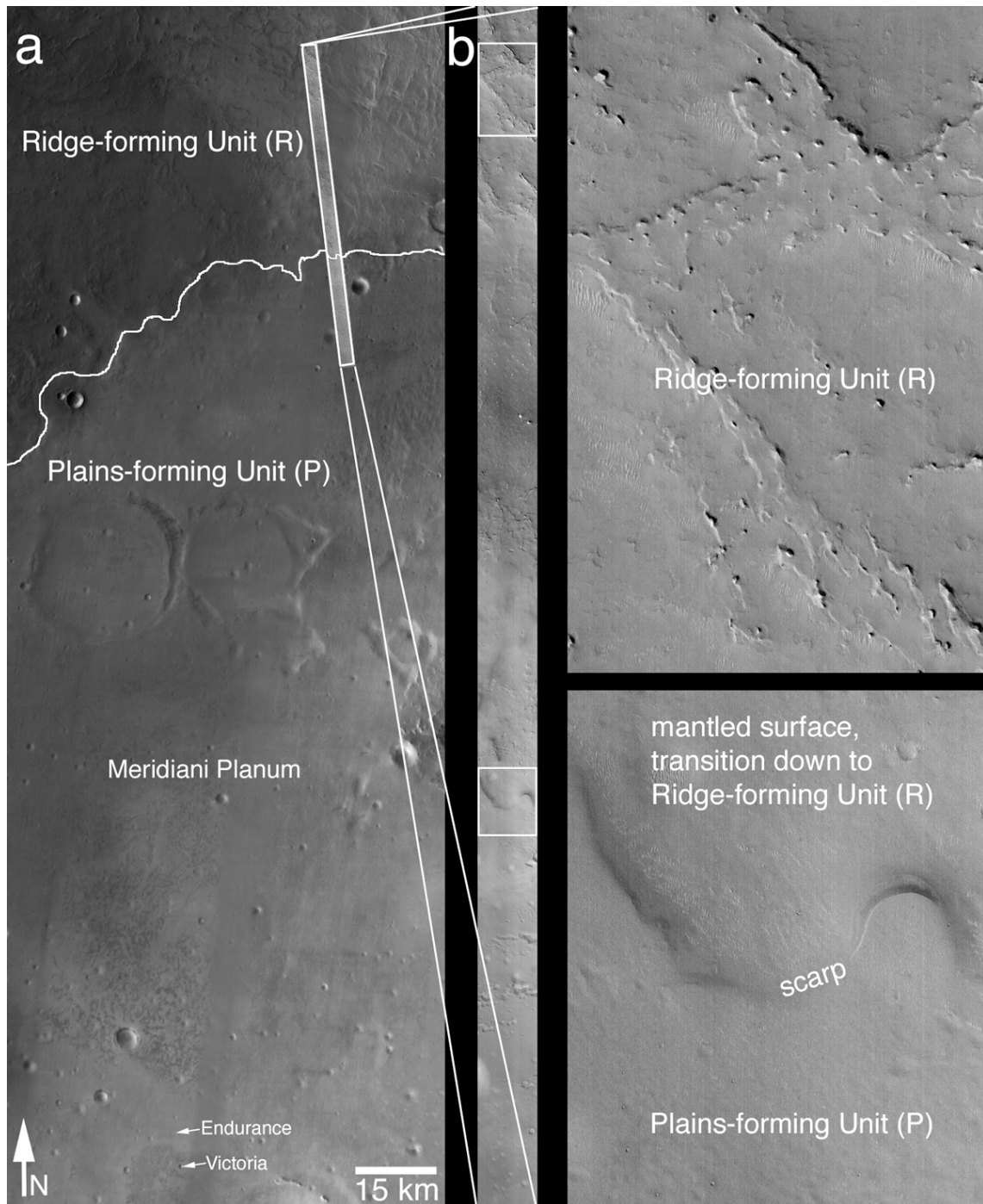


Figure 23. **(a)** Relation of plains-forming unit to underlying ridge-forming unit. The MER-B site is in the vicinity of Endurance and Victoria craters. This is a mosaic of sub-frames of THEMIS IR band 9 images, I01835005, I06666018, I07415019, I08526015, and I10710003 ([figure23a.png](#)). **(b)** The transition from the plains-forming unit to the ridge-forming unit is illustrated in MOC image S08-03049. The full image is shown on the left, sub-frames are on the right and their locations are indicated by white boxes. Each image covers an area 3 km wide. From MGS MOLA observations, the scarp is ~50 m high ([figure23b.png](#)).

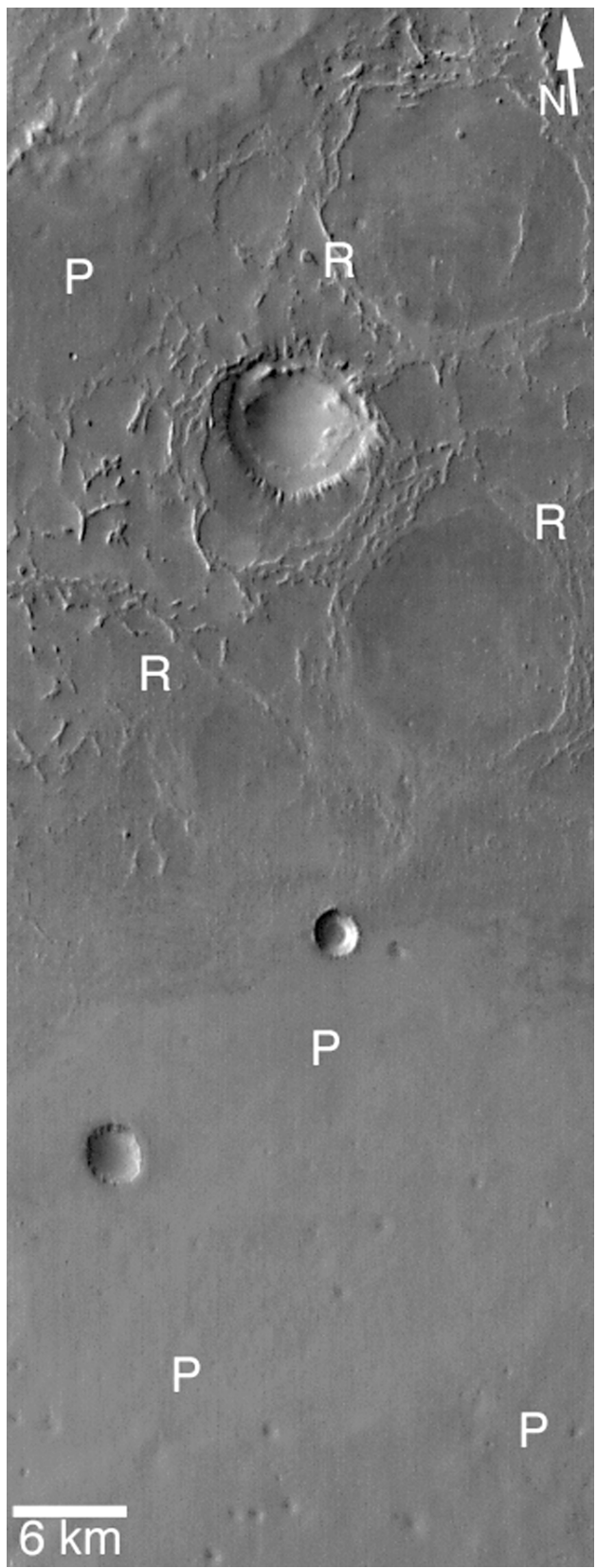


Figure 24. Image showing stratigraphic relation between plains-forming unit (P) and underlying, ridge-forming unit (R). This is a sub-frame of THEMIS IR band 9 image I04756005, located near 2.0°N, 2.6°W ([figure24.png](#)).

While it is possible that the observations in Figures 37 and 38 indicate that the bedrock of eastern Sinus Meridiani is composed of light-toned, layered rock of properties similar to or indistinguishable from those of light-toned, sedimentary rocks in central and northern Sinus Meridiani, it is also possible that these patches and exposures are not representative of the bulk bedrock of the region. However, there are no exposures that would indicate that the bulk bedrock is not layered or light-toned.

Cratered terrain south of Meridiani Planum

As with eastern Sinus Meridiani, patches of light-toned, layered rock outcrops are also found in the heavily cratered terrain south of Meridiani Planum. Figure 39 shows two examples. In addition to these, several craters also exhibit rock properties similar to those in craters formed in Meridiani Planum rocks. Figure 40 shows a key example. The first crater (Figure 40a) formed in the heavily cratered terrain of southern Sinus Meridiani. The rock exposed in the walls of this crater is light-toned and layered. The material eroded by mass movement from the crater walls has accumulated on the floor and lower walls in the form of a talus that is darker than the rock from which it was derived. The second crater shows the same relationships—light-toned, layered wall rock and a dark-toned talus. The erosional expression of the wall rock and the depositional pattern of the talus deposits are nearly identical in the two craters, but different relative to similar-sized craters elsewhere on the planet. One might conclude from these observations that the second crater formed in material of the same physical properties as the first crater. However, the second crater is located in northern Sinus Meridiani, in the plains-forming unit (P) of Meridiani Planum. Although the two craters formed in different rock units, the rocks apparently have similar properties.

Another attribute of the heavily cratered terrain south and east of Meridiani Planum that is shared with the rocks of northern and central Sinus Meridiani is the interbedding of impact craters. For example, Figure 41 shows several examples of 1–2 km diameter craters that were filled or partially filled and later at least partially exhumed from within the strata of the layered, cratered terrain south of Meridiani Planum. Figure 42 shows another example—a much larger crater (~70 km diameter, larger than the craters in Figures 33 and 35) in southern Sinus Meridiani that was nearly filled and later cut by a valley.

The heavily cratered terrain to the north, west, south, and east of Meridiani Planum is not a monolithic material. The rock is layered, possibly light-toned, and includes interbedded craters of a range of diameters. While the erosional expression of the cratered surfaces in south and east Sinus Meridiani differ from that of Meridiani Planum and the cliff-forming rocks of north Sinus Meridiani, the rock properties may be similar. The implication of these observations and the stratigraphic placement of the Meridiani Planum rocks relative to the cratered terrain south of the plains, are further explored in the discussion section below.

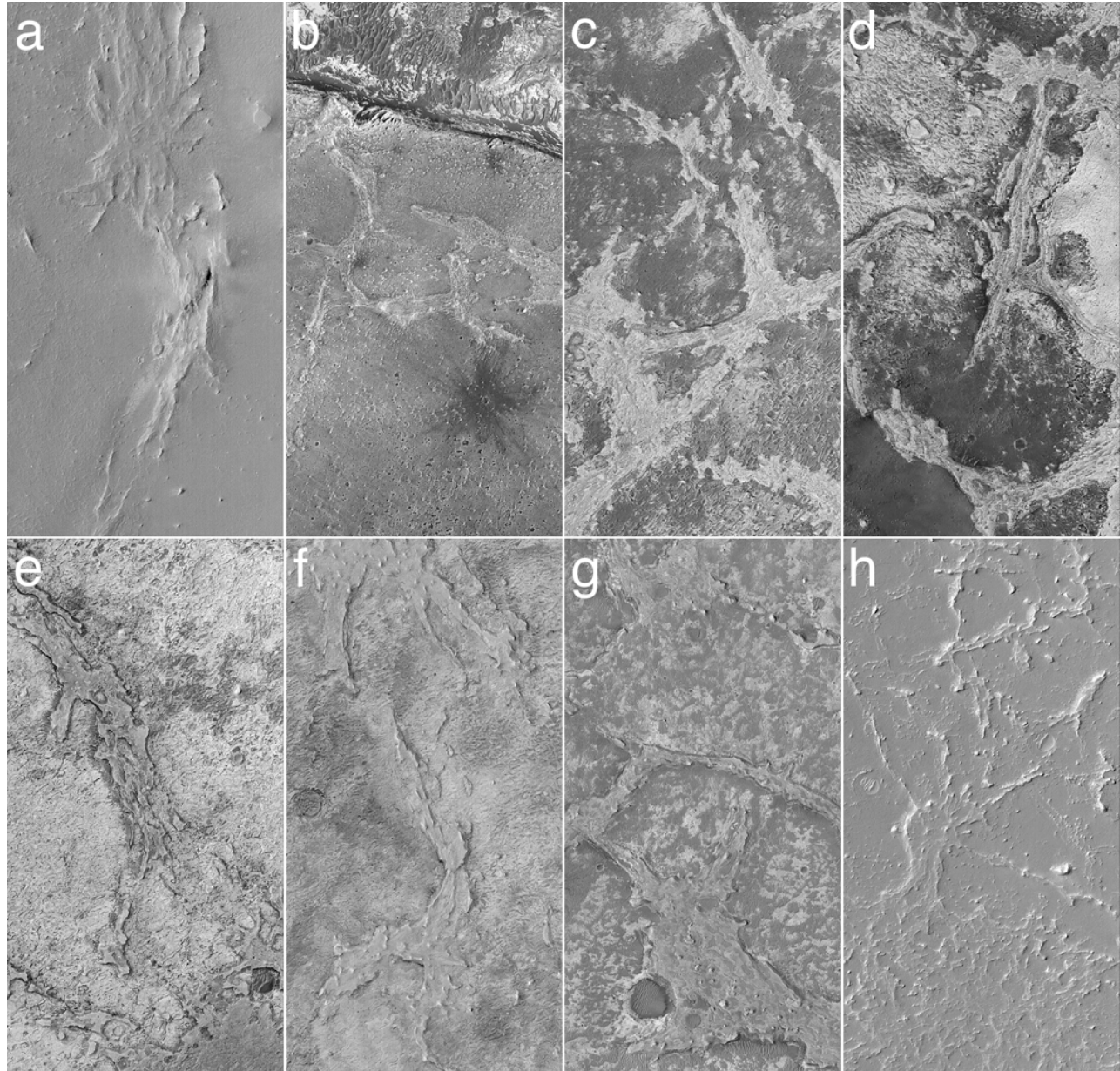


Figure 25. Sub-frames of MOC images showing examples of ridges in eroded, ridge-forming unit (R) from all across northern Sinus Meridiani. Albedo variations between all of the images are largely a product of overlying mantles or regolith of varied thickness and spatial distribution. All images cover the same surface area, 3 km by 5.9 km. **(a)** A sub-frame of image E18-00327, near 4.2°N, 353.2°W ([figure25a.png](#)). **(b)** A portion of MOC image M02-02530, near 1.9°N, 353.4°W ([figure25b.png](#)). **(c)** M12-01466, near 0.2°S, 356.2°W ([figure25c.png](#)). **(d)** M13-02257, near 0.1°S, 357.2°W ([figure25d.png](#)). **(e)** E18-01425, near 2.2°N, 2.0°W ([figure25e.png](#)). **(f)** R16-02367, near 4.0°N, 3.1°W ([figure25f.png](#)). **(g)** M04-01901, near 3.0°N, 4.5°W ([figure25g.png](#)). **(h)** A sub-frame of MOC image E22-00884, near 6.2°N, 5.8°W ([figure25h.png](#)).

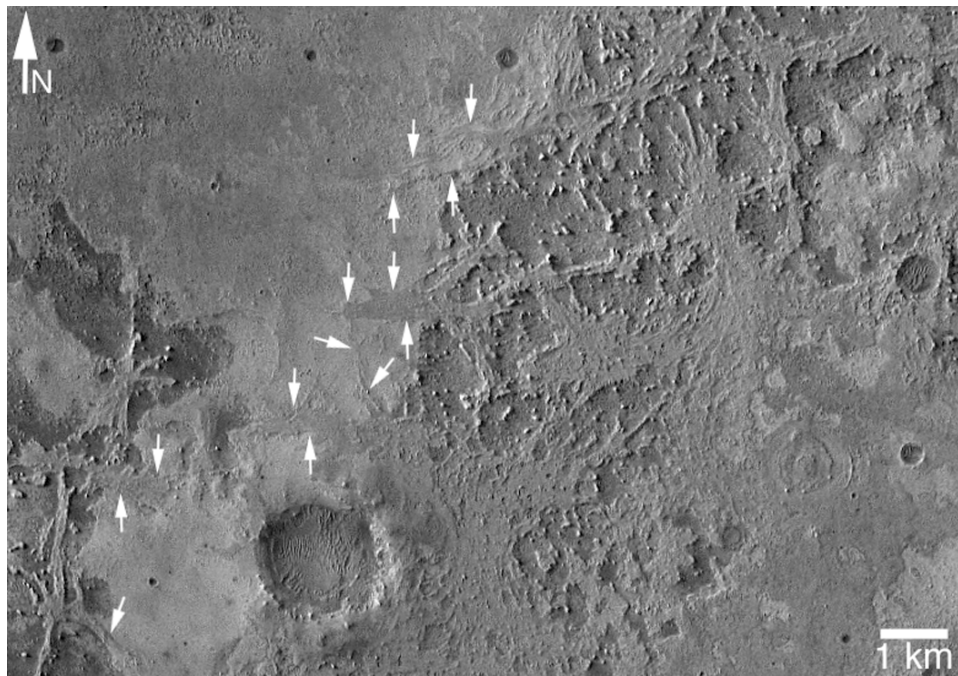


Figure 26. The depressions and spaces between the ridges of the ridge-forming unit were once occupied by light-toned rock. Unknown is whether the ridges formed and then the spaces between them were filled, or whether the ridges consist of material that filled cracks or voids within a host rock. The arrows in this figure show the location of ridges that are still embedded within light-toned rock. This is a sub-frame of THEMIS image V11134006, located near 0° , 357.1°W ([figure26.png](#)).

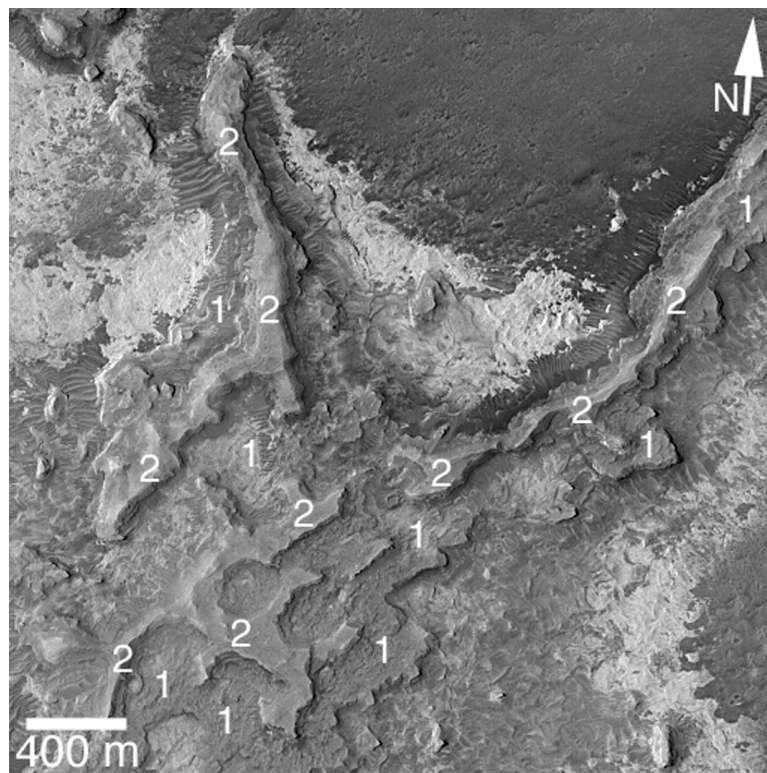


Figure 27. The material comprising each ridge of the ridge-forming unit (R) may be layered. This example, a sub-frame of MOC image M03-01935, shows an eroded ridge of the ridge-forming unit. Numbers 1 and 2 indicate two apparent layers within the ridge. This image is located near 5.1°N , 2.6°W ([figure27.png](#)).

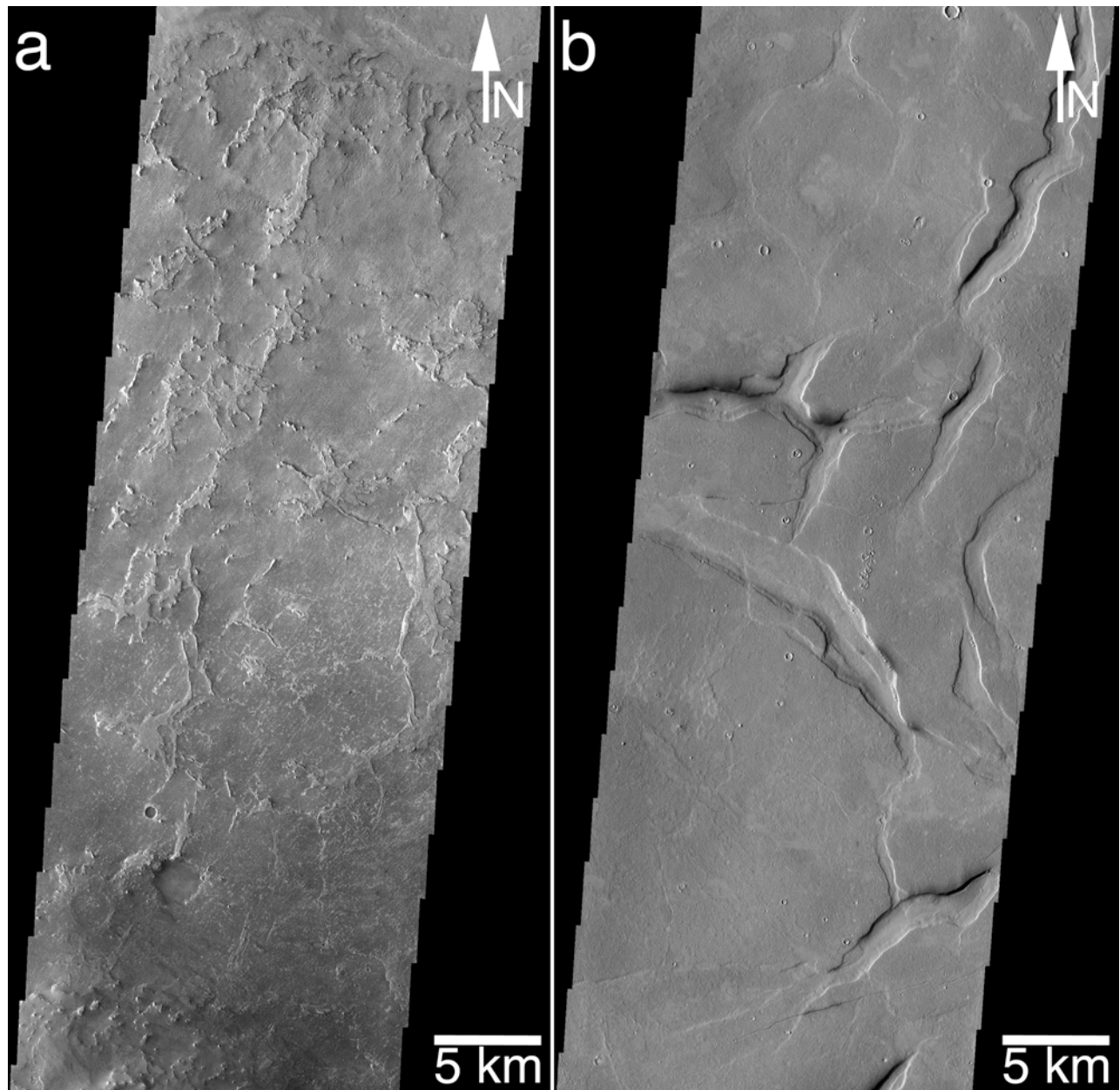


Figure 28. The origin of the ridges of the ridge-forming unit is not known. A possibility is suggested by the similarity of the scale of the ridges to the cracks, troughs, and fissures of the Adamas Labyrinthus in northern Elysium Planitia. The Sinus Meridiani ridges might be the remains of material that filled similar cracks and troughs. **(a)** A typical THEMIS VIS view of ridges of the ridge-forming unit of Sinus Meridiani in a sub-frame of image V06254018, located near 2.2°N, 3.1°W ([figure28a.png](#)). **(b)** A typical THEMIS VIS view of the cracks and fissures of the Adamas Labyrinthus in sub-frame of image V05489013, located near 39.2°N, 255.8°W ([figure28b.png](#)).

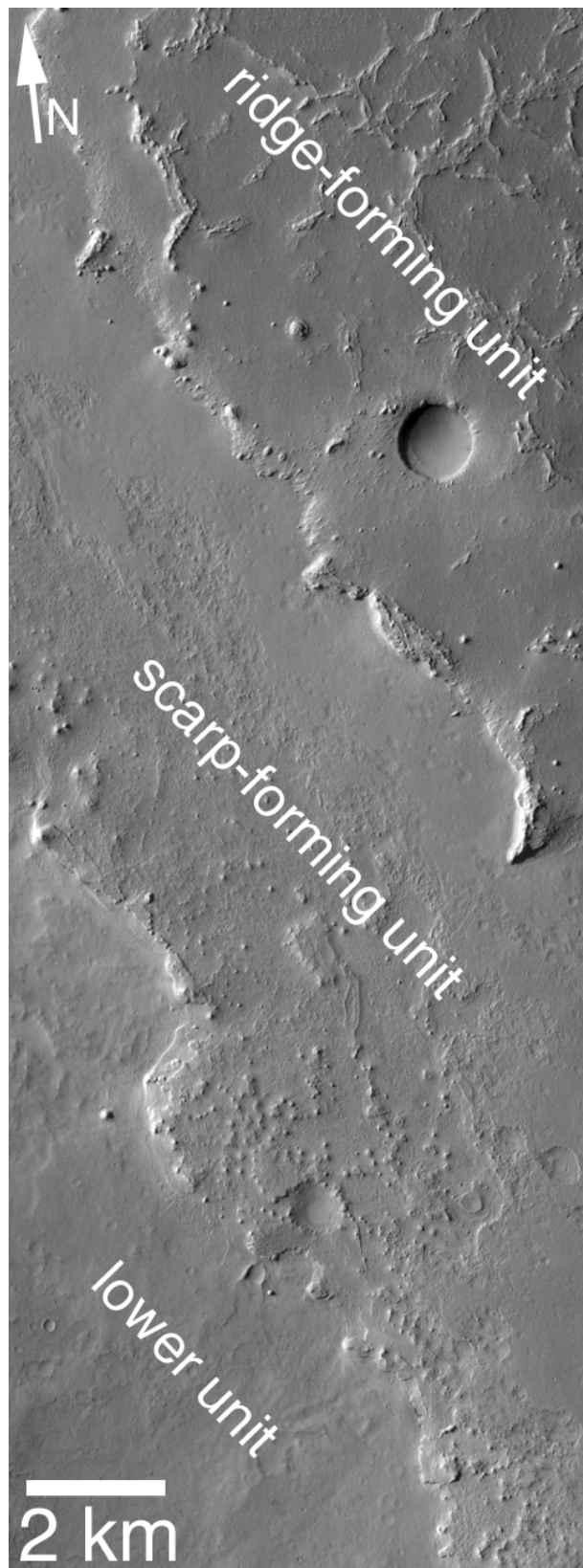


Figure 29. THEMIS VIS view of scarps and contacts between the scarp-forming unit (S), the ridge-forming unit (R), and the older, lower unit (L). This is a sub-frame of V03720003, located near 3.7°N, 1.9°W ([figure29.png](#)).

Observation 5: Light-toned, layered, plains-forming rock is not unique to Sinus Meridiani

The theme of filled, buried, and exhumed valleys and impact craters in a layered upper martian crust—a story common throughout Sinus Meridiani—repeats itself all over the martian surface ([Malin and Edgett 2001](#)). This theme is especially prominent across Arabia Terra where craters of tens to hundreds of kilometers in diameter have been filled, buried, and in some cases have begun to be exhumed. Figure 43 shows a small example. A key distinction between Arabia Terra and Sinus Meridiani is that the eroded landscape of Arabia is mostly covered by thick mantles of dust, as inferred from MOC images and thermal inertia derived from infrared observations (Christensen 1986).

The fifth key observation that places the sedimentary rocks of the MER-B site into context centers on whether the materials outcropping in Sinus Meridiani are unique. When the initial global exploration of MOC images of sedimentary rock outcrops was published by Malin and Edgett (2000), it seemed that the occurrence of such rocks beneath relatively flat, regionally-extensive plains was largely limited to Sinus Meridiani. Most of the occurrences were in craters, chaotic terrain, and the chasms of the Valles Marineris (Malin and Edgett 2000). The notable exception was the suite of light-toned materials outcropping along the course and near the mouth of Mawrth Vallis in western Arabia Terra. Since that time, an additional suite of light-toned, layered rock outcrops has been identified; this group forms the plains into which some of the chasms of the Valles Marineris and Juventae Chasma are cut.

It is critical here to recognize that the observations presented in this section are not intended to imply that the rocks cut by Mawrth Vallis or by the Valles Marineris are the same geologic units as those in Sinus Meridiani, any more than a red sandstone outcropping in Utah would be of the same geologic formation as a red sandstone in Australia, or a gray limestone in Indiana would have any relation to a gray shale in southwest Colorado.

Mawrth Vallis

Mawrth Vallis is considered to be one of the circum-Chryse outflow channels (e.g., Rotto and Tanaka 1995). However, it is unusual relative to other martian outflow channels because it seems to begin fully born in the middle of nowhere, without the usual association that other circum-Chryse channels have with chasms or chaotic terrain. Figure 44 shows that Mawrth Vallis begins at nearly its full width just northwest of Trouvelot Crater. The source area and upper reaches of Mawrth Vallis might be either filled and buried and occur beneath the plains into which the Trouvelot Crater impact occurred (and perhaps were partially destroyed by this crater), or might have cut through strata that once occurred above Trouvelot Crater and were long ago eroded away. Regardless, in the context of Sinus Meridiani geology, what is important about Mawrth Vallis is that it cuts a bedrock of light-toned, layered material that is grossly

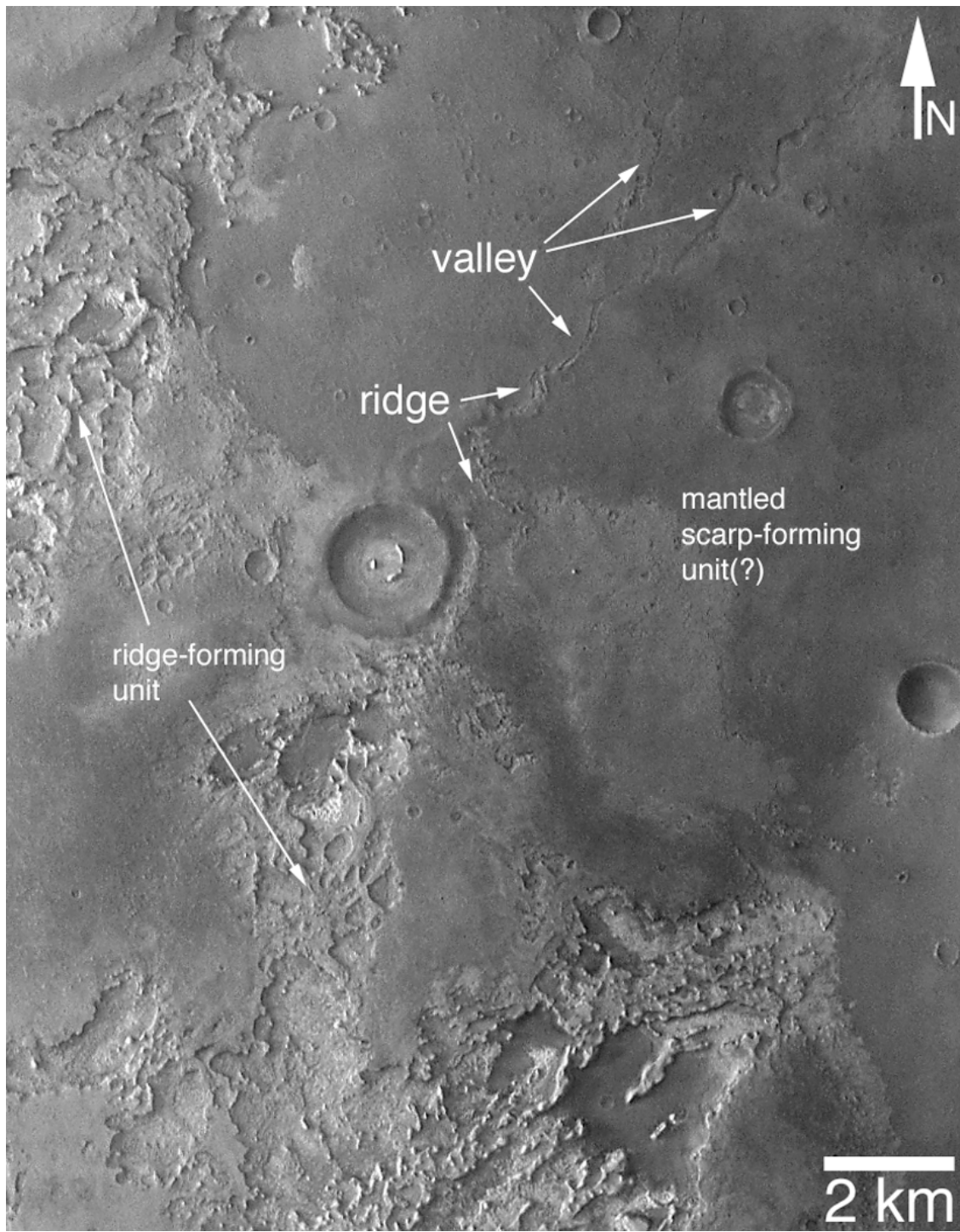


Figure 30. Exhumed valleys and valley networks, in some places found in inverted (ridge) form, and in some places found in negative relief (valley) form, are most common in Sinus Meridiani in the rock unit that underlies the ridge-forming unit; in other words, the scarp-forming unit. This picture shows a partially exhumed valley system that cut rock that lies below the ridge-forming unit. Dark-toned material mantles and obscures the bedrock into which the valley is cut. This is a sub-frame of THEMIS image V06229014, located near 3.7°N , 1.9°W ([figure30.png](#)).

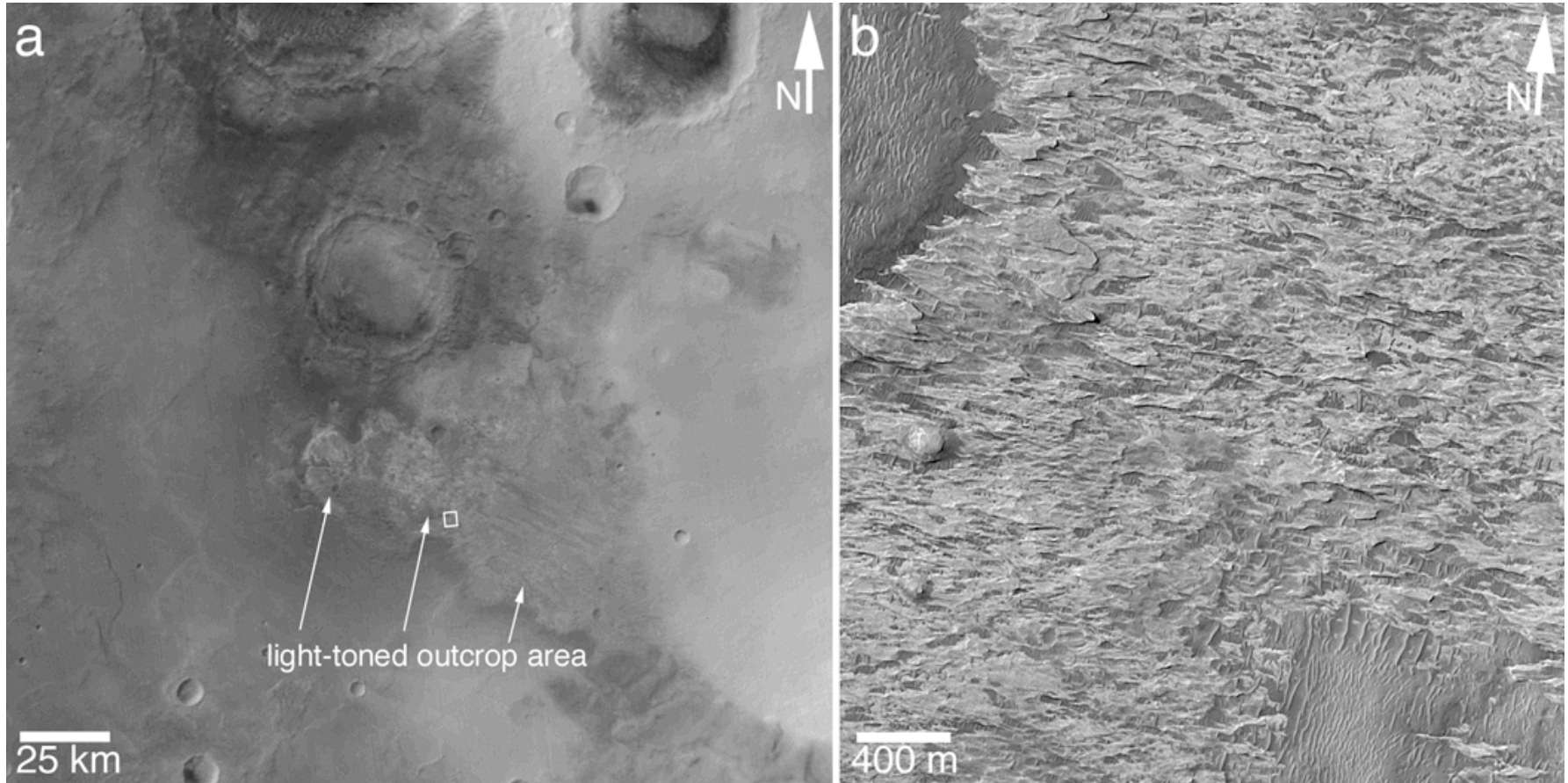


Figure 31. Light-toned sedimentary rock outcrops of the lower unit of the > 800 m stratigraphy in the Sinus Meridiani region. **(a)** Sub-frame of MOC red wide angle image M01-00457, showing the location of the light-toned outcrops. The materials occur west of Meridiani Planum, near 0° , 9°W ([figure31a.png](#)). **(b)** MOC narrow angle view of some of the light-toned rock outcrops in the region. The white box in (a) shows the location of these outcrops. This is a sub-frame of R20-01579, located near 0° , 8.9°W ([figure31b.png](#)).

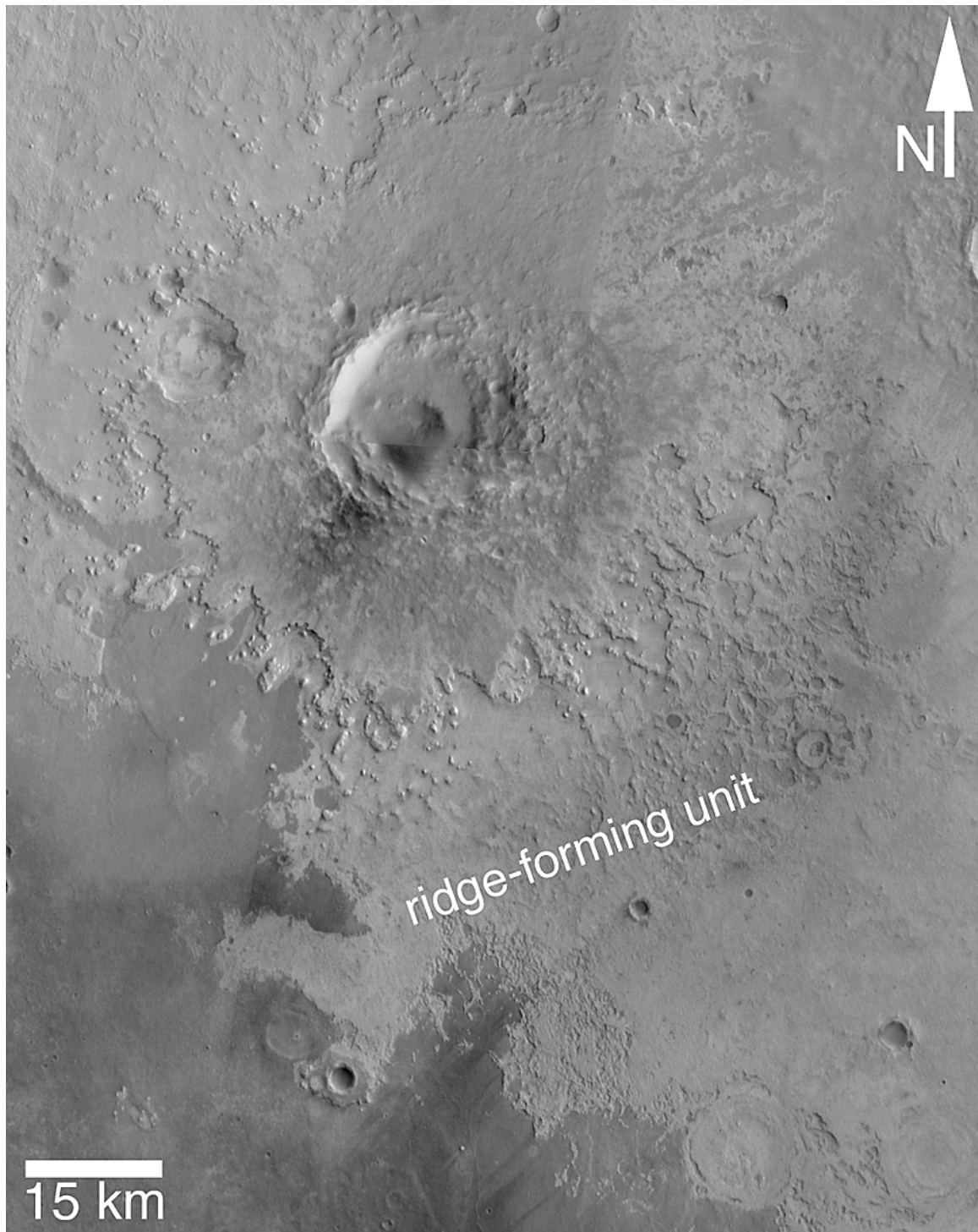


Figure 32. More than 150 m of layered rock are preserved beneath the ejecta of this pedestal crater in northwest Sinus Meridiani (crater 5 in Figure 18) near 7.2°N, 1.8°W. Below the rocks of the pedestal lies the ridge-forming unit. Therefore, the rocks contained within the pedestal include the plains-forming unit (including rocks contemporary with those explored by MER-B). This is a map-projected mosaic of the following THEMIS IR band 9 images: I01423006, I01398010, I01086005, I01061005, I01036006, I01735006, I02484009, I02509009, I02846002, I03208002, I03233012, I03595002, I04369005, I04756005. To enhance the visual appearance and approximate the visible albedo pattern of the region, the dynamic range of each individual image was inverted such that higher temperature surfaces appear dark ([figure32.png](#)).

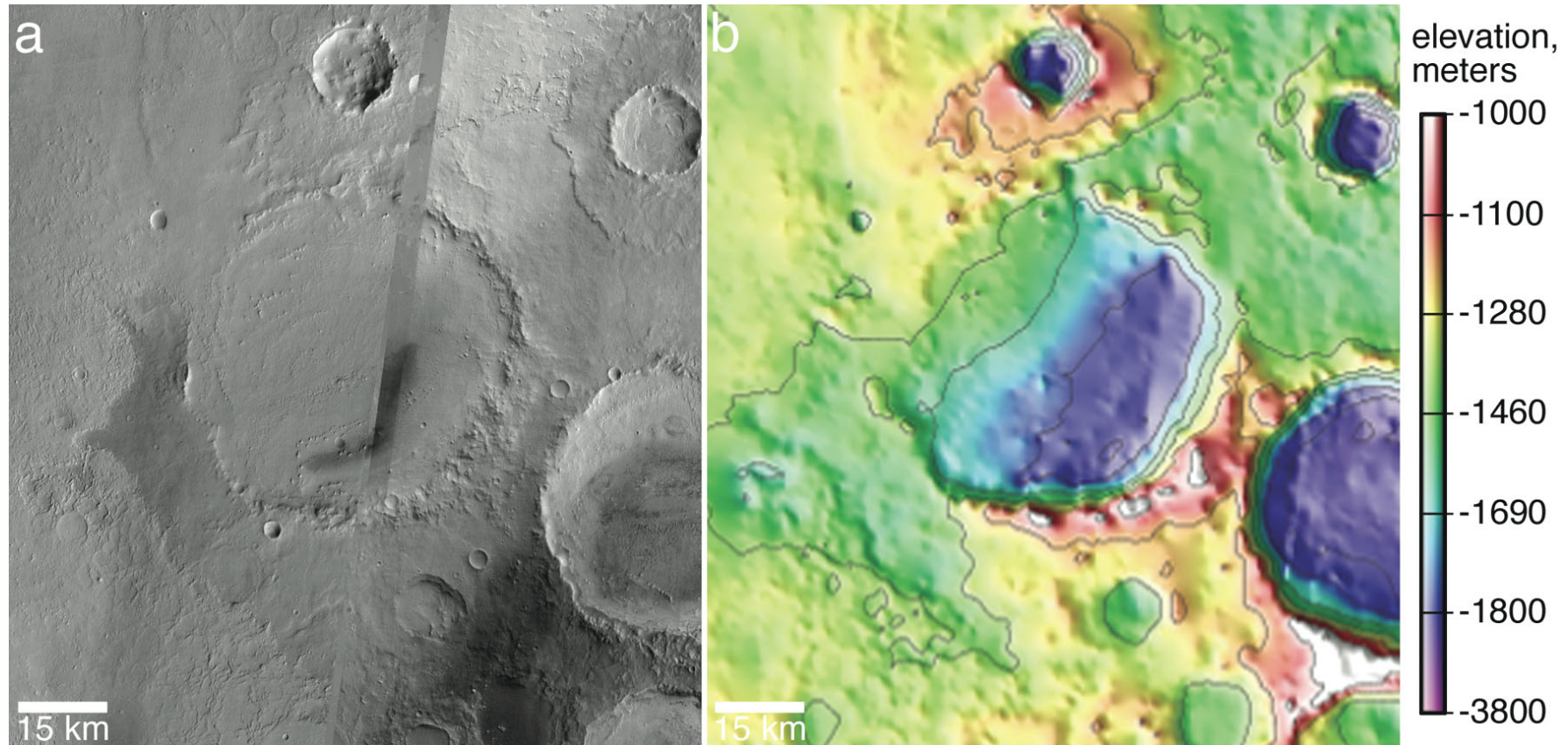


Figure 33. Crater 4 in Figures 17 and 18 is about 55 km in diameter—nearly the size of crater 1 at 8°N , 7°W —and is embedded within and only partially exhumed from the sedimentary bedrock of the northwest Sinus Meridiani region. **(a)** This is a map-projected mosaic of THEMIS band 9 infrared images I04831011, I01448009, I01498005, I01810005, I02584002, I03670002, I06666018, and I08139016. To enhance the visual appearance and approximate the visible albedo pattern of the region, the dynamic range of each individual image was inverted, such that the higher temperature surfaces appear dark ([figure33a.png](#)). **(b)** Topographic map derived from MGS MOLA observations, showing that the crater is only partly exhumed. This is a sub-section of the topographic map shown in Figure 17b ([figure33b.png](#)).

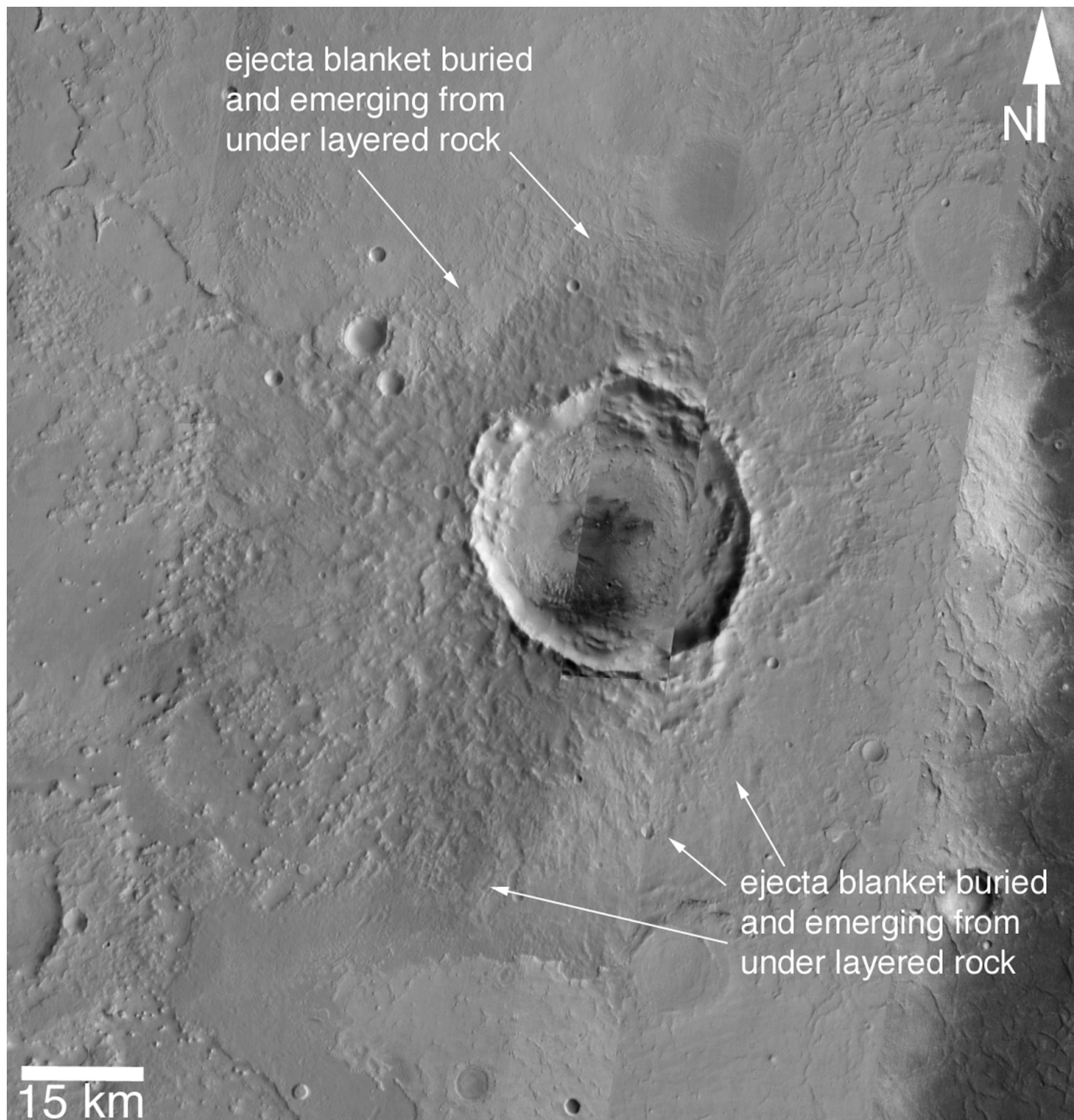


Figure 34. The ejecta blanket of this impact crater (crater 3 in Figure 18) is sandwiched between layered rock units in the cratered terrain west of Sinus Meridiani. The ejecta west of the crater has been completely exhumed; the ejecta to the south, east, and north of the crater is still largely buried beneath the surface. See Figure 18 for the stratigraphic placement of this crater's ejecta blanket, which lies between the ridge-forming unit and the scarp-forming unit. This is a map-projected mosaic of the following THEMIS IR band 9 images: I04856002, I04831011, I08164024, I04419010, I03695002, I01136002, I01498005, I01523017, I01860006, I02584002, I02609002, I0367002, I07415019, and I06666018. To enhance the visual appearance and approximate the visible albedo pattern of the region, the dynamic range of each individual image was inverted, such that higher-temperature surfaces appear dark ([figure34.png](#)).

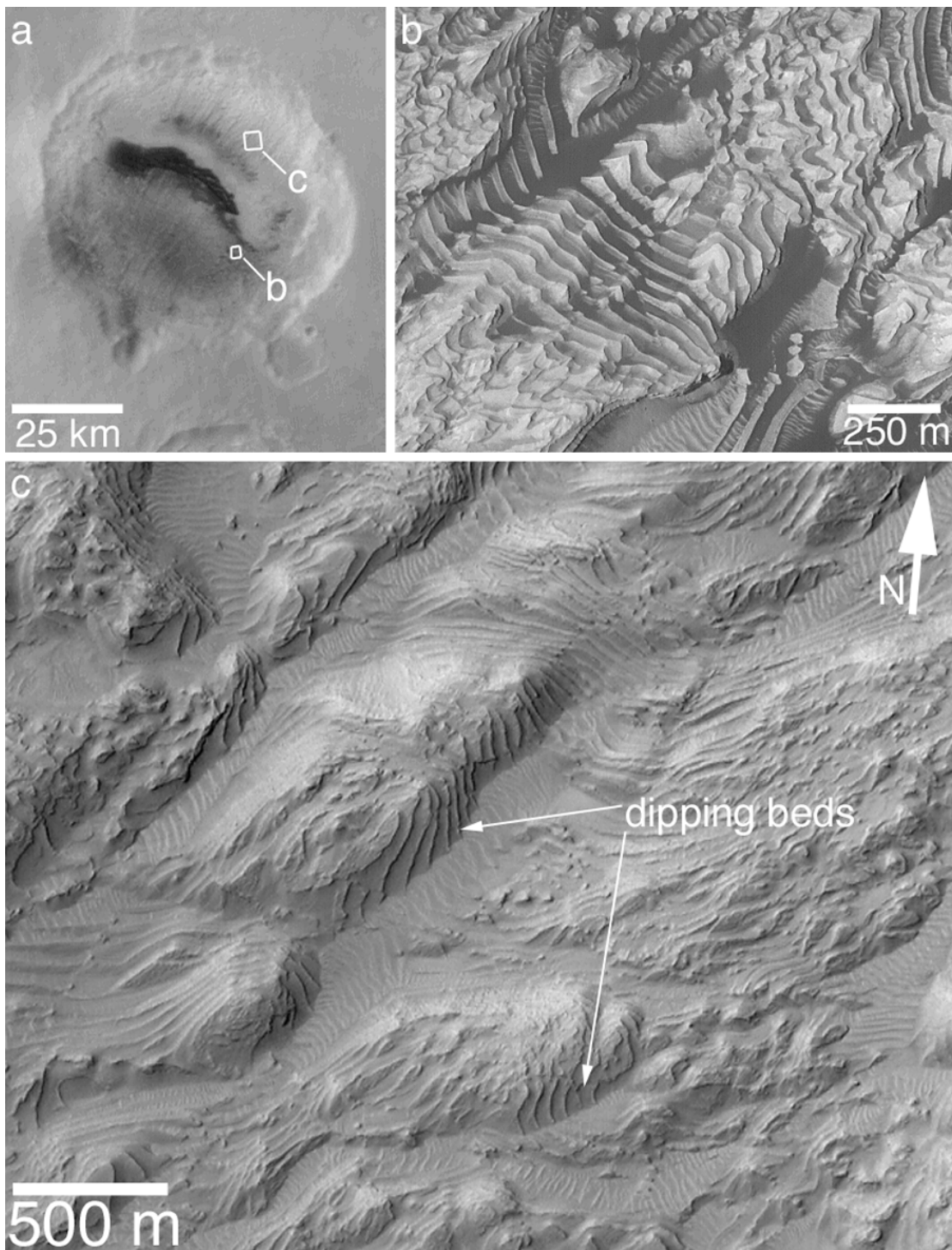


Figure 35. An unnamed, 60 km diameter crater at 8°N , 7°W (crater 1 in Figure 18). **(a)** MOC red wide angle view of the crater; a sub-frame of image M01-00847. The white boxes show the locations of narrow angle images in **(b)** and **(c)** ([figure35a.png](#)). **(b)** MOC narrow angle view of layers, contrast-enhanced by the presence of dark, windblown sand within the crater. Hundreds of repeated beds of similar thickness and erosional expression are present in the 8°N , 7°W crater. Although the crater is surrounded by mantled, layered sedimentary rock units, similar layers do not occur outside of the crater. This is a sub-frame of E05-00804 ([figure35b.png](#)). **(c)** Examples of dipping beds. Layers dip toward the interior of the crater, conforming to the original crater wall/floor topography. This is a sub-frame of MOC image E01-00102 ([figure35c.png](#)).

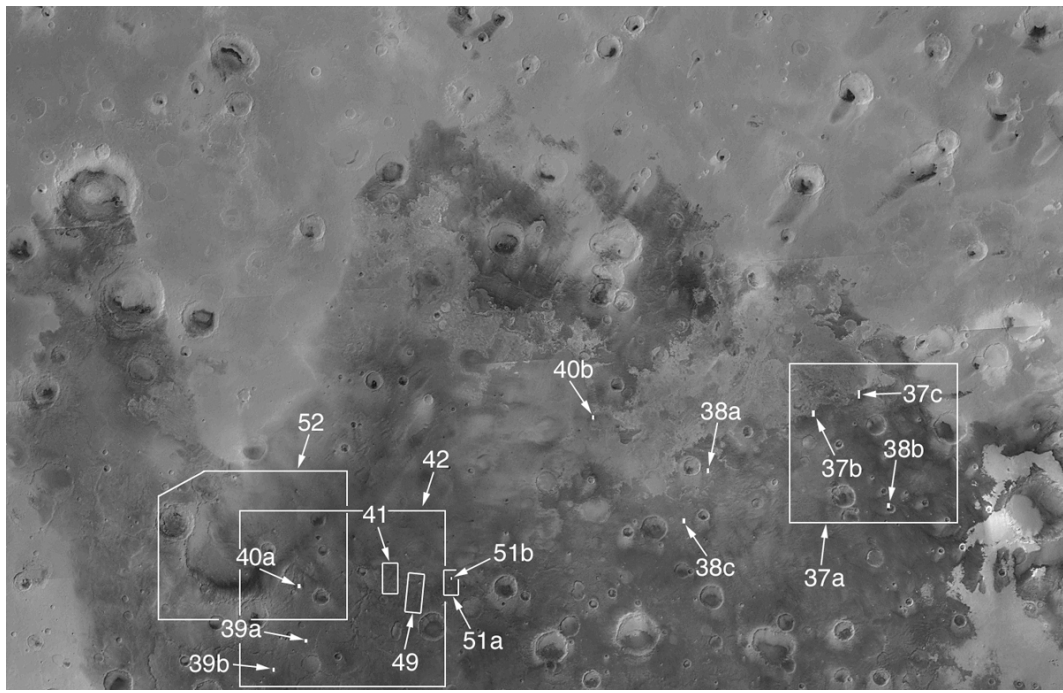


Figure 36. Map of Sinus Meridiani, showing the location of MOC, THEMIS, and Viking orbiter images in Figures 37–42, and 49, 51, 52 ([figure36.png](#)).

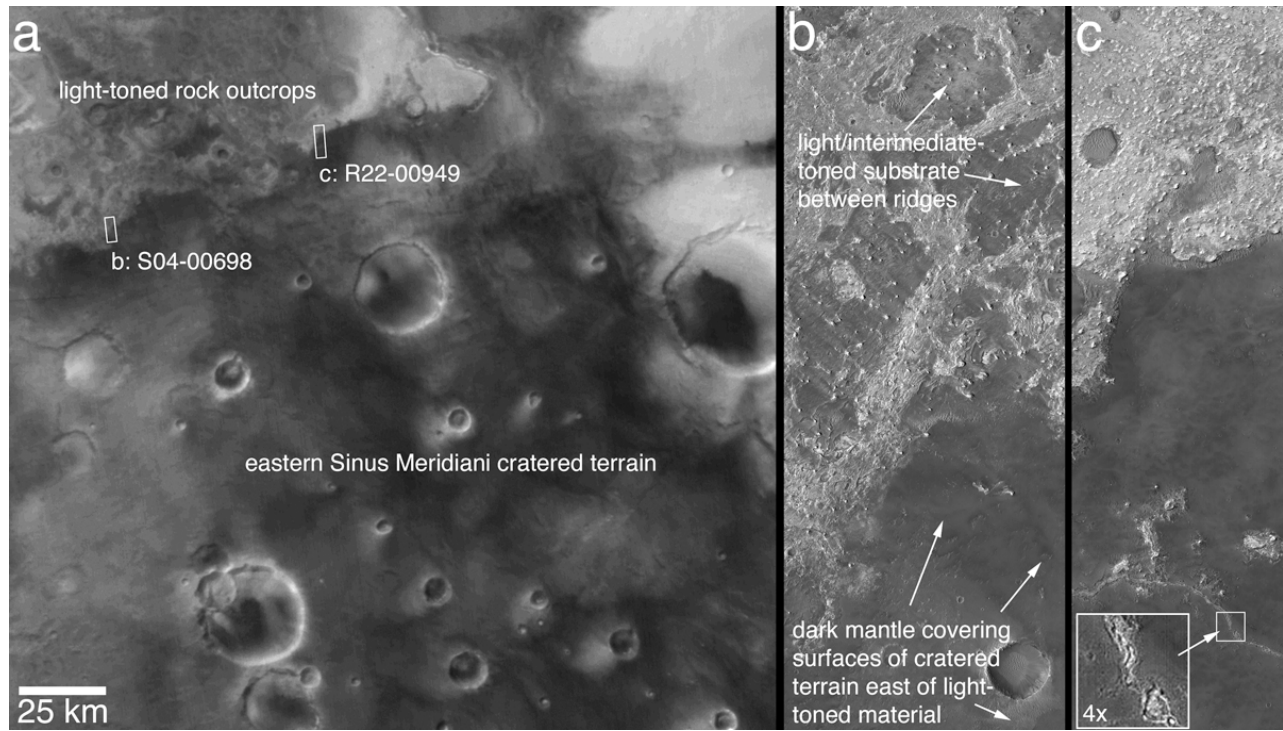


Figure 37. Examples of relations between light-toned rock outcrops and cratered terrain of eastern Sinus Meridiani. **(a)** Context in MOC red wide angle mosaic; north is up ([figure37a.png](#)). **(b)** Portion of MOC image S04-00698, showing indistinct nature of transition from light-toned rock to dark-toned, mantled surface of eastern Sinus Meridiani. Light- and intermediate-toned rock lies in lowlands between the light-toned ridges of the ridge-forming unit (R) outcropping in this area. This image is located near 0.1°N , 354.2°W ([figure37b.png](#)). **(c)** Sub-frame of MOC image R22-00949, showing high-standing, light-toned rock overlying a flatter, lower-lying substrate that is covered by a dark-toned mantle. The nature of the substrate beneath the mantle is uncertain, but the narrow valley in the southern quarter of the image exhibits light-toned outcrops. If the light-toned outcrops are the bedrock beneath the dark-toned mantle, rather than the remains of a light-toned material that filled the valley, then this observation suggests the bedrock beneath the dark-toned surface has a light tone. This image is located near 0.5°N , 353.1°W ([figure37c.png](#)).

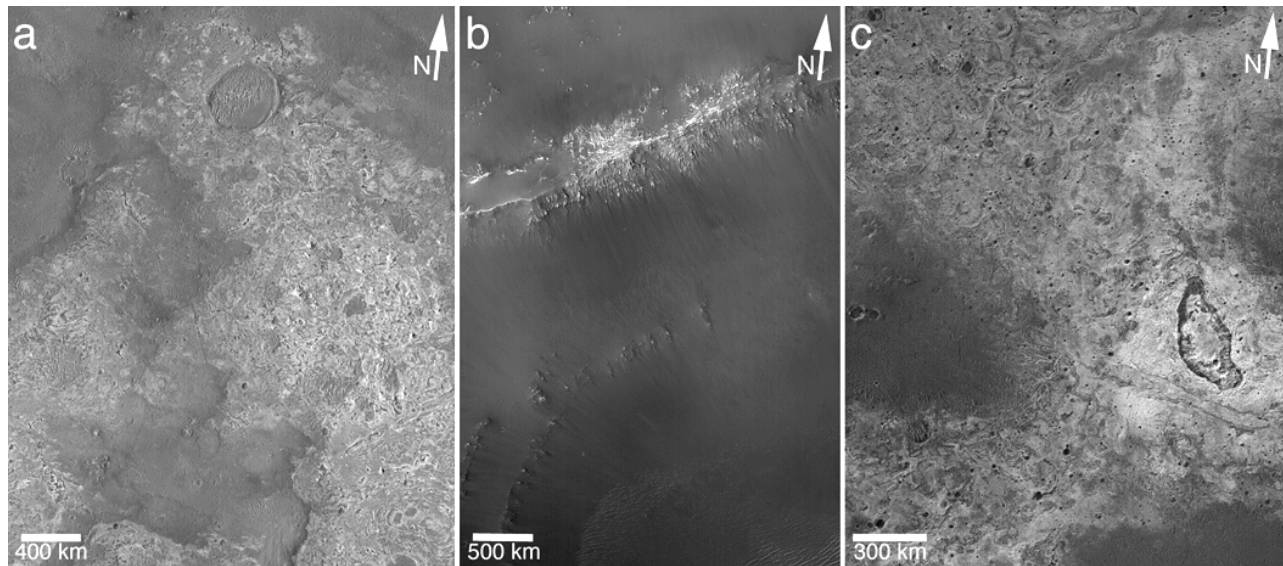


Figure 38. Windows through the dark mantling material in the heavily cratered terrain of eastern Sinus Meridiani reveal light-toned, layered bedrock that is similar to the materials outcropping in central and northern Sinus Meridiani. (a) Light-toned outcrops near 1.3°S , 356.5°W , in a sub-frame of MOC image S04-00262 ([figure38a.png](#)). (b) Light-toned, layered rock exposed in the wall of an impact crater near 2.0°S , 352.5°W , in a portion of MOC S05-01437 ([figure38b.png](#)). (c) Light-toned outcrops near 2.3°S , 357.1°W , in a portion of image S01-00728 ([figure38c.png](#)).

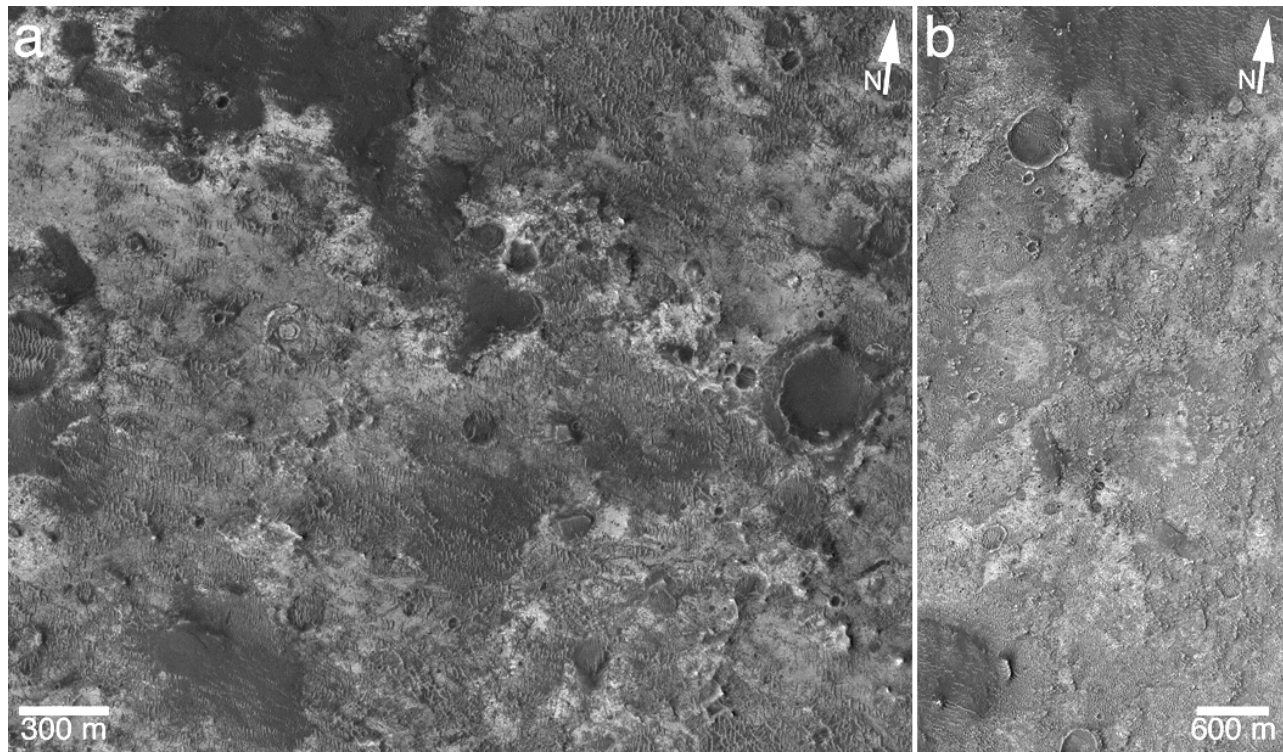


Figure 39. Examples of light-toned bedrock outcrops in southern Sinus Meridiani in the rugged, heavily cratered terrain south of the Meridiani Planum southern boundary. Dark-toned mantles and small ridge-forming materials (or windblown ripples) still partially cover the light-toned substrate in each example. (a) A sub-frame of MOC S06-02362, located near 5.0°S , 5.5°W ([figure39a.png](#)). (b) A sub-frame of MOC image R04-00059, located near 5.7°S , 6.3°W ([figure39b.png](#)).

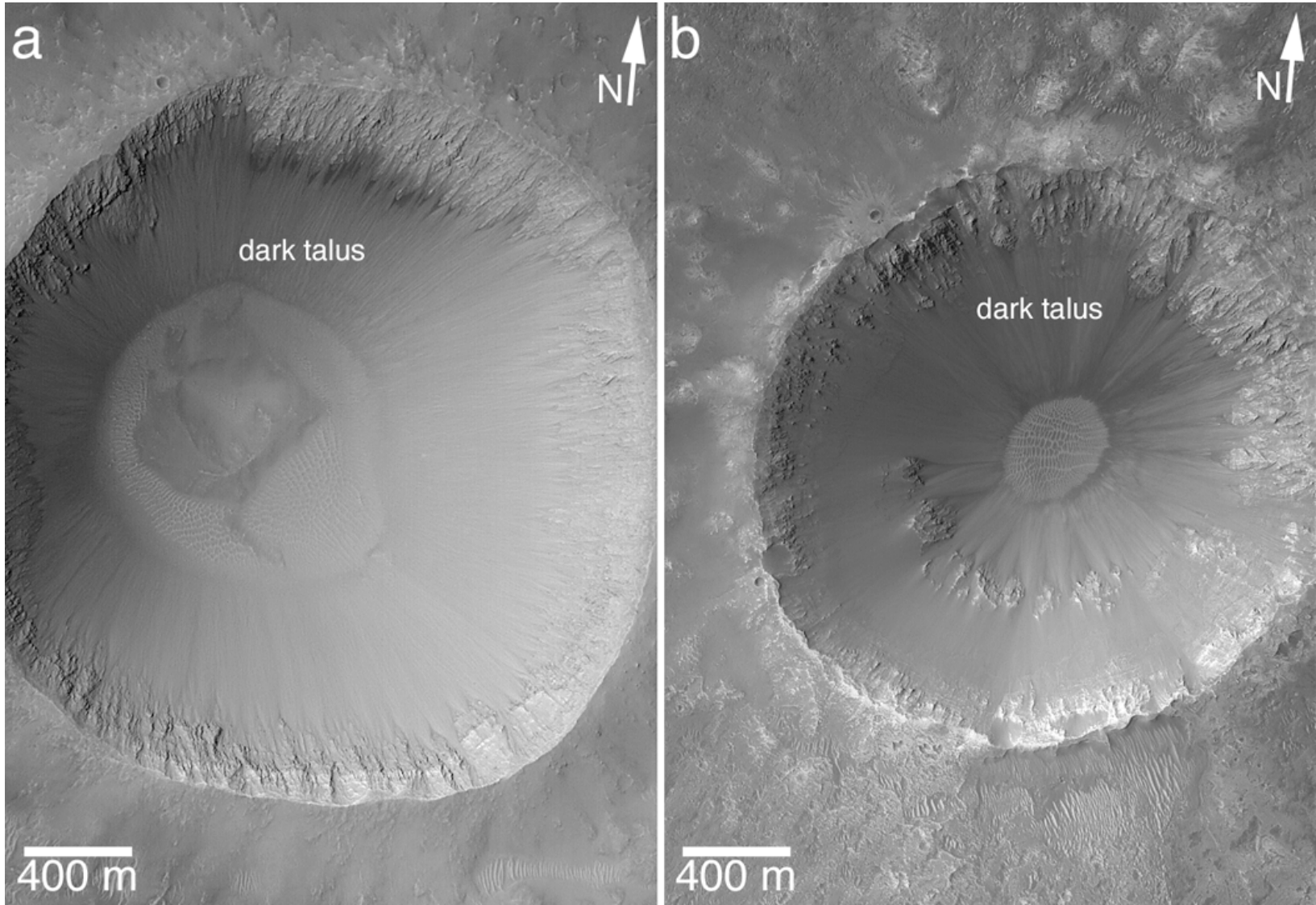


Figure 40. The similarity in the erosional expression of wall rock and in the presence of dark-toned talus derived from light-toned layered rock in these two impact craters suggests that both craters formed in a target material of similar physical properties and composition. Very few martian craters observed by the MGS MOC exhibit this particular suite of characteristics. (a) A crater formed in the rugged, heavily cratered terrain south of the Meridiani Planum southern boundary. This is a sub-frame of MOC image S04-00313, located near 3.8°S, 5.7°W ([figure40a.png](#)). (b) A crater formed in Meridiani Planum in a known substrate of light-toned, layered, sedimentary rock. This is a sub-frame of MOC image E04-00595, located near 0.1°S, 359.1°W ([figure40b.png](#)).

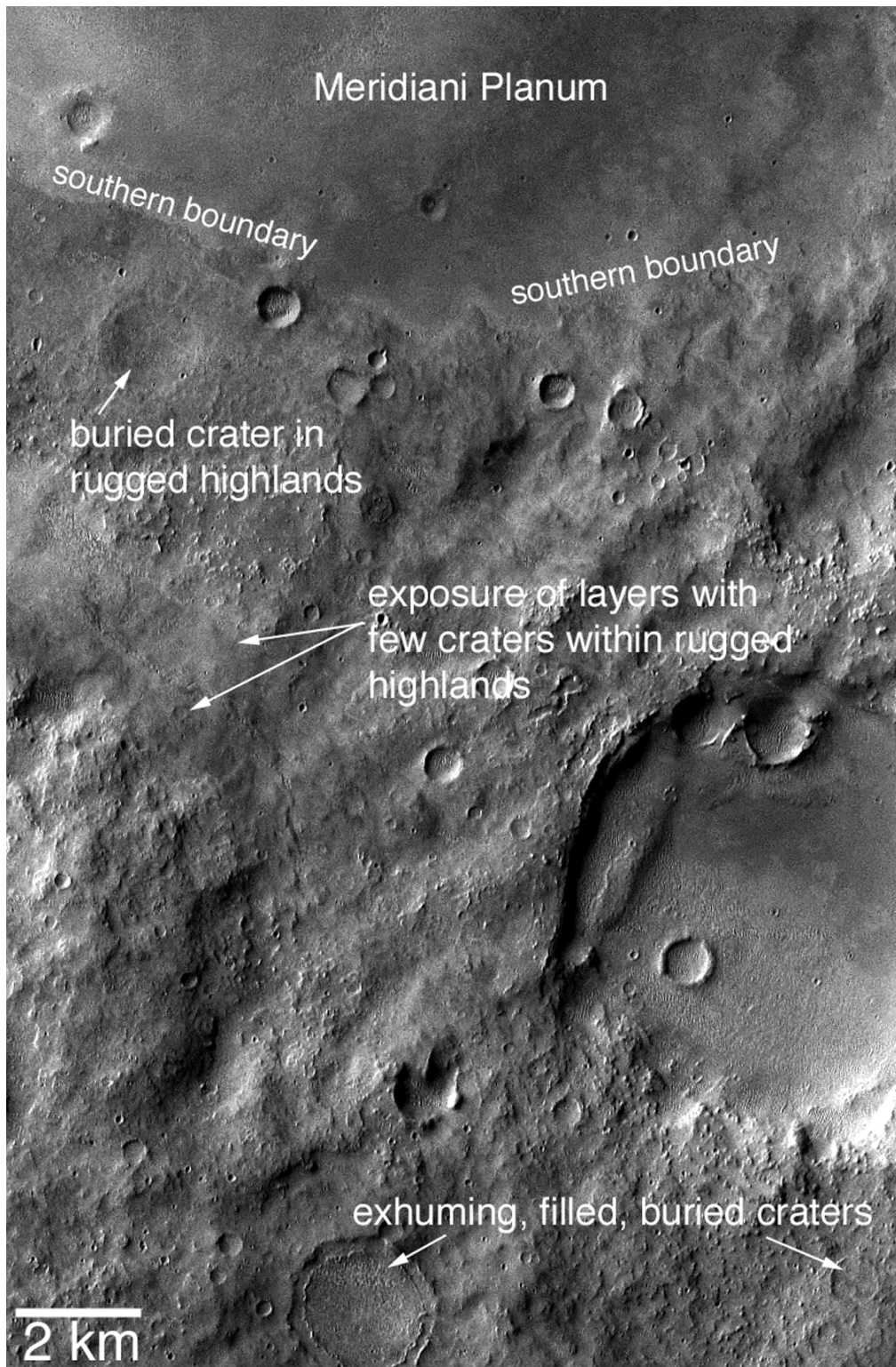


Figure 41. A typical view of the contact between Meridiani Planum and the rugged cratered highlands of southern Sinus Meridiani. The bedrock of the cratered terrain is also layered, and interbedded within this material is an array of filled, buried, and exhuming impact craters. While the erosional expression of the southern cratered highlands is different than that of Meridiani Planum and the light-toned, layered rock outcrops of northern Sinus Meridiani, the southern cratered highland shares the characteristics of layering and interbedded impact craters. This is a sub-frame of THEMIS VIS image V11572001, located near 3.6°S, 3.7°W ([figure41.png](#)).

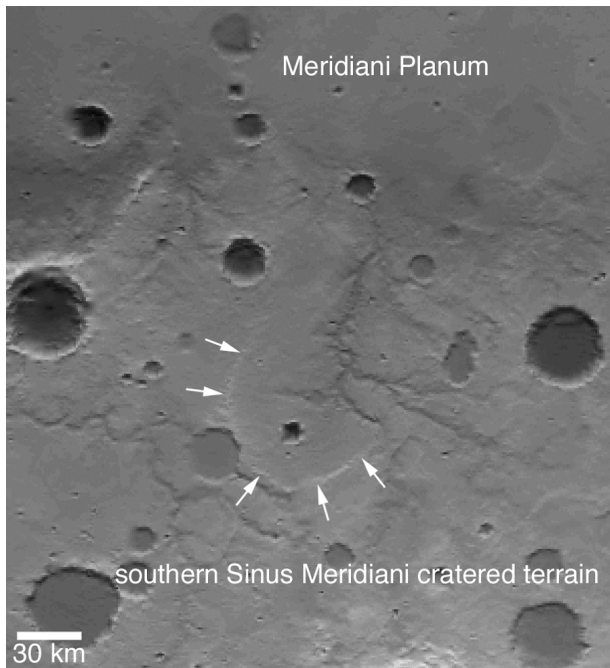


Figure 42. Example of a nearly filled, nearly buried, ~70 km diameter crater (arrows) in the heavily cratered terrain of southern Sinus Meridiani. The size of this crater should be compared with crater 4 in Figure 33 (55 km diameter) and crater 1 in Figure 35 (60 km diameter). This figure is a simple cylindrical projected shaded relief map constructed from MGS MOLA data. The ~70 km diameter feature is centered near 5.2°S, 4.7°W, north is up ([figure42.png](#)).

similar to some of the sedimentary rock occurrences in the Meridiani region (Figures 44, 45). Some of the materials have fine-scale layering that is visible in MOC images (Figure 45a), and many of the outcrops are superposed by dark-toned, mesa-forming material similar to dark mesa-forming occurrences in Sinus Meridiani (Figure 45b).

Plains cut by the Valles Marineris and Juventae Chasma

Figure 46 shows the Valles Marineris region including Juventae Chasma. The plains into which these troughs and chasms are cut have been considered to be volcanic for more than three decades. McCauley (1978), Scott and Tanaka (1986), and Whitbeck et al. (1991) mapped the plains as a unit interpreted as flood basalts because the plains are grossly similar to those of the lunar maria (relatively uncratered and bearing mare-type “wrinkle” ridges). At the west end of the Valles Marineris system, the Labyrinthus Noctis and parts of western Tithonium and Ius Chasms cut plains that have lava flows and small shield volcanoes. But MOC high-resolution images of other areas along the course of the Valles Marineris system show no volcanic landforms and abundant small outcrops of light-toned, layered rock that exhibit erosional expressions and bedding properties similar to occurrences of sedimentary rock found elsewhere on Mars, including Sinus Meridiani. Outcrops are especially common south of Ius Chasma, south of Melas Chasma, between Ius/Melas and west Candor Chasma, and west of



Figure 43. Example of eroded, layered bedrock and exhuming craters in eastern Arabia Terra near 24.7°N, 308.2°W. This is a sub-frame of THEMIS VIS image V01571010 ([figure43.png](#)).

Juventae Chasma (Figure 47). Like the layered rocks of Sinus Meridiani, those exposed in the Valles Marineris region form vast, relatively flat plains, and in some places they exhibit small exhumed and partially-destroyed impact craters.

Implications for Sinus Meridiani rocks

The observation of light-toned, layered rock outcrops in the vicinity of Mawrth Vallis and the Valles Marineris provides a temporal as well as global context for the MER-B results.

The temporal context is as follows:

- 1) The light-toned, layered rocks of the Mawrth Vallis region are cut by that valley. This implies that the rocks are quite old, old enough to have been solid rock at the time the valley formed. Figure 44c shows, too, that a crater of ~100 km diameter, and several smaller ones, formed in the light-toned rock. Because the materials are heavily cratered, they most likely date back to the Noachian Period.
- 2) The light-toned, layered rocks cut by the Valles Marineris chasms are at and just beneath lightly cratered plains considered to be Hesperian in age (McCauley 1978; Whitbeck et al. 1991).
- 3) That environments could exist in both the Noachian and in the Hesperian that would lead to deposition of material that forms rocks similar to those of Sinus

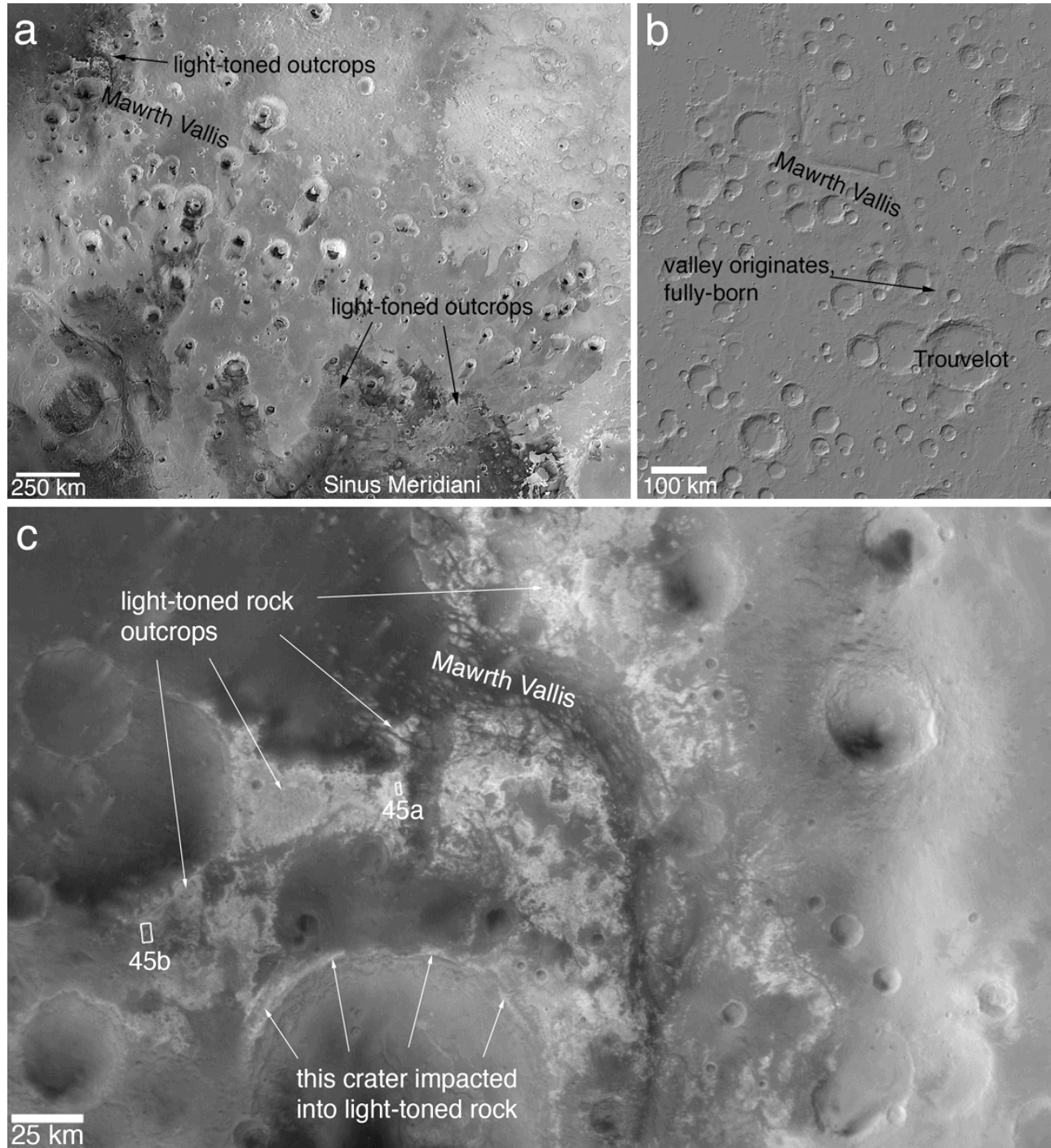


Figure 44. Mawrth Vallis and its light-toned rock outcrops. North is up in all three pictures. **(a)** Regional view showing the location of Mawrth Vallis relative to the Sinus Meridiani region. The base map is a mosaic of MGS MOC red wide angle images acquired in May 1999, from the MOC Geodesy Campaign ([figure44a.png](#)). **(b)** A shaded relief map derived from MGS MOLA data. The map shows that Mawrth Vallis begins, fully-born, just north of Trouvelot Crater. There are no contributory valleys nor evidence for a valley source in the regions south of Trouvelot ([figure44b.png](#)). **(c)** MOC red wide angle view of the majority of light-toned rock outcrops in the Mawrth Vallis region. This figure, centered near 25.4°N, 19.3°W, shows the location of MOC narrow angle images in Figure 45. This is a mosaic of sub-frames of M01-00664, M01-01055, and M01-01446 ([figure44c.png](#)).

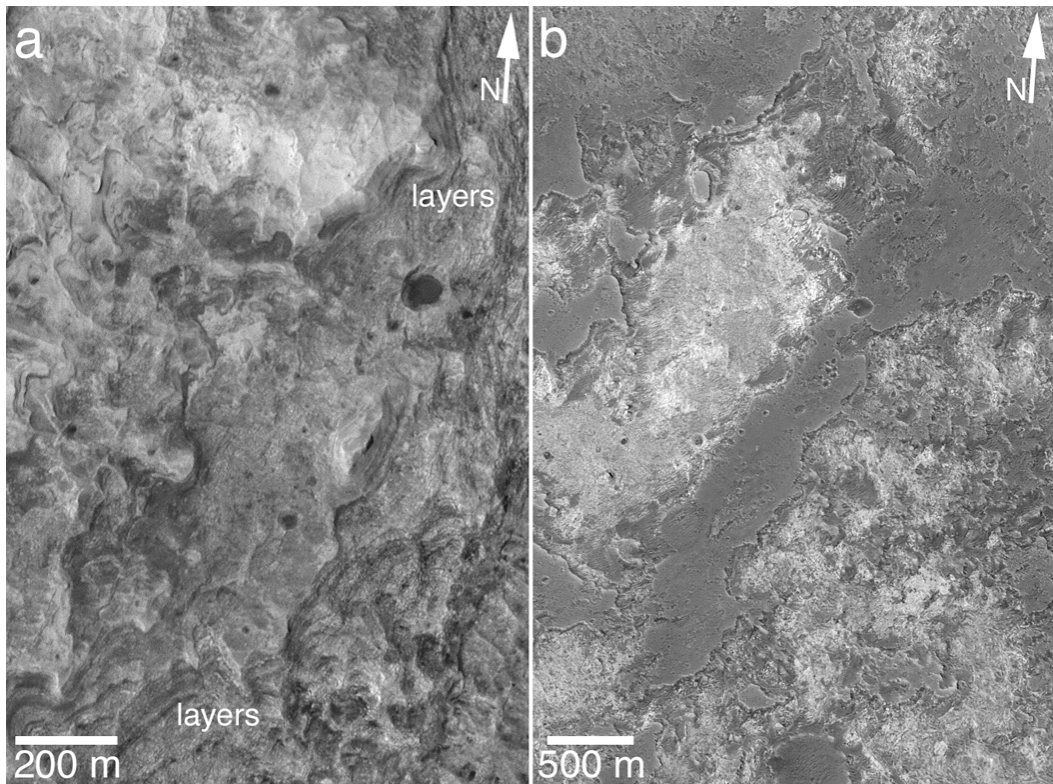


Figure 45. MOC views of light-toned rock outcrops near Mawrth Vallis. **(a)** Stair-stepped layered outcrops in light-toned bedrock. This is a sub-frame of MOC image R23-01316, located near 25.6°N, 20.2°W ([figure45a.png](#)). **(b)** Light-toned outcrops overlain by dark mesa-forming material. This is a sub-frame of MOC M03-01810, located near 24.8°N, 21.8°W ([figure45b.png](#)).

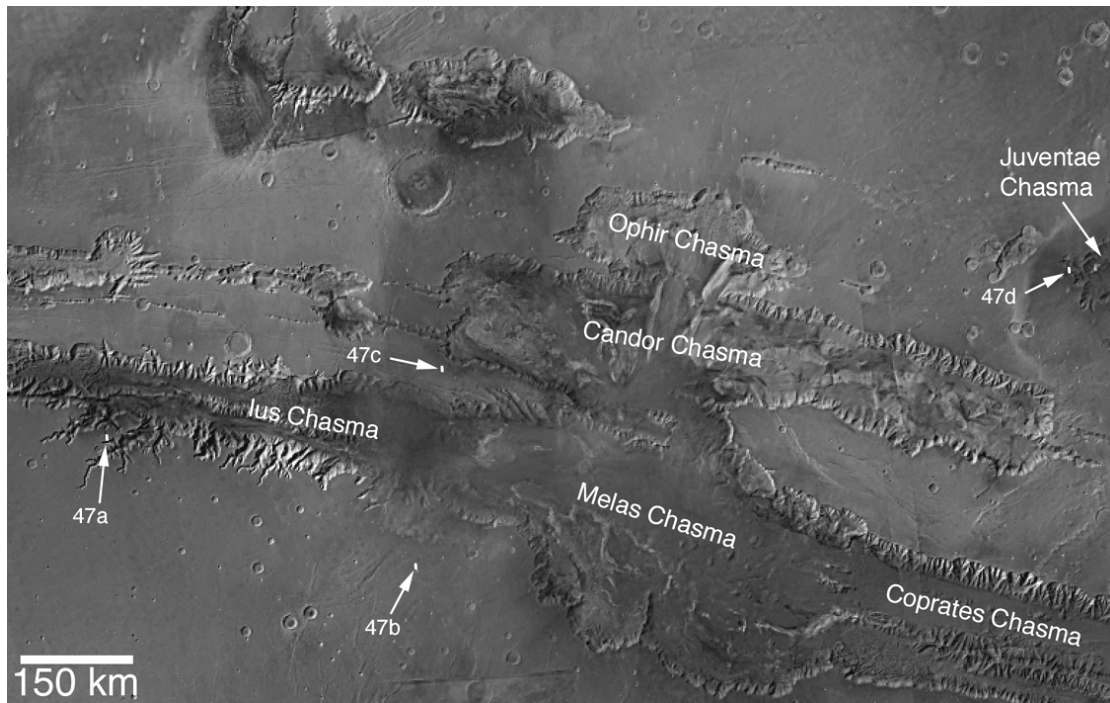


Figure 46. Map of a portion of the Valles Marineris region, showing the location of the four MOC images in Figure 47, which show light-toned, layered, sedimentary rock outcrops in the plains cut by the Valles Marineris troughs. The base map is a mosaic of MGS MOC red wide angle images acquired during the MOC Geodesy Campaign ([Caplinger and Malin 2001](#)) ([figure46.png](#)).

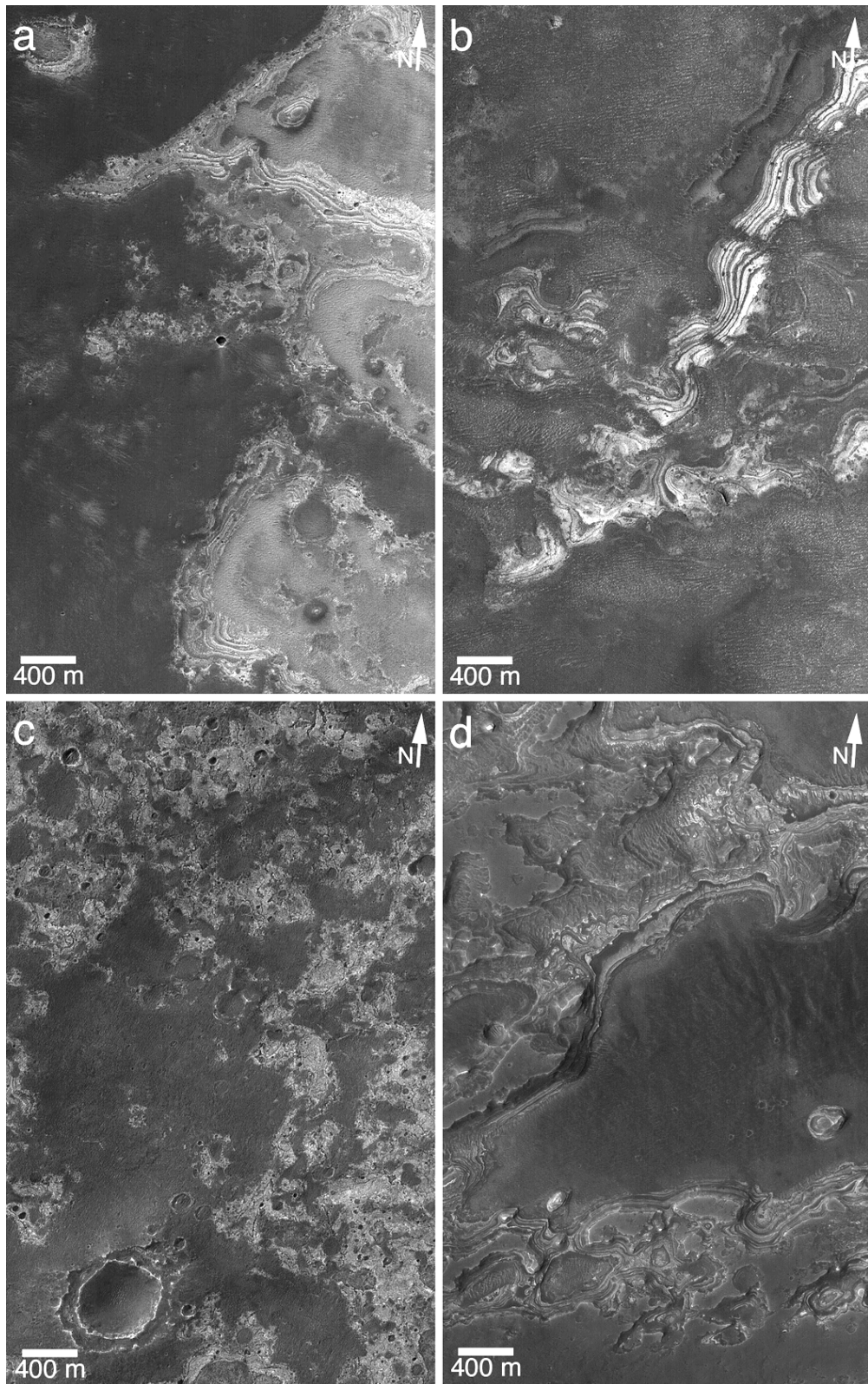


Figure 47. Examples of light-toned, layered, sedimentary rock outcrops in the plains cut by troughs of the Valles Marineris. (a) Outcrops located on the plains south of Ius Chasma in a sub-frame of MOC image R16-01143, located near 8.4°S , 84.9°W ([figure47a.png](#)). (b) Outcrops south of Melas Chasma in a sub-frame of MOC image R15-00758, near 11.2°S , 78.1°W ([figure47b.png](#)). (c) Outcrops on the plains between western Melas and western Candor chasms, sub-frame of MOC image R20-00356, near 6.9°S , 77.5°W ([figure47c.png](#)). (d) Sedimentary rock outcrops located west of Juventae Chasma near 4.8°S , 63.8°W ; this is a sub-frame of MOC R04-01154 ([figure47d.png](#)).

Meridiani suggests the that the rocks of Meridiani Planum do not necessarily date back to the Noachian, they could be Hesperian. The regional and topographic setting of the light-toned rock exposed in the vicinity of Mawrth Vallis suggests these rocks might occur, stratigraphically, somewhere below the ~800 m of strata exposed in the Sinus Meridiani region.

The rocks explored by MER-B and the other light-toned, layered, sedimentary rocks exposed by erosion in the Sinus Meridiani region are not the only such occurrences of extensive, light-toned, layered rock on Mars. Further, if it is true that the rocks at the MER-B site and throughout Sinus Meridiani were subjected to diagenesis in the presence of groundwater—and that some of these rocks might also be the products of subaqueous sedimentation—then it might also be true that the light-toned, layered rocks beneath the plains into which the Valles Marineris are cut have a history involving water and/or groundwater. This would imply a very different story for the many kilometers of layered rock cut by the Valles Marineris chasms than the volcanic history that is commonly assumed (e.g., McEwen et al. 1999).

Discussion

Summary of observations

The previous five sections presented an overview and basic framework for the geology of the Sinus Meridiani region. The five key observations that place the rocks examined by the MER-B team into context, are:

- 1) The rocks outcropping in the Sinus Meridiani region are more diverse than the suite of materials explored at the Mars Exploration Rover (MER-B) site.
- 2) Impact craters—of a range of diameters (from tens of meters to tens of kilometers)—and former valleys and streams are interbedded with the rocks exposed in the Sinus Meridiani region.
- 3) The ~7 meters of stratigraphic section observed by the MER-B team in the craters Eagle, Fram, and Endurance, cover less than 1% of the total >800 m of stratigraphic section observed in orbiter images of the region.
- 4) The bedrock of the heavily cratered terrain adjacent to Meridiani Planum is layered, possibly light-toned, and contains interbedded filled, buried, and exhumed impact craters.
- 5) Light-toned, layered, plains-forming rocks are not unique to Meridiani Planum and the Sinus Meridiani region; similar rocks are cut by Mawrth Vallis and form the plains cut by the Valles Marineris. These occurrences suggest the possibility that the rocks at the MER-B site may be younger than Noachian in age (i.e., Hesperian).

Relation of Meridiani Planum bedrock to the heavily cratered terrain

One of the key issues raised by this study is the relation between the light-toned, layered, sedimentary rocks of northern and central Sinus Meridiani to the heavily cratered terrain that is north, south, east, and west of the region. The traditional view is one of superposition—the layered rocks of Meridiani Planum are superimposed on a previous heavily cratered surface ([Schultz and Lutz 1988](#); Edgett and Parker 1997; [Hynek et al. 2002](#); [Arvidson et al. 2003](#); [Christensen and Ruff 2004](#)). The traditional view is illustrated in “cartoon” form in Figure 48a. The features that are actually observed—layered bedrock in both the cratered terrain and Meridiani Planum region, including the interbedding of large craters to the north and west of Meridiani Planum—are illustrated in Figure 48b.

The assumption illustrated in Figure 48a has its roots in lunar geology and in the poorer knowledge of the nature of the martian heavily cratered terrain during the 25 years between the Mariner 9 and Mars Global Surveyor missions. On the Moon there are two basic units: the heavily cratered highlands and the more lightly cratered maria. The lunar highlands are generally considered to be composed of anorthosite that has been severely brecciated by impacts, and the somewhat younger maria are flood basalts that superpose and embay the more ancient highland materials. On Mars, a hidden assumption that has persisted for several decades is that the heavily cratered terrain—sometimes called the “cratered highlands” although some areas in Arabia and Xanthe are below 0 km elevation—is something that might be monolithic, like the lunar highlands, and whether monolithic or not, it is often assumed to be the starting point for martian geology.

In other words, the hidden assumption holds that a heavily cratered terrain was formed, and then things happened to it—valley networks were created, other forms of erosion occurred, and volcanism and sedimentation superimposed their products on the cratered terrain. The notion that the martian cratered “highlands” may be a monolithic material is captured in the desire expressed by some investigators over the past decade (e.g., De Hon 1994; Murchie and Treiman 1994; Barlow 1999; Gilmore and Tanaka 2001) that a lander or rover should be dispatched to “a highlands site” as if one landing in the heavily cratered terrain of Mars would help characterize all of it, at least to the level that a landing in the lunar highlands would for the Moon.

The lunar-like view of the layered rocks of Meridiani Planum is further enhanced by a specific physiographic feature along the southern margin of Meridiani Planum. Labeled as the “southern boundary” in Figures 2, 41, and 49, this is the only clear boundary along which there is a sharp transition from surfaces that are lightly cratered (plains-forming material, unit (P)) to those that are rugged and more heavily cratered. Other transitions from the ~800 m of Meridiani Planum/northern Sinus Meridiani strata to cratered terrain are less distinct and—in the north and west—include the intermingling of what can be considered heavily cratered terrain bedrock with the sedimentary rock stratigraphy.

The relationship between Meridiani Planum bedrock and the

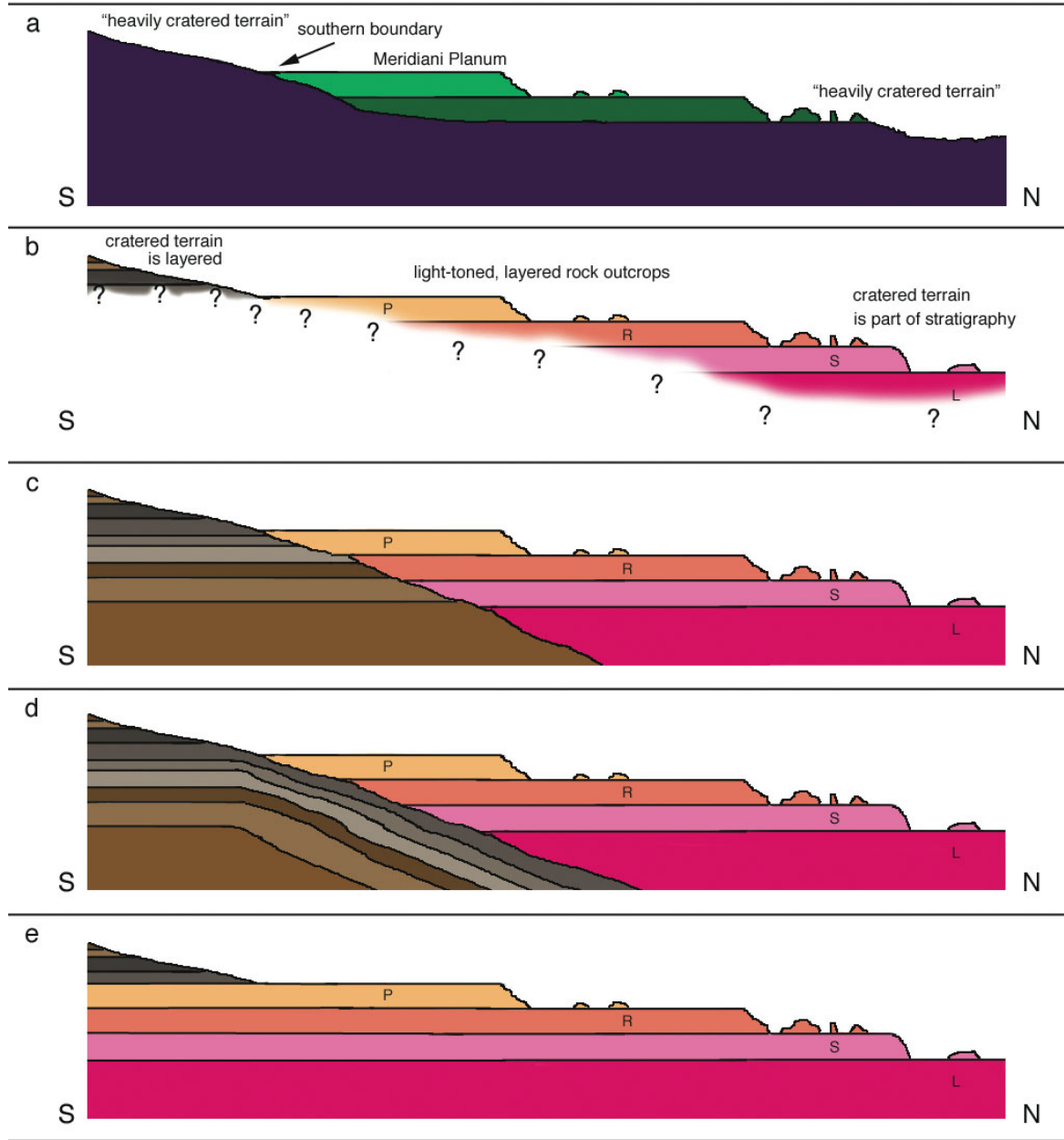


Figure 48. Simplified (cartoon) south-to-north cross-sections describing alternative views of the subsurface beneath western Sinus Meridiani. Features labeled P, R, S, and L, represent the units in Figure 18. **(a)** The traditional, lunar-like view, in which green represents a layered “deposit” superimposed on a heavily cratered terrain (purple). **(b)** A sketch of features observable from orbit—the cratered terrain north of Meridiani Planum is an extension of the layered, sedimentary rocks beneath the plains; and the rugged, cratered highlands south of the plains are also layered and light-toned but have a different erosional expression, and thus might be a different material. **(c)** One alternative interpretation of the relation between the rocks of Meridiani Planum and those to the south of the southern boundary; this view holds that an impact or erosional event separates the strata of material south of Meridiani Planum from those to the north. **(d)** An alternative in which the rocks found south of Meridiani Planum are dipping beneath those of and to the north of Meridiani Planum. **(e)** A third, less-likely alternative in which the heavily cratered rocks south of Meridiani Planum are actually younger than the more lightly cratered rocks found to the north—a product of rapid sedimentation of the P, R, S, and L units—and the capability of a given rock unit to retain craters ([figure48.png](#)).

heavily cratered terrain to the north, east, and west is different than that of the relationship along the southern boundary. The situation is reminiscent of some of the artwork of M. C. Escher (1898–1972). Escher produced several pieces in which staircases seemed to go both up and down (“House of Stairs,” 1951; “Ascending and Descending,” 1960), or a waterfall seemed to feed itself, falling down only to be recaptured and transported to the top of the falls without flowing up hill (“Waterfall,” 1961). If one approaches martian geology with a lunar- or Mariner/Viking-trained perspective, then the relationship along the southern boundary is the one that makes sense and defines the stratigraphic position of the Meridiani Planum bedrock. But the other relationships, to the north, west, and east, do not make sense in this perspective and seem instead to be like Escher’s waterfall or staircases.

How are these views to be reconciled? The approach lies in the nature of both the heavily cratered terrain and the ~800 m of sedimentary rock stratigraphy in the Meridiani Planum region. Both materials are layered, both contain interbedded craters and valleys, and both have surfaces—exposed at the interface with the martian atmosphere—that have undergone erosion. And, in the north and west, the two become one—the lower strata of the Meridiani Planum stratigraphy and the bedrock into which large craters in southwest Arabia Terra formed, are the same.

Martian geology cannot be considered in terms of surfaces—it is a three-dimensional problem. The upper crust of Mars is composed of a complex interbedding of layered rock, filled and buried impact craters, valleys, and previously-eroded surfaces. Frey et al. (2003) recognized in MOLA topography the presence in the cratered highlands of many buried impact craters and basins. They suggested that these represent a buried surface; Malin and Edgett (2001) and work presented here argue that there are/were many cratered surfaces buried and complexly interbedded within the upper crust of Mars.

Another issue is that of crater retention. Some rocks are more easily eroded than others, and thus do not retain as many impact craters as do more resistant rocks of similar, or even younger, age. This is evident, for example, when one compares the plethora of small craters (< 200 m diameter) preserved on the hard lava flow surfaces of relatively young martian volcanoes such as Olympus and Ascraeus Mons, with the almost uncratered surfaces of light-toned, layered rock outcrops in Sinus Meridiani, west Candor Chasma, and elsewhere. In other words, heavily cratered surfaces are not always indicative of the oldest rocks; the resistance of the material to erosion is important in crater retention.

Figure 48c–e illustrates three alternative perspectives on the rock beneath Sinus Meridiani. All three recognize the observations diagrammed in Figure 48b. The actual configuration of the strata is likely to be much more complicated than the views presented here—the illustrations do not account for the possibility of facies changes, interbedding and lateral pinching-out of rock units, or other complexities. The true situation could be a hybrid of two or all three of these alternatives. In two of the cases—Figures

48c and 48d—something changes beneath Meridiani Planum. This is suggested by the observations because the rocks beneath the plains-forming unit (P) in northern Sinus Meridiani are, clearly, those of the ridge-forming unit (R), but the rocks beneath the plains-forming unit along the southern boundary of Meridiani Planum are those that comprise the rugged, heavily cratered terrain of southern Sinus Meridiani.

Figure 48c suggests that the change beneath Meridiani Planum near the southern boundary may be one in which erosion or impact cratering created a sharp transition. That the transition could be the product of an impact event might be strengthened by the proposal of [Newsom et al. \(2003\)](#) that northern Sinus Meridiani is the site of a very ancient, multi-ringed basin. However, another possible impact basin outline is illustrated in Figure 50.

Figure 48d suggests that the change beneath Meridiani Planum might be the product of crustal warping—like the intra-cratonic warps on Earth, such as those that formed the Williston and Michigan Basins in North America—so that the rocks of the cratered terrain dip below Meridiani Planum.

Finally, Figure 48e illustrates a radical interpretation. In this case, the southern boundary is the product of southward retreat by erosion of the layered rocks of the heavily cratered terrain. Figure 51 shows a scarp facing north along the southern boundary—a relationship at odds with the view that the boundary is produced by deposition of the plains-forming unit on top of the cratered terrain, but not the norm in the region. Figure 49, on the other hand, shows outliers of plains-forming (P) material overlying the rugged surface of the cratered terrain. If Figure 48e is the correct interpretation, then the issues of crater retention and rapid burial or burial in a thickened sequence of rock, would need to be invoked to explain how a rock unit that lies stratigraphically above the plains-forming unit (P) could be so much more heavily cratered.

What lies beneath the MER-B site?

Figures 48c and 48d present the more likely relationships, albeit in very simple form, between the rocks of Meridiani Planum and those of the cratered terrain of southern Sinus Meridiani. If one were to drill downward from the plains at the MER-B site, would one encounter rocks of the ridge-forming unit (R) followed by rocks of the scarp-forming unit (S) and lower unit (L)? Or would one encounter the layered rocks of the cratered terrain of south Sinus Meridiani? The complication illustrated in Figure 48 regarding the fact that the plains-forming unit (P) overlies one thing in the north (unit R), and something else in the south (the material that is expressed by a rugged, cratered surface), means that understanding what lies beneath the rover site cannot be determined with certainty.

However, a few things can be observed. The first is that the plains-forming unit (P) has—with it—small, interbedded impact craters. Craters have been filled, buried, and in some cases exhumed or partially exhumed. Thus, beneath the

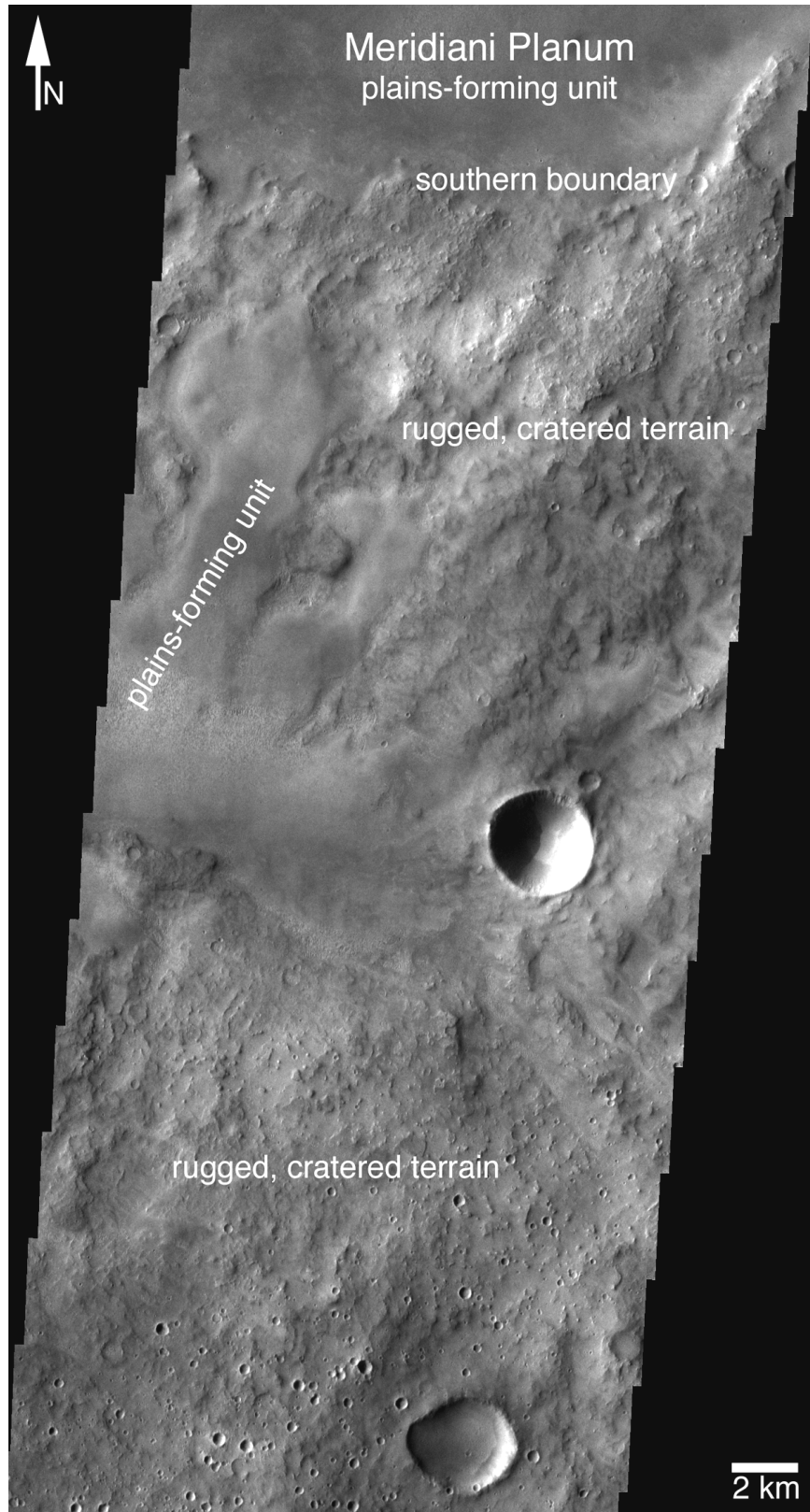


Figure 49. A sub-frame of THEMIS VIS image V10636002, showing an outlier of plains-forming material that occurs south of the Meridiani Planum southern boundary. This relation suggests that the bedrock of the rugged, cratered terrain of southern Sinus Meridiani is likely to be older than the plains-forming rock, and that these previously-eroded, cratered surfaces may be exhumed ([figure49.png](#)).

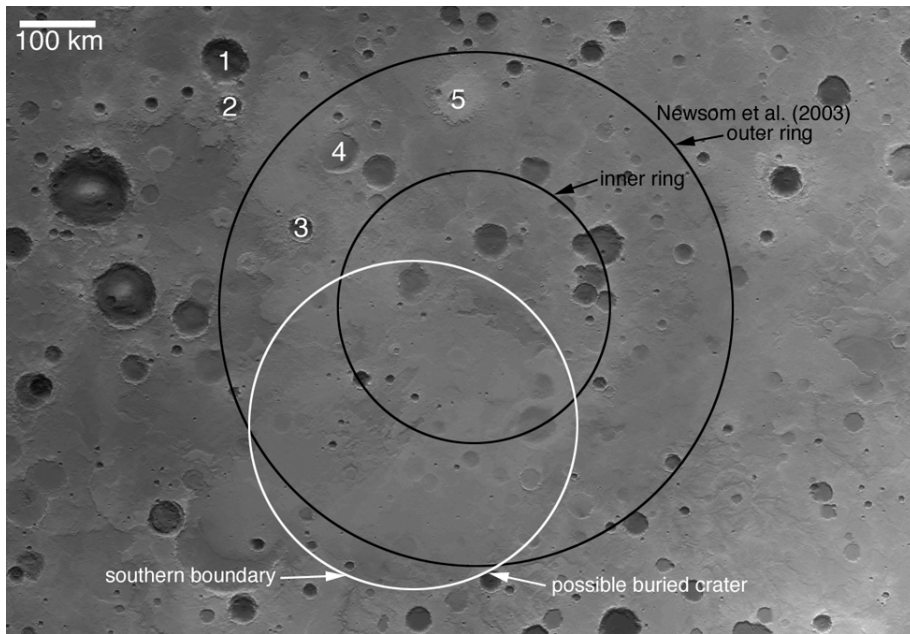


Figure 50. Newsom et al. (2003) proposed that northern Sinus Meridiani is underlain by the remains of a large, eroded, multi-ringed impact basin. Their outlines are shown in black. An alternative, smaller basin is suggested by the configuration of the southern boundary at the south edge of Meridiani Planum. Either of these alternatives would result in a subsurface configuration similar to "c" in Figure 48. However, it is equally possible that no ancient impact basin(s) are present at this location. For reference, the numbers, 1–5, correspond to those in Figures 17 and 18. This map is derived from MGS MOLA observations ([figure50.png](#)).

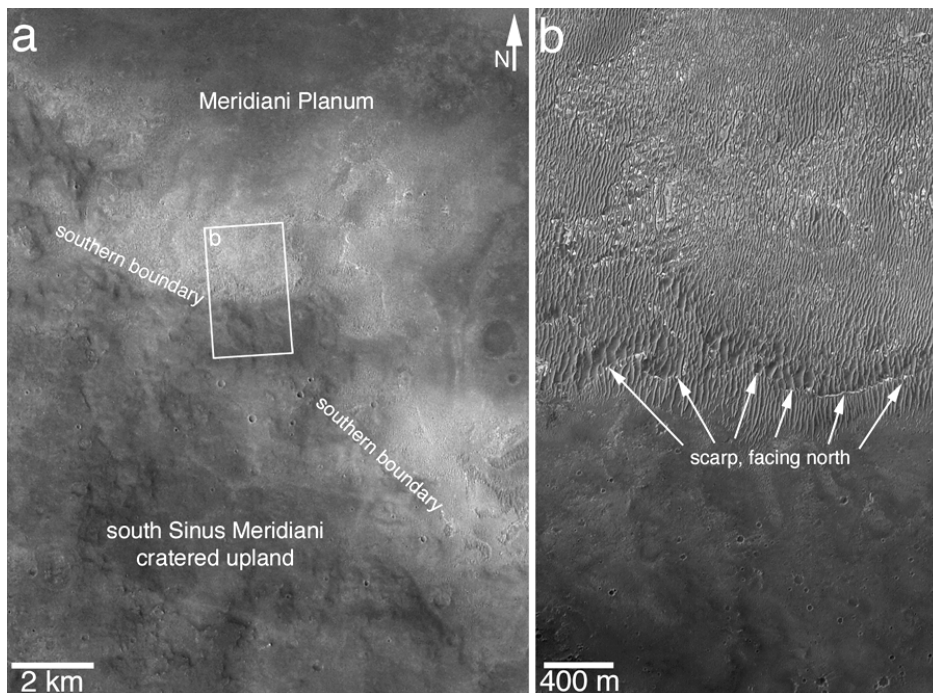


Figure 51. Example of retreating scarp relation between Meridiani Planum and the bedrock of the rugged, cratered upland of southern Sinus Meridiani. This relationship is atypical. **(a)** A sub-frame of THEMIS VIS image V08789001, located near 4.0° S, 2.3° W ([figure51a.png](#)). **(b)** A sub-frame of MOC image M00-02021, showing the north-facing scarp cut into the bedrock of the rugged, cratered upland. The scarp is only a few meters high and somewhat obscured by small ridge-forming material ([figure51b.png](#)).

plains that the rover is operating upon, there may be additional small craters that formed on surfaces that were later buried and became a part of the plains-forming bedrock. The other observation is that of a ~140 km diameter crater that is partially exhumed from beneath the sedimentary rock of west-central Sinus Meridiani (Figure 52). The MER-B site is near the buried northeast rim—on the outward-facing slope of this rim—of this crater. Thus, if one were to drill downward from the MER-B site, one might encounter brecciated rock and ejecta from this crater.

Exhumed craters

The exhumation of buried landforms is common on Mars, as initially noted by Malin (1976) and reiterated upon receipt of MOC data by [Malin and Edgett \(2001\)](#) and [Edgett and Malin \(2002\)](#), among others. Exhumation of ancient terrain elements is not unique to Mars. For example, there is a rather famous relationship between Precambrian knobs of rhyolite and on-lapping Upper Cambrian marine sedimentary

rocks in the St. Francois Mountains of southeastern Missouri in North America, illustrated by an outcrop near the Taum Sauk Power Plant ([Kisvarsanyi and Hebrank 1987](#)). While the rocks in Sinus Meridiani are generally flat-lying, rocks—like those at the Taum Sauk Power Plant site—can be locally dipping in response to underlying topographic features such as crater walls and rims. Such appears to be the case, for example, in the unnamed crater at 8°N, 7°W (Figure 35).

Preservation of impact craters in the martian rock record may argue that the processes involved with both burial and exhumation were relatively benign or gentle. Differences between bedding inside and outside of craters may argue that the depositional environments were different as well. For example, the craters may have been lacustrine settings while the terrain outside of craters could have experienced more episodes of subaerial sedimentation. Gentle burial of craters implies that the processes involved were of relatively low

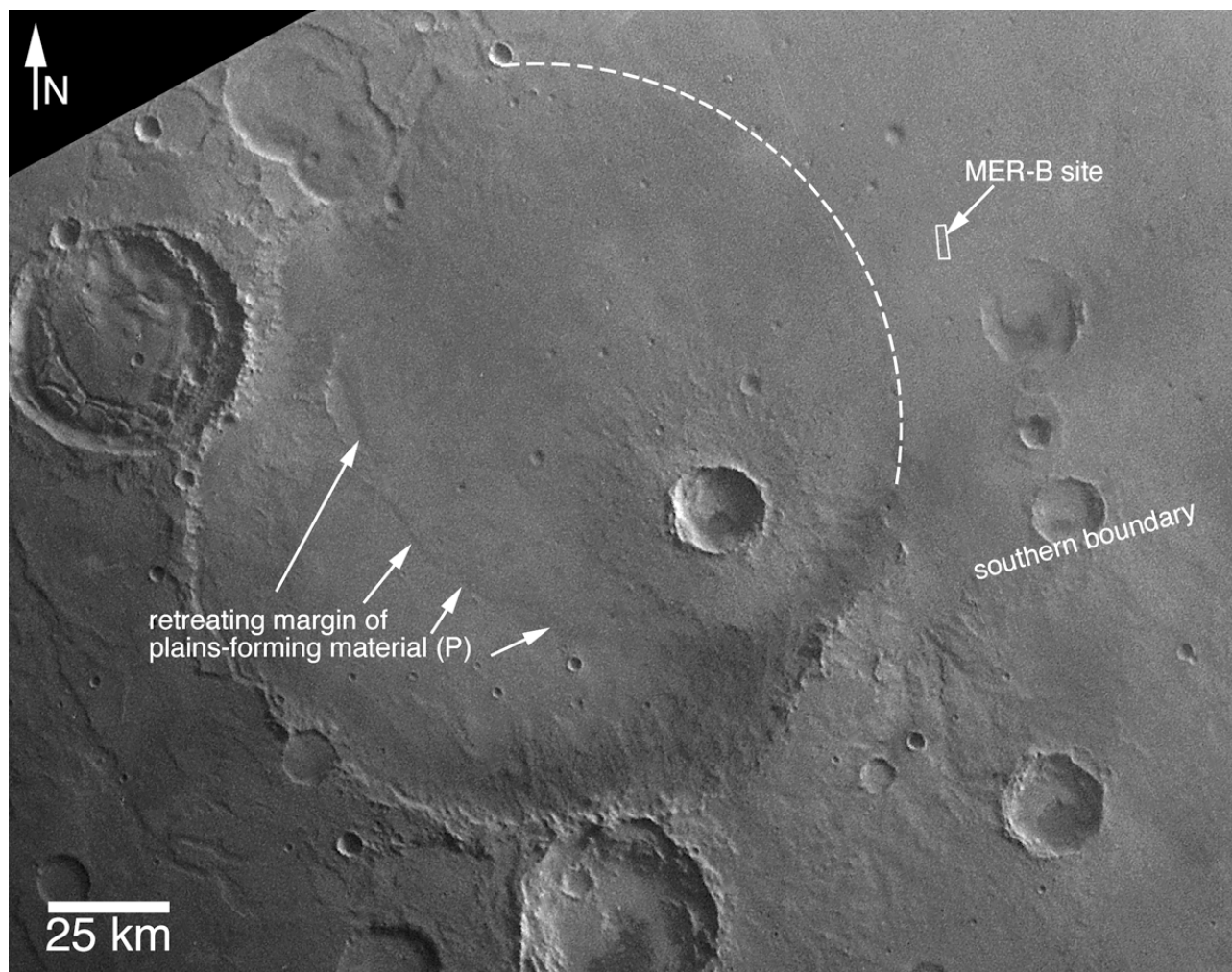


Figure 52. Beneath the plains-forming rock of the MER-B site might lie rugged, brecciated rock associated with a ~140 km diameter impact basin that is only partially exhumed. The dotted arc indicates the approximate location of the buried crater rim which is manifested at the surface in a suite of rises/hills that can be identified in orbiter images and maps derived from MGS MOLA topography. The box at the MER-B site indicates the zone from Eagle and Endurance Craters, south to Victoria Crater, and encompasses the entire area in which the rover worked during 2004 and 2005. This is a mosaic of two Viking orbiter images, 653a57 and 653a59 ([figure52.png](#)).

energy or so rapid that sedimentation dominated over erosion of the landscape. Gentle exhumation implies that the processes involved, also, were of relatively low energy. However, the number of craters destroyed by erosion is unknown. It is possible that erosion and exhumation of craters has not been particularly gentle and that for every crater exhumed and appearing to be in nearly-pristine form, many more craters of similar size have been destroyed.

Erosion

Among the unanswered questions about the geologic processes that have shaped the Sinus Meridiani region, perhaps the most challenging is that of erosion. The rocks described here had to have been deposited, buried, lithified, and then later brought back to the surface and exposed such that they can be identified in orbiter images.

The rocks have, therefore, been eroded. Pedestal craters have formed, cliffs and scarps have formed, craters have been exhumed, and some of the material filling the craters has been removed from them. And all of these things have happened without leaving behind very many clues as to the nature of the processes involved.

Very few yardangs, a good indicator of wind erosion (Blackwelder 1934), are found in the region—some occur west of Meridiani Planum in terrain mapped as being a surface expression of the lower unit (L). No valley networks cut the uppermost rock units—the plains-forming unit (P) or the ridge-forming unit (R). Thus, it is not clear whether wind or running water played a role in the incredible amount of erosion that must have occurred in the region. Wind erosion, however, does not always produce yardangs, and wind can transport materials shed from the outcrops by weathering and other erosive processes. The scarps, cliffs, buttes, and mesas in the region suggest two other contributors to landscape degradation in the region—gravity, which slowly removes material by mass movement—and groundwater, the percolation and seepage of which may have influenced and enhanced scarp retreat through undermining and collapse (e.g., Higgins and Osterkamp 1990)—followed by breakdown and removal of the debris, perhaps by wind.

Where did the material come from, and where did it go?

Another challenging question is one that plagues nearly every occurrence of layered and eroded rock on Mars. Where did the materials come from and where did they go after they were eroded?

On Earth, some clastic sedimentary rock stratigraphies tell a story of mountain ranges that have come and gone. They are only known from the sediment they shed. Across southern Ohio, for example, one can trace the sedimentologic record of the three Paleozoic orogenies that occurred in eastern North America even though the geomorphic evidence of only the very last (the Appalachian) is preserved. If one were studying the sedimentary rocks of the Colorado Plateau in the 19th Century, one might have found it very difficult to

imagine the comings and goings of mountain ranges, volcanoes, deserts, and seas recorded there—or, at least, one would be challenged to understand these things in the absence of the plate tectonics paradigm. On Mars our problems are compounded by the fact that only a very, very tiny amount of the martian bedrock has been examined (the material at the MER landing sites), and the rest of the science rests on those things that can be determined from orbit.

The sedimentary rocks of Mars might record the comings of goings not of tectonic ranges but of localized “mountains” created by impacts. The rocks likely also include the weathered and eroded products of earlier sedimentary and igneous rocks. As for where the material eroded from the Sinus Meridiani region may have gone, this is equally unknowable. The sediments derived from the weathering and erosion of these rocks were deposited elsewhere, perhaps in some cases to become new sedimentary rock.

Summary and Conclusions

The light-toned, layered rocks exposed in Sinus Meridiani are sedimentary rocks. They exhibit a level of diversity of properties not unlike that of the sedimentary rocks exposed on North America’s Colorado Plateau. More than 800 m of stratigraphic section can be viewed in orbiter images. The 2004 MER-B rover activities have explored < 1% of this section. The bedrock of the heavily cratered terrain to the north, south, east, and west of Meridiani Planum is also light-toned and layered, and may be composed of similar material. To the north and west of Meridiani Planum, the large (tens of km diameter) impact craters of the heavily cratered terrain in the regions are an integral part of the Sinus Meridiani stratigraphy. Some of the diversity of the rocks in the region is reflected in differences in bedding style between rocks occurring inside and outside of impact craters; these differences suggest that the depositional setting inside a crater and outside and adjacent to the crater were different. The Sinus Meridiani region also exhibits interbedded valleys or valley networks, some of which have been exhumed and others of which have been inverted by erosion.

The upper crust of Mars in the Sinus Meridiani region is a layered, cratered, and “valley-ed” volume. Erosional expressions (including the exhumation of large craters and inversion of valleys) similar to those of Sinus Meridiani occur across Arabia Terra and in other cratered highlands of Mars. Unfortunately, the bedrock of Arabia Terra is typically hidden by thick mantles of fines. However, rocks bearing some similarity to those in Sinus Meridiani are exposed and observable in orbiter images at Mawrth Vallis and in the plains cut by the Valles Marineris; their presence suggests that the rocks examined by MER-B could be Hesperian rather than Noachian in age. The rocks cut by the Valles Marineris have long been assumed to be volcanic (mostly lava flows); the observation of sedimentary rocks similar to those of Sinus Meridiani opens up the possibility that those materials, too, may have involved deposition in or at least diagenesis in the presence of water or groundwater.

Directory of supporting data

root directory

- edgett_mars_2005_0002.pdf this file
- Fig. 1 figure01a.png, figure01b.png, figure01c.png full-resolution unannotated images
- Fig. 2 figure02inset.png, figure02.png full-resolution unannotated images
- Fig. 3 figure03.png full-resolution unannotated image
- Fig. 4 figure04.png full-resolution unannotated image
- Fig. 5 figure05a.png, figure05b.png, figure05c.png full-resolution unannotated image
- Fig. 6 figure06a.png, figure06b.png, figure06c.png full-resolution unannotated images
- Fig. 7 figure07a.png, figure07b.png full-resolution unannotated image
- Fig. 8 figure08.png full-resolution unannotated image
- Fig. 9 figure09a.png, figure09b.png full-resolution unannotated images
- Fig. 10 figure10.png full-resolution unannotated image
- Fig. 11 figure11.png full-resolution unannotated image
- Fig. 12 figure12.png full-resolution unannotated image
- Fig. 13 figure13.png full-resolution unannotated image
- Fig. 14 figure14a.png, figure14b.png full-resolution unannotated images
- Fig. 15 figure15a.png, figure15b.png full-resolution unannotated images
- Fig. 16 figure16a.png, figure16b.png, figure16c.png, figure16d.png, figure16e.png full-resolution unannotated images
- Fig. 17 figure17a.png, figure17b.png, full-resolution unannotated images
- Fig. 18 figure18.png full-resolution geologic sketch map and stratigraphic column, with annotations
- Fig. 19 figure19.png full-resolution unannotated image
- Fig. 20 figure20.png full-resolution unannotated image
- Fig. 21 figure21a.png, figure21b.png, figure21c.png, figure21d.png, figure21e.png full-resolution unannotated images
- Fig. 22 figure22a.png, figure22b.png full-resolution unannotated images
- Fig. 23 figure23a.png, figure23b.png full-resolution unannotated images
- Fig. 24 figure24.png full-resolution unannotated image
- Fig. 25 figure25a.png, figure25b.png, figure25c.png, figure25d.png, figure25e.png, figure25f.png, figure25g.png, figure25h.png full-resolution unannotated images
- Fig. 26 figure26.png full-resolution unannotated image
- Fig. 27 figure27.png full-resolution unannotated image
- Fig. 28 figure28a.png, figure28b.png full-resolution unannotated images
- Fig. 29 figure29.png full-resolution unannotated image
- Fig. 30 figure30.png full-resolution unannotated image
- Fig. 31 figure31a.png, figure31b.png full-resolution unannotated images
- Fig. 32 figure32.png full-resolution unannotated image
- Fig. 33 figure33a.png, figure33b.png full-resolution unannotated images
- Fig. 34 figure34.png full-resolution unannotated image
- Fig. 35 figure35a.png, figure35b.png, figure35c.png full-resolution unannotated images
- Fig. 36 figure36.png full-resolution unannotated image
- Fig. 37 figure37a.png, figure37b.png, figure37c.png full-resolution unannotated images
- Fig. 38 figure38a.png, figure38b.png, figure38c.png full-

resolution unannotated images

- Fig. 39 figure39a.png, figure39b.png full-resolution unannotated images
 - Fig. 40 figure40a.png, figure40b.png full-resolution unannotated images
 - Fig. 41 figure41.png full-resolution unannotated image
 - Fig. 42 figure42.png full-resolution unannotated image
 - Fig. 43 figure43.png full-resolution unannotated image
 - Fig. 44 figure44a.png, figure44b.png, figure44c.png full-resolution unannotated images
 - Fig. 45 figure45a.png, figure45b.png full-resolution unannotated images
 - Fig. 46 figure46.png full-resolution unannotated image
 - Fig. 47 figure47a.png, figure47b.png, figure47c.png, figure47d.png full-resolution unannotated images
 - Fig. 48 figure48.png full-resolution annotated diagram
 - Fig. 49 figure49.png full-resolution unannotated image
 - Fig. 50 figure50.png full-resolution unannotated image
 - Fig. 51 figure51a.png, figure51b.png full-resolution unannotated images
 - Fig. 52 figure52.png full-resolution unannotated image
- data**—This directory contains MOC images used in the figures that were acquired April–September 2005 (mission subphases S05–S10). These had not yet been archived with the NASA PDS at the time the paper was published. These data have not been validated by the MOC archiving team.
- cumindex.txt explanation of content of the .txt files
- S05-00383.gif unprocessed image
 S05-00383.txt ancillary information
 - S05-00568.gif unprocessed image
 S05-00568.txt ancillary information
 - S05-01437.gif unprocessed image
 S05-01437.txt ancillary information
 - S06-02362.gif unprocessed image
 S06-02362.txt ancillary information
 - S08-03049.gif unprocessed image
 S08-03049.txt ancillary information
 - S09-02562.gif unprocessed image
 S09-02562.txt ancillary information
 - S10-01115.gif unprocessed image
 S10-01115.txt ancillary information

Acknowledgements

I am profoundly thankful to M. C. Malin for his patience and the hundreds of hours—over the past 8 years—of discussion, targeting, analysis, and review, that have contributed to the ideas expressed in this work. I appreciate the constructive comments, which led to improvements in the manuscript, provided by reviewers L. S. Crumpler and E. Stofan, and the Associate Editor, J. B. Plescia. I also give sincere thanks to the hundreds of engineers and scientists that managed, fabricated, tested, launched, operated, and archived data from the instruments aboard MGS, Mars Odyssey, and MER-B. I am equally thankful for those that developed the tools essential for data analysis and operation of the spacecraft and their instruments. This research was conducted via the MGS MOC investigation (Jet Propulsion Laboratory contract 959060), the Mars Odyssey THEMIS investigation (Arizona State University contract 01-081, under JPL contract 1228404), and the NASA Mars Data Analysis Program (contract NASW-01004).

References

- Allen, C. C., F. Westall, and R. T. Schelble (2001) "Importance of a martian hematite site for astrobiology" *Astrobiology* 1(1), 111–123.
- Antoniadi, E. M. (1930) *La Planète Mars*, Hermann, Paris.
- Arvidson, R. E. F. P. Seelos IV, K. S. Deal, W. C. Koeppen, N. O. Snider, J. M. Kieniewicz, B. M. Hynek, M. T. Mellon, and J. B. Garvin (2003) "Mantled and exhumed terrains in Terra Meridiani, Mars" *Journal of Geophysical Research* 108(E12), 8073. [doi:10.1029/2002JE001982](https://doi.org/10.1029/2002JE001982)
- Arvidson, R. E. et al. (2004) "Localization and physical property experiments conducted by Opportunity at Meridiani Planum" *Science* 306, 1730–1733. [doi:10.1126/science.1104211](https://doi.org/10.1126/science.1104211)
- Arvidson, R. E., F. Poulet, J.-P. Bibring, M. Wolff, A. Gendrin, R. V. Morris, J. J. Freeman, Y. Langevin, N. Mangold, and B. Bellucci (2005) "Spectral reflectance and morphologic correlations in eastern Terra Meridiani, Mars" *Science* 307, 1591–1594. [doi:10.1126/science.1109509](https://doi.org/10.1126/science.1109509)
- Baker, A. A. (1936) "Geology of the Monument Valley–Navajo Mountain region, San Juan County, Utah" *United States Geological Survey Bulletin* 865, 1–106.
- Barlow, N. G. (1999) "Potential highlands landing sites for Mars Surveyor 2001" Second Mars Surveyor Landing Site Workshop in Buffalo, New York, NASA Ames Research Center, Moffett Field, California.
- Bell, J. F. III et al. (2003) "Mars Exploration Rover Athena Panoramic Camera (Pancam) investigation" *Journal of Geophysical Research* 108(E12), 8063. [doi:10.1029/2003JE002070](https://doi.org/10.1029/2003JE002070)
- Blackwelder, E. (1934) "Yardangs" *Geological Society of America Bulletin* 45, 159–165.
- Buczkowski, D. L. and G. E. McGill (2002) "Topography within circular grabens: Implications for polygon origin, Utopia Planitia, Mars" *Geophysical Research Letters* 29(7), 1155. [doi:10.1029/2001GL014100](https://doi.org/10.1029/2001GL014100)
- Caplinger, M. A. and M. C. Malin (2001) "Mars Orbiter Camera geodesy campaign" *Journal of Geophysical Research* 106(E10) 23,595–23,606. [doi:10.1029/2000JE001341](https://doi.org/10.1029/2000JE001341)
- Catling, D. C. and J. M. Moore (2003) "The nature of coarse-grained crystalline hematite and its implications for the early environment of Mars" *Icarus* 165, 277–300. [doi:10.1016/S0019-1035\(03\)00173-8](https://doi.org/10.1016/S0019-1035(03)00173-8)
- Chan, M. A., B. Beitler, W. T. Parry, J. Ormö, and G. Komatsu (2004) "A possible terrestrial analogue for haematite concretions on Mars" *Nature* 429, 731–734. [doi:10.1038/nature02600](https://doi.org/10.1038/nature02600)
- Chan, M. A., B. Beitler, W. T. Parry, J. Ormö, and G. Komatsu (2005) "Red rock and red planet diagenesis: Comparisons of Earth and Mars concretions" *Geological Society of America Today* 15(8), 4–10. [doi:10.1130/1052-5173\(2005\)015<4:RRARPD>2.0.CO;2](https://doi.org/10.1130/1052-5173(2005)015<4:RRARPD>2.0.CO;2)
- Chapman, M. G. and K. L. Tanaka (2002) "Related magma–ice interactions: Possible origins of chasmata, chaos, and surface materials in Xanthe, Margaritifer, and Meridiani Terra, Mars" *Icarus* 155, 324–339. [doi:10.1006/icar.2001.6735](https://doi.org/10.1006/icar.2001.6735)
- Christensen, P. R. (1986) "Regional dust deposits on Mars: Physical properties, age, and history" *Journal of Geophysical Research* 91(B3), 3533–3545.
- Christensen, P. R. (1986) "The spatial distribution of rocks on Mars" *Icarus* 68, 217–238. [doi:10.1016/0019-1035\(86\)90020-5](https://doi.org/10.1016/0019-1035(86)90020-5)
- Christensen P. R. and S. W. Ruff (2004) "Formation of the hematite-bearing unit in Meridiani Planum: Evidence for deposition in standing water" *Journal of Geophysical Research* 109, E08003. [doi:10.1029/2003JE002233](https://doi.org/10.1029/2003JE002233)
- Christensen, P. R. et al. (2000) "Detection of crystalline hematite mineralization on Mars by the Thermal Emission Spectrometer: Evidence for near-surface water" *Journal of Geophysical Research* 105(E4), 9623–9642. [doi:10.1029/1999JE001093](https://doi.org/10.1029/1999JE001093)
- Christensen, P. R., R. V. Morris, M. D. Lane, J. L. Bandfield, and M. C. Malin (2001) "Global mapping of martian hematite mineral deposits: Remnants of water-driven processes on early Mars" *Journal of Geophysical Research* 106(E10), 23,873–23,885. [doi:10.1029/2000JE001415](https://doi.org/10.1029/2000JE001415)
- Christensen, P. R. et al. (2003) "Morphology and composition of the surface of Mars: Mars Odyssey THEMIS results" *Science* 300, 2056–2061. [doi:10.1126/science.1080885](https://doi.org/10.1126/science.1080885)
- Christensen, P. R. et al. (2004) "The Thermal Emission Imaging System (THEMIS) for the Mars 2001 Odyssey mission" *Space Science Reviews* 110, 85–130. [doi:10.1023/B:SPAC.0000021008.16305.94](https://doi.org/10.1023/B:SPAC.0000021008.16305.94)
- Christensen, P. R. et al. (2004) "Mineralogy at Meridiani Planum from the Mini-TES experiment on the Opportunity rover" *Science* 306, 1733–1739. [doi:10.1126/science.1104909](https://doi.org/10.1126/science.1104909)
- Darton, N. H. (1910) "A reconnaissance of parts of northwestern New Mexico and northern Arizona" *United States Geological Survey Bulletin* 435, 1–88.
- De Hon, R. A. (1994) "A highland sample strategy for Pathfinder" Mars Pathfinder Landing Site Workshop, Lunar and Planetary Institute Technical Report 94-04, Houston, 24–25.
- Edgett, K. S. (1997) "Nature and source of low-albedo surface material in the sandy aeolian environment of Sinus Meridiani, Mars" *Geological Society of America Annual Meeting Abstracts with Programs* 29(6), A214.
- Edgett, K. S. and M. C. Malin (2002) "Martian sedimentary rock stratigraphy: Outcrops and interbedded craters of northwest Sinus Meridiani and southwest Arabia Terra" *Geophysical Research Letters* 29(24), 2179. [doi:10.1029/2002GL016515](https://doi.org/10.1029/2002GL016515)
- Edgett, K. S. and M. C. Malin (2004) "The geologic record of early Mars: A layered, cratered, and 'valley-ed' volume" *Lunar and Planetary Science XXXV, Abstract No. 1188*, Lunar and Planetary Institute, Houston.
- Edgett, K. S. and T. J. Parker (1997) "Water on early Mars: Possible subaqueous sedimentary deposits covering ancient cratered terrain in western Arabia and Sinus Meridiani" *Geophysical Research Letters* 24(22), 2897–2900.
- Frey, H. V., J. H. Roark, K. M. Shockley, E. L. Frey, and S. E. H. Sakimoto (2002) "Ancient lowlands on Mars" *Geophysical Research Letters* 29(10), 1384. [doi:10.1029/2001GL013832](https://doi.org/10.1029/2001GL013832)
- Frey, H. V., E. L. Frey, W. K. Hartmann, and K. L. Tanaka (2003) "Evidence for buried 'Pre-Noachian' crust pre-dating the oldest observed surface units on Mars" *Lunar and Planetary Science XXXIV, Abstract No. 1848*, Lunar and Planetary Institute, Houston.
- Gilmore, M. S. and K. L. Tanaka (2001) "Potential Noachian-aged sites for MER-B" First Landing Site Workshop for the 2003 Mars Exploration Rovers, Abstract No. 9029, Lunar and Planetary Institute, Houston.
- Golombek, M. P. et al. (2003) "Selection of the Mars Exploration Rover landing sites" *Journal of Geophysical Research* 108(E12), 8072. [doi:10.1029/2003JE002074](https://doi.org/10.1029/2003JE002074)
- Greeley, R. and J. E. Guest (1987) "Geologic map of the eastern equatorial region of Mars" *United States Geological Survey Miscellaneous Investigations*

- Series, Map I-1802-B, scale 1:15,000,000.
- Greeley, R. and S. D. Thompson (2003) "Mars: Aeolian features and wind predictions at the Terra Meridiani and Isidis Planitia potential Mars Exploration Rover landing sites" *Journal of Geophysical Research* 108(E12), 8093. [doi: 10.1029/2003JE002110](https://doi.org/10.1029/2003JE002110)
- Grotzinger, J. P. and the Athena Science Team (2004) "Stratification, sediment transport, and the early west surface of Meridiani Planum" *Eos, Transactions of the American Geophysical Union* 85(7), Fall Meeting Supplement, Abstract P24A-01.
- Hartmann, W. K. (2005) "Martian cratering 8: Isochron refinement and the chronology of Mars" *Icarus* 174(2), 294–320. [doi: 10.1016/j.icarus.2004.11.023](https://doi.org/10.1016/j.icarus.2004.11.023)
- Hartmann, W. K. and G. Neukum (2001) "Cratering chronology and the evolution of Mars" *Space Science Reviews* 96, 165–194.
- Hartmann, W. K., J. Anguita, M. A. de la Casa, D. C. Berman, and E. V. Ryan (2001) "Martian cratering 7: The role of impact gardening" *Icarus* 149, 37–53. [doi: 10.1006/icar.2000.6532](https://doi.org/10.1006/icar.2000.6532)
- Herkenhoff, K. E. et al. (2004) "Evidence from Opportunity's Microscopic Imager for water on Meridiani Planum" *Science* 306, 1727–1730. [doi: 10.1126/science.1105286](https://doi.org/10.1126/science.1105286)
- Higgins, C. G. and W. R. Osterkamp (1990) "Seepage-induced cliff recession and regional denudation" in C. G. Higgins and D. R. Coates, Eds., *Groundwater Geomorphology, The Role of Subsurface Water in Earth-Surface Processes and Landforms*, Geological Society of America Special Paper 252, 291–317.
- Hynek, B. M. (2004) "Implications for hydrologic processes on Mars from extensive bedrock outcrops throughout Terra Meridiani" *Nature* 431, 156–159. [doi: 10.1038/nature02902](https://doi.org/10.1038/nature02902)
- Hynek, B. M., R. E. Arvidson, and R. J. Phillips (2002) "Geologic setting and origin of Terra Meridiani hematite deposit on Mars" *Journal of Geophysical Research* 107(E10), 5088. [doi: 10.1029/2002JE001891](https://doi.org/10.1029/2002JE001891)
- Kisvarsanyi, E. B., and A. W. Hebrank (1987) "Taum Sauk Power Plant section; buried and exhumed hills of Precambrian rhyolite, the St. Francois Mountains, Missouri" in *Centennial Field Guide Volume 3, North-Central Section of the Geological Society of America*, 167–168. [doi: 10.1130/0-8137-5403-8\(1987\)003<0167:TSPPSB>2.0.CO;2](https://doi.org/10.1130/0-8137-5403-8(1987)003<0167:TSPPSB>2.0.CO;2)
- Klingelhöfer, G. et al. (2004) "Jarosite and hematite at Meridiani Planum from Opportunity's Mössbauer spectrometer" *Science* 306, 1740–1745. [doi: 10.1126/science.1104653](https://doi.org/10.1126/science.1104653)
- Lane, M. D., R. V. Morris, S. A. Mertzman, and P. R. Christensen (2002) "Evidence for platy hematite grains in Sinus Meridiani, Mars" *Journal of Geophysical Research* 107(E12), 5126. [doi: 10.1029/2001JE001832](https://doi.org/10.1029/2001JE001832)
- Lane, M. D., P. R. Christensen, and W. K. Hartmann (2003) "Utilization of the THEMIS visible and infrared imaging data for crater population studies of the Meridiani Planum landing site" *Geophysical Research Letters* 30(14), 1770. [doi: 10.1029/2003GL017183](https://doi.org/10.1029/2003GL017183)
- Maizels, J. (1990) "Raised channel systems as indicators or palaeohydrologic change: a case study from Oman" *Palaeogeography, Palaeoclimatology, Palaeoecology* 76, 241–277.
- Maki, J. N. et al. (2003) "Mars Exploration Rover engineering cameras" *Journal of Geophysical Research* 108(E12), 8071. [doi: 10.1029/2003JE002077](https://doi.org/10.1029/2003JE002077)
- Malin, M. C. (1976) "Nature and origin of intercrater plains on Mars" in *Studies of the Surface Morphology of Mars*, Ph.D. dissertation, California Institute of Technology, Pasadena, 101–176.
- Malin, M. C. and K. S. Edgett (2000) "Sedimentary rocks of early Mars" *Science* 290, 1927–1937.
- Malin, M. C. and K. S. Edgett (2001) "Mars Global Surveyor Mars Orbiter Camera: Interplanetary cruise through primary mission" *Journal of Geophysical Research* 106(E10), 23,429–23,570. [doi: 10.1029/2000JE001455](https://doi.org/10.1029/2000JE001455)
- Malin, M. C. and K. S. Edgett (2003) "Evidence for persistent flow and aqueous sedimentation on early Mars" *Science* 302, 1931–1934. [doi: 10.1126/science.1090544](https://doi.org/10.1126/science.1090544)
- Malin, M. C., G. E. Danielson, A. P. Ingersoll, H. Masursky, J. Veverka, M. A. Ravine, and T. A. Soulanille (1992) "Mars Observer Camera" *Journal of Geophysical Research* 97(E5), 7699–7718.
- McCauley, J. F. (1978) "Geologic map of the Coprates Quadrangle of Mars" United States Geological Survey Miscellaneous Investigations Series, Map I-897, scale 1:5,000,000.
- McEwen, A. S., M. C. Malin, M. H. Carr, and W. K. Hartmann (1999) "Voluminous volcanism on early Mars revealed in Valles Marineris" *Nature* 397, 584–586.
- McEwen, A. S., B. S. Preble, E. P. Turtle, N. A. Artemieva, M. P. Golombek, M. Hurst, R. L. Kirk, D. M. Burr, and P. R. Christensen (2005) "The rayed crater Zunil and interpretations of small impact craters on Mars" *Icarus* 176(2), 351–381. [doi: 10.1016/j.icarus.2005.02.009](https://doi.org/10.1016/j.icarus.2005.02.009)
- McGill, G. E. and L. S. Hills (1992) "Origin of giant martian polygons" *Journal of Geophysical Research* 97(E2), 2633–2647.
- McLennan, S. M. et al. (2005) "Provenance and diagenesis of the evaporite-bearing Burns Formation, Meridiani Planum, Mars" *Earth and Planetary Science Letters*. [doi: 10.1016/j.epsl.2005.09.041](https://doi.org/10.1016/j.epsl.2005.09.041)
- Miller, R. P. (1937) "Drainage lines in bas-relief" *Journal of Geology* 45(4), 432–438.
- Murchie, S. and A. Treiman (1994) "Tartarus Colles: A sampling of the martian highlands" *Mars Pathfinder Landing Site Workshop, Lunar and Planetary Institute Technical Report 94-04*, Houston, 32–33.
- Murchie, S., J. Mustard, J. Bishop, J. Head, C. Pieters, and S. Erard (1993) "Spatial variations in the spectral properties of bright regions on Mars" *Icarus* 105, 454–468. [doi: 10.1006/icar.1993.1141](https://doi.org/10.1006/icar.1993.1141)
- Newsom, H. E., C. A. Barber, T. M. Hare, R. T. Schelble, V. A. Sutherland, and W. C. Feldman (2003) "Paleolakes and impact basins in southern Arabia Terra, including Meridiani Planum: Implications for the formation of hematite deposits" *Journal of Geophysical Research* 108(E12), 8075. [doi: 10.1029/2002JE001993](https://doi.org/10.1029/2002JE001993)
- North American Commission on Stratigraphic Nomenclature (1983) "North American stratigraphic code" *American Association of Petroleum Geologists Bulletin* 67(5), 841–875.
- Ormö, J., G. Komatsu, M. A. Chan, B. Beitler, and W. T. Parry (2004) "Geological features indicative of processes related to the hematite formation in Meridiani Planum and Aram Chaos, Mars: A comparison with diagenetic hematite deposits in southern Utah, USA" *Icarus* 171, 295–316. [doi: 10.1016/j.icarus.2004.06.001](https://doi.org/10.1016/j.icarus.2004.06.001)
- Presley, M. A. (1986) "The origin and history of surficial deposits in the central equatorial region of Mars" M.S. Thesis, Washington University, St. Louis.
- Rhodes, D. D. (1987) "Table Mountain of Calaveras and Tuolumne counties, California" *Centennial Field Guide Volume 1, Cordilleran Section of the Geological Society of America*, 269–272. [doi: 10.1130/0-8137-5401-1\(1987\)001<0269:TMOCAT>2.0.CO;2](https://doi.org/10.1130/0-8137-5401-1(1987)001<0269:TMOCAT>2.0.CO;2)

- Rieder, R. et al. (2004) "Chemistry of rocks and soils at Meridiani Planum from the Alpha Particle X-ray Spectrometer" *Science* 306, 1746–1749. [doi:10.1126/science.1104358](https://doi.org/10.1126/science.1104358)
- Rotto, S. and K. L. Tanaka (1995) "Geologic/geomorphologic map of the Chryse Planitia region of Mars" United States Geological Survey Miscellaneous Investigations Series, Map I-2441, scale 1:5,000,000.
- Schultz, P. H. and A. B. Lutz (1988) "Polar wandering on Mars" *Icarus* 73, 91–141. [doi:10.1016/0019-1035\(88\)90087-5](https://doi.org/10.1016/0019-1035(88)90087-5)
- Schultz, P. H., R. A. Schultz, and J. Rogers (1982) "The structure and evolution of ancient impact basins on Mars" *Journal of Geophysical Research* 87(B12), 9803–9820.
- Scott, D. H. and M. H. Carr (1978) "Geologic map of Mars" United States Geological Survey Miscellaneous Investigations Series, Map I-1083, scale 1:25,000,000.
- Scott, D. H. and K. L. Tanaka (1986) "Geologic map of the western equatorial region of Mars" United States Geological Survey Miscellaneous Investigations Series, Map I-1802-A, scale 1:15,000,000.
- Shoemaker, E. M. and R. J. Hackman (1962) "Stratigraphic basis for a lunar time scale" in Z. Kopal and Z. K. Michailov, editors, *The Moon, International Astronomical Union Symposium 14*, Leningrad 1960 Proceedings, Academic Press, New York, 289–300.
- Smith, D. E. et al. (2001) "Mars Orbiter Laser Altimeter: Experiment summary after the first year of global mapping of Mars" *Journal of Geophysical Research* 106(E10), 23,689–23,722. [doi:10.1029/2000JE001364](https://doi.org/10.1029/2000JE001364)
- Soderblom, L. A. et al. (2004) "Soils of Eagle Crater and Meridiani Planum at the Opportunity rover landing site" *Science* 306, 1723–1726. [doi:10.1126/science.1105127](https://doi.org/10.1126/science.1105127)
- Squyres, S. W. et al. (2004) "The Opportunity rover's Athena science investigation at Meridiani Planum, Mars" *Science* 306, 1698–1703. [doi:10.1126/science.1106171](https://doi.org/10.1126/science.1106171)
- Squyres, S. W. et al. (2004) "In situ evidence for an ancient aqueous environment at Meridiani Planum, Mars" *Science* 306, 1709–1714. [doi:10.1126/science.1104559](https://doi.org/10.1126/science.1104559)
- Stokes, W. L. (1969) *Scenes of the Plateau Lands and How They Came to Be*, Starstone, Salt Lake City.
- Sullivan, R. et al. (2005) "Aeolian processes at the Mars Exploration Rover Meridiani Planum landing site" *Nature* 436, 58–61. [doi:10.1038/nature03641](https://doi.org/10.1038/nature03641)
- Sumner, D. Y. (2004) "Poor preservation potential of organics in Meridiani Planum hematite-bearing sedimentary rocks" *Journal of Geophysical Research* 109(E12), E12007. [doi:10.1029/2004JE002321](https://doi.org/10.1029/2004JE002321)
- Tanaka, K. L. (1986) "The stratigraphy of Mars" *Proceedings of the Seventeenth Lunar and Planetary Science Conference, Part 1*, *Journal of Geophysical Research* 91(B13), E139–E158.
- Thomas, M., J. D. A. Clarke, and C. F. Pain (2005) "Weathering, erosion and landscape processes on Mars identified from recent rover imagery, and possible Earth analogues" *Australian Journal of Earth Sciences* 52, 365–378. [doi:10.1080/08120090500134597](https://doi.org/10.1080/08120090500134597)
- Varekamp, J. C. (2004) "Copahue Volcano: A modern terrestrial analog for the Opportunity landing site?" *Eos, Transactions of the American Geophysical Union* 85(41), 401, 407. [doi:10.1029/2004EO410002](https://doi.org/10.1029/2004EO410002)
- Whitbeck, N. E., K. L. Tanaka, and D. H. Scott (1991) "Geologic map of the Valles Marineris region, Mars" United States Geological Survey Miscellaneous Investigations Series, Map I-2010, scale 1:2,000,000.
- Wilhelms, D. E. (1972) "Geologic mapping of the second planet" *NASA/United States Geological Survey Interagency Report, Astrogeology* 55, 1–36.
- Wilhelms, D. E. (1990) "Geologic mapping" in *Planetary Mapping*, edited by R. Greeley and R. M. Batson, Cambridge University Press, New York, 208–260.
- Williams, R. M. E. and K. S. Edgett (2005) "Valleys in the martian rock record" *Lunar and Planetary Science XXXVI*, Abstract No. 1099, Lunar and Planetary Institute, Houston.
- Williams, R. M. E., M. C. Malin, and K. S. Edgett (2005) "Remnants of the courses of fine-scale, precipitation-fed runoff streams preserved in the martian rock record" *Lunar and Planetary Science XXXVI*, Abstract No. 1173, Lunar and Planetary Institute, Houston.
- Zimbelman, J. R. and R. A. Craddock (1991) "An evaluation of probable bedrock exposure in the Sinus Meridiani region of the martian highlands" *Proceedings of Lunar and Planetary Science* 21, 645–655.
- Zuber, M. T., D. E. Smith, S. C. Solomon, D. O. Muhleman, J. W. Head, J. B. Garvin, J. B. Abshire, and J. L. Buffon (1992) "The Mars Observer Laser Altimeter investigation" *Journal of Geophysical Research* 97(E5), 7781–7797.